Research Based Development of Innovative and Indigenous Technologies for Nuclear Physics Laboratories

A Thesis submitted to the Central University of Himachal Pradesh

for the Partial Fulfilment of the Degree of

DOCTOR OF PHILOSOPHY

In the School of Physical and Material Sciences,

In the Department of Physics and Astronomical Science

under the supervision of

Prof.(Dr.) O.S.K.S. Sastri

by

Jithin Bhagavathi

October, 2020

CENTRAL UNIVERSITY OF HIMACHAL PRADESH

Dated: October 2020

Department of Physics & Astronomical Science

School of Physical & Material Sciences

Central University of Himachal Pradesh, Dharamshala

[Established under the Central Universities Act 2009]

PO Box 21, Dharamshala, District Kangra,

Himachal Pradesh [India] - 176215

CERTIFICATE

This to certify that I, **Jithin Bhagavathi**, have carried out the research embodied in the present thesis for the full period prescribed under Ph.D. ordinances of the University.

I declare to the best of my knowledge that no part of this Thesis was earlier submitted for the award of research degree of any University.

Name: Jithin Bhagavathi

Enrolment No.: CUHP17RDPHY05

SIGNATURE OF THE SUPERVISORS **HEAD OF THE DEPARTMENT**

Dated: October 2020

Department of Physics & Astronomical Science

School of Physical & Material Sciences

Central University of Himachal Pradesh, Dharamshala

[Established under the Central Universities Act 2009]

PO Box 21, Dharamshala, District Kangra,

Himachal Pradesh [India] - 176215

UNDERTAKING

I, **Jithin Bhagavathi**, hereby undertake that I have carried out the research embodied in the present thesis and that the work is original and without plagiarism. In case any such evidence is found, my degree is liable to be cancelled by the university .

Name: Jithin Bhagavathi

Enrolment No.: CUHP17RDPHY05

This is to certify that the above claim is correct to the best of my knowledge

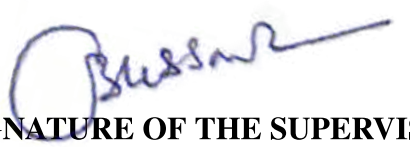

SIGNATURE OF THE SUPERVISORS

Dedicated to All My Mentors. . .

Acknowledgements

First and foremost, I am indebted to my guide, Prof O.S.K.S. Sastri for enabling me to pursue this research and allowing tremendous creative liberties and decision making freedom. His constant support, guidance and encouragement has been crucial in completing this work. He has also offered complete support in outreach programmes, so that the results out this work could reach the academic community.

I am grateful to IUAC, New Delhi for making reference designs of alpha detector systems available in the open domain. The prototype design Alpha Spectrometers designed by Dr Ajith Kumar and Er. V.V.V. Satyanarayana, being used at Panjab University offered insight into their functioning and identifying potential areas for improvement. Technical advice from Er S Venkataramanan, Er Arti Gupta and Er Ruby Shanthi were instrumental during the development of the analog signal processing stages. The advice and support from Dr. Sugathan P and Dr. Saneesh N was extremely helpful on getting usable results from custom built gamma detectors. I am grateful to Georges Khaznadar for his assistance with packaging software for Debian based platforms.

Several professors from various institutes have offered their valuable time and resources to test and validate the designed equipment along with their students. The active feedback and advice from Prof. Devinder Mehta, and Er. Ashwini Jain from Panjab University have greatly helped us in our journey. Their vast experience in training students in the field of nuclear and radiation physics has been put to good use. Help from Dr. A M Vinod Kumar, Calicut University, Dr K K Abdulla and Dr Subha P A, Farooq College, Calicut, in the testing of the gamma spectrometer are highly appreciated. I would also like to thank Dr. Padmanabh Rai, for providing us with single crystal diamonds fabricated at his research facility.

The PER group at CUHP headed by Prof O.S.K.S Sastri has been instrumental in publishing the research that has led up to the development of the various instruments, and has been involved in further documenting the latest progress. Special thanks to the entire group - Jyoti Ma'am, Vandana Ma'am, Swapna, Aditi, and all my friends for making this a memorable experience. Swapna Gora has extensively used and characterized the Alpha Spectrometer, as well as published data from novel experiments conducted with it.

Many thanks to Dr. Sheetal Dewan for being an inspiration, and for facilitating post processing of the single crystal diamonds at Dr Vinay Gupta's lab, at the Physics Department of Delhi University. Dr. Surbhi Gupta and Surbhi Jain spent much of their valuable time to get the single crystal diamonds coated using the e-beam instrument, and are experts at what they do.

I am indebted to Dr. D K Avasthi, Amity University for reviewing and providing valuable suggestions on the gamma-gamma coincidence unit. My gratitude extends to Prof. Alpana Goel and Prof. A N Garg for deploying the setup at their university, which has helped me fine tune the instrument. Dr. Santosh Babu Gunda, NISER, has also played an active role in evaluating this instrument and has provided guidance on changes necessary for making it more student friendly.

The contribution of the undergraduate students at the Central University of Himachal Pradesh who have used the Alpha Spectrometer in its nascent stages and offered their valuable feedback has been invaluable in refining the designs.

This progress has been massively facilitated due to financial and material support via CSpark Research, a company I founded with the initial financial support from my father, Dr Ajith Kumar. He has actively helped me in defining the goals. My Mom and Brother have wholly supported me and also contributed to the fabrication and testing tasks. Mr Brijmohan Saini and his skilled team have been indispensable for machining vacuum chambers and enclosures designed for this research.

To my batchmates at the university - Rishu, Monal, Aditi, Ankush, and Anil - it was wonderful knowing all of you, and thanks for making it a memorable experience. To Kanika and Mayrika, there is not enough gossip in the world for us to share. Thank you for keeping the RD room alive.

The existence of Free and Open Source software has been crucial for this work. Our gratitude towards the developers of the KiCAD EDA, Python, PyQt, Numpy, Scipy, PyQtgraph and the GNU/Linux operating system cannot be expressed enough.

And finally, to all the teachers who have shown faith in my work, and invested their time and effort to encourage further developments , I cannot thank you enough.

Contents

List of Figures

List of Tables

List of Publications

1. Jithin B.P. and O.S.K.S. Sastri, "Novel coincidence setup using indigenously developed portable USB gamma spectrometer and associated analysis software," *Nuclear Instruments and Methods in Physics Research, Section A: Accelerators, Spectrometers, Detectors and Associated Equipment*, vol. 964, p. 163 793, 2020, ISSN: 01689002. DOI: 10.1016/j.nima.2020.163793Paper

2. Jithin B.P., V. V. V. Satyanarayana, S. Gora, *et al.*, "Measurement Model of an Alpha Spectrometer for Advanced Undergraduate Laboratories," *Physics Education*, vol. 35, no. Jan-March 2019, 2019. [Online]. Available: http://www.physedu.in/pub/2019/PE18-08-518

3. Jithin B.P., S. Gora, V. Satyanarayana, *et al.*, "Gamma Spectra of Non-Enriched Thorium Sources using PIN Photodiode and PMT based Detectors," *Physics Education*, no. Apr jun 2020, 2020. [Online]. Available: http://www.physedu.in/pub/2020/PE19-12-600

4. S. Gora, Jithin B.P., V. V. V. Satyanarayana, *et al.*, "Alpha Spectrum of 212 Bi Source Prepared using Electrolysis of Non-Enriched ThNO 3 Salt," *Physics Education -IAPT*, vol. 35, no. Jan-Mar 2019, 2019. [Online]. Available: http://www.physedu.in/pub/2019/PE18-07-511

5. Jithin B.P., "SEELablet : A Technological Platform for Development of Innovative Experiments for Undergraduate Education," *APT Tunes*, vol. May 2018, 2018. [Online]. Available: https://aptkerala.org/images/stories/apttunes/APT_TUNES2018.pdf

6. O. S. K. S. Sastri, S. Aditi, J. Bhardwaj, *et al.*, "Numerical Solution of Square Well Potential With Matrix Method Using Worksheets," *IAPT*, no. Jan - Mar 2020, 2019. [Online]. Available: http://www.physedu.in/pub/2020/PE19-11-590

7. A. Sharma, S. Gora, J. Bhagavathi, *et al.*, "Simulation study of nuclear shell model using sine basis," *American Journal of Physics*, vol. 576, 2020. DOI: 10.1119/10.0001041

Conference Publications

1. Jithin B.P. and O.S.K.S Sastri, "Indigenously developed gamma spectrometer," in *Proceedings of the DAE Symp. on Nucl. Phys. 63 (2018) 1072*, 2018, pp. 1072–1073. [Online]. Available: http://sympnp.org/proceedings/63/G19.pdf

2. Jithin B.P. and O.S.K.S. Sastri, "Gated MCA technique for demonstration of coincidence phenomena with a set of indigenously developed gamma spectrometers," in *Recent Issues in Nuclear and Particle Physics, Viswa Bharati*, 2019

3. Jithin B.P. and O.S.K.S. Sastri, "Compact dual-parameter MCA for γ-γ Coincidence Measurements," in *Proceedings of the DAE Symp. on Nucl. Phys. 64 (2019) 920*, 2019. [Online]. Available: http://sympnp.org/proceedings/64/G37.pdf

4. Jithin B.P. and O.S.K.S. Sastri, "Background Gamma Radiation Surveying in the IndianPeninsula with a Portable USB Spectrometer," in *Proceedings of the DAE Symp. on Nucl. Phys. 64 (2019)*, 2019. [Online]. Available: http://sympnp.org/proceedings/64/G28.pdf

5. Jithin B.P., "Learning Microcontrollers with Python," in *Scipy India*, 2019

6. Jithin B.P., "Simulation of N-Well Kronig- Penney Potential using Matrix Approach.," in *NACISP-2018*, IAPT, 2018

Workshops and outreach programs

1. 3 Day workshop on Computer Interfaced Science Experiments, Calicut University

2. India Science Fest, IISER Pune

3. SciPy.in-2019 International Conference.

4. 1 Day workshop on Computer Interfaced Science Experiments, P T Sarvajanik College, Surat

5. Science Hack Day 2019, Belgaum

Software published as Open Source

- Jithin B P, *CN Spec Source Code*. [Online]. Available: https://github.com/csparkresearch/cnspec
- Jithin B.P., *KuttyPy Source Code*, 2019. [Online]. Available: github.com/csparkresearch/kuttypy-gui

Abstract

Name of the student: **Jithin Bhagavathi** Roll No: **CUHP17RDPHY05**
Degree for which submitted: **PhD** Department: **Physics and Astronomical Science**
Thesis title: **Research Based Development of Innovative and Indigenous Technologies for Nuclear Physics Laboratories**
Thesis supervisor: **Prof. O.S.K.S. Sastri**
Month and year of thesis submission: **October 2020**

The goal of this thesis is to design, develop, and deploy equipment along with novel experiments with high instructional value essential for research and education in the field of nuclear radiation physics. This field is largely constrained by high equipment prices driven by a shortage of indigenous intellectual property as well as local manufacturing, and as a consequence gets minimal hands-on instruction in the vast majority of science institutions across India.

We have compiled a list of essential equipment critical for tackling this challenge, and have developed the necessary detector technology, electronics designs, and complementary firmware and software code to keep costs at a minimum. Additionally, our designs have been validated with experiments with pedagogical value performed using the final devices.

The key instruments developed are a USB powered multi-channel analyzers(MCA) for measuring energy spectrum, Alpha Particle and Gamma Ray spectrometers with signal processing electronics, and a Gamma-Gamma coincidence measurement setup. Additionally, a detector array, and a portable cellphone powered gamma spectrometer design has also been explored.

The significance of this study lies in the completeness of the developed instruments including technical and scientific documentation, and their demonstrated ability to be deployed to universities for teaching and research.

CHAPTER 1

Introduction

Nuclear physics is the field of science that explores the building blocks of atomic nuclei and their interactions. Discoveries in nuclear physics have led to applications in the fields of power generation, nuclear medicine and magnetic resonance imaging, isotopes that help studying biology, radiocarbon dating in geology and archaeology, and of course, warfare. Experimental nuclear physics depends heavily on the detection and analysis of radiation emitted by the nuclei. For that reason, teaching nuclear physics requires equipment that can detect and analyzse different types of radiation emitted by the nucleus. Enhancing experimental facilities to support research and instruction in this field has been the primary objective of this work.

1.1 Motivation for the Research

Nuclear science has immense importance in fields ranging from medical sciences to power generation [16], and defence. In the Indian context, the importance of teaching nuclear and radiation physics goes beyond a pure research perspective. A large number of particle accelerators are being deployed across the country for medical and research applications [17]. A press information bureau report by the department of atomic energy, government of India, provides an overview of the goals concerning use of nuclear sources in health, power generation, and defence[18].

The nuclear share of power generation in India is stated to be 3.4% as of 2016, and is projected to increase. According to the government sources, sanctioned funds for nuclear

power generation plants under construction exceeds Rs. 35,000 crores. In the year 2017, the central government proposed doubling the nuclear power generation to 14,000MW, and this is to be done through indigenous development [19] [20]. As of 2018, 6 nuclear power plants with a combined capacity of 4.4GWe are under construction, and are expected to be completed by 2024-25[21]. India hopes to exploit its vast thorium resources for power generation in fast breeder reactors since reserves of natural uranium are poor [22]. Nuclear waste management, and environment safety audits will become more important as the country undergoes this shift. A huge workforce trained in nuclear and radiation physics is essential for the success of such initiatives.

It is generally the mandate of universities to create a trained human resource pool essential for the requirements of a nation. As far as education in the field of nuclear and radiation physics is concerned, the present situation in India is far from satisfactory. Nuclear physics as a subject is taught in very few universities, and that itself is mostly restricted to theory. We perceive that a major reason for this scenario is the lack of equipment to teach experimental nuclear physics at undergraduate and post graduate levels.

A variety of institutions are offering courses in radiation physics, however, factors such as a lack of indigenous equipment, high prices, and difficulties involved in procurement of radioactive sources, has resulted in neglect of experimental labs in this field. Human resource development is integral to economic and scientific progress, and this requires education at the graduate level and beyond. However, as of 2013 only 6 universities[23] have been awarding degrees dedicated to nuclear engineering . As a result, training in experimental nuclear physics is largely restricted to a handful of institutions under the Department of Atomic Energy (DAE), Inter-University Accelerator Accelerator Centre, New Delhi, and a few rare university departments. Currently, experimental nuclear physics is largely dependent on costly imported laboratory equipment and this fact prevents adapting it on a larger scale and deploying across the university network. The initial financial implications and the permanent dependency on foreign vendors for maintenance are major hurdles that require immediate attention.

Therefore, there is an urgent need for indigenous development of instrumentation for research and teaching in nuclear physics, and also to develop new experiments that rely on easily accessible apparatus and raw materials. The developed instruments should be affordable, rugged, power efficient, and user friendly. In addition, all components must

be available easily in order to facilitate manufacturing with a minimal price point and easy maintenance. One can therefore say that the education, research, and applications of nuclear physics requires a rapid shift to indigenous development.

1.1.1 Nuclear physics experiments at the post graduate level

A list of experiments included in the nuclear physics syllabus of many Indian universities is shown below. [24], to give some impression about the present scenario.

1. Dead time measurement and characterization of a G.M. counter.
2. To study the distribution of counts per unit time, and analyze the Source strength of a beta-source using a G.M. counter.
3. Analyze the pulse height of gamma ray spectra.
4. To study the attenuation of beta rays by Al sheets, and deduce the end-point energy.
5. Detect gamma radiation with a scintillation counter.
6. Calibrate gamma ray spectra using a scintillation counter.
7. Identify weakly radioactive samples, and determine their activity.
8. Calibrate a gamma-ray spectrometer, and determine its energy resolution.
9. Time resolution and calibration of a coincidence set-up using a multi-channel analyzer.
10. Observe the Formation of alpha particle tracks on Solid State Nuclear Track, and count them.

In the majority of teaching institutions, the only equipment available to study radiation is the Geiger-Muller counter. Equipment to measure the energy of gamma rays is rarely seen in our laboratories. The cost of a gamma spectrometer is way beyond the routine budget of our teaching laboratories, and such equipment if acquired, are mostly through the occasional project funding. Lack of follow-up funds for repair and maintenance pushes many of these acquired systems out of operation. These factors make including nuclear

spectroscopy experiments in the M.Sc curriculum almost impossible, and doing it at the B.Sc level is highly improbable.

The gravity of this situation becomes evident when you contrast it with the situation in developed countries. We quote the following line from a public document titled "Managing Ionising Radiations and Radioactive Substances in Schools and Colleges" from CLEAPSS[25], the School Science Service in UK. *"CLEAPSS publications are normally strictly confidential, with circulation restricted to members and associate members only. However, this revised edition is made publicly available to promote teaching practical radioactivity in schools, and in a well-managed way"*. The full document can be accessed from [25]. It states that elementary radiation experiments using a GM counter are included at the school level, and radiation safety guidelines applicable to schools are prepared and circulated, for encouraging such studies.

Awareness about radioactivity among the public is very low in our country, and the reason can be traced to the lack of initiatives similar to that of CLEAPSS. Such initiatives also require availability of equipment to support them. One of the main reasons for our lack of progress in this field is the paucity of affordable equipment.

In technology, market forces dictate the pace of innovation as well as the cost of end products. The downside of such an evolution is that several niche, yet critical products suffer from lack of sufficient $R\&D$. Development of scientific equipment require high R&D effort and the low volume production makes them expensive, that in turn affects quality hands-on education. The associated costs for simple spectroscopy related experiments exceeds several Lakhs INR and a large fraction of it goes to imported equipment with high cost of maintenance and essential repairs.

In view of the limited funds available with the vast majority of universities, equipment with a much lower price point is highly sought after, and that requires indigenous development of technology.

1.2 Basic Building Blocks for Radiation Detection

Before delving into the details of the instruments for radiation detection and analysis, it is necessary to gain some understanding of the fundamentals of the radiation detection

process.

The basic building blocks common for all radiation detection systems are the Detector, Pre-amplifier, Shaping amplifier, and the Digitizer. The specifications of each building block may vary with the nature of the concerned application. A brief introduction to the basic building blocks and processes involved are given below, and a simplified schematic of a typical system is outlined in Figure 1.1.

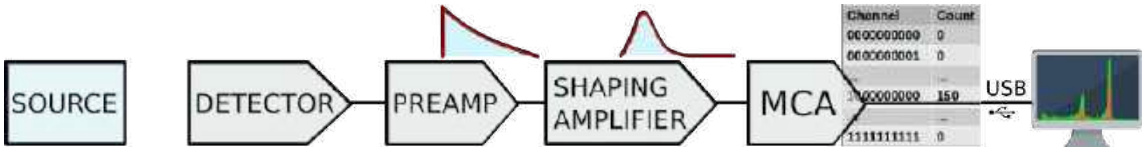

FIGURE 1.1: Schematic of a Radiation Detection System

The Detector assembly generates an electrical signal on the arrival of a charged particle or a gamma ray photon. The magnitude of this signal is so small that it cannot be measured directly (Except for detectors like the Geiger-Muller counter where internal amplification is achieved by applying a high voltage). The detector output is fed to a Pre-amplifier that generates a voltage pulse output corresponding to the charge generated by input radiation event. The next stage is a shaping amplifier that processes the pre-amplifier output to make it suitable for digitization. The shaping amplifier output pulse height is then digitized using an Analog to Digital converter having a definite number of channels, for example 1024 channels in the case of a 10 bit ADC. Each digitization increments the count in the corresponding channel and we get a histogram, a pulse height distribution. After calibration, this represents the energy spectrum of the incident radiation. Subsequent paragraphs give a brief introduction of these subsystems. A detailed treatment of this topic is given in the book by Knoll [26].

1.2.1 The Detector

Radiation, either a charged particle or a gamma ray photon, is detected by observing the results of its interactions with the detector material, that consists of electrons and nuclei. Charged particles can be further classified into light or heavy depending on their mass, compared to that of an electron. The choice of detector heavily depends on this classification. In order to gain some understanding about the working of the radiation

detectors, We need to consider the nature of interactions between the incoming radiation and the detector material.

1. **Heavy charged particles:** Protons, alpha particles, and ions of heavier elements fall into this category. When a heavy charged particle enters a volume of matter, Coulomb interaction with the electrons dominates. There is a very small probability that it will undergo large angle scattering as a consequence of a collision with a nucleus. Since the incident particle is thousands of times heavier than an electron it travels in a fairly straight line. After undergoing a large number of collisions with electrons, transferring some energy each time, it eventually comes to a stop, by ionizing the detector atoms. The mean energy loss per distance is given by the Bethe formula. The range of alpha particles in solids is of the order of tens of microns. For this reason, the thickness of the detector material required to measure the energy of heavy ions is relatively small. The interaction of the incident particle results in the creation of charge pairs inside the detector volume, that can be collected by applying an external electric field. The amount of charge is proportional to the energy of the incident particle.

2. **Light charged particles:** Electrons and positrons are the primary members of this category. Light particles can undergo large angle elastic scattering with electrons in the detector medium without losing energy. But energy can be lost by various processes such as ejecting electrons from their atomic shells and by the emission of bremsstrahlung radiation. The main difference is the larger distance they travel before coming to rest compared to heavy charged particles with the same energy. As a result, larger detector volumes are required for energy measurements.

3. **Gamma ray photons:** The main modes of interaction of gamma rays with matter are *photoelectric absorption, Compton scattering, and electron-positron pair production*. In photoelectric absorption, a gamma ray interacts with a bound atomic electron and loses all of its energy and ceases to exist as a gamma ray. Some of the energy is used to overcome the electron binding energy, and most of the remainder is transferred to the freed electron as kinetic energy. A very small amount of recoil energy remains with the atom to conserve momentum. In most detectors, the emitted electron is stopped in the active volume of the detector, which results in an output photon pulse whose amplitude is proportional to the energy deposited by

the photo-electron. Photoelectric absorption is important for gamma-ray detection because it is only in this interaction that the gamma ray gives up all its energy, and the resulting pulse composes the full-energy peak region.

An incident gamma ray can also get Compton scattered by an electron in the detector. The incident and scattered photon energies are related by the equation $E' = \frac{E}{1+E(1-cos\theta)/m_oc^2}$. Maximum energy transferred is given by $E_T = E(1 - 1/(1 + \frac{2E}{m_oc^2}))$, and this happens when $\theta = 180^o$. The scattered electron is usually stopped in the detection medium, and the detector produces an output pulse that is proportional to the energy lost by the incident gamma ray. The result is energy deposition in the detector ranging from zero to a maximum called the Compton edge energy. It is not possible to relate the Compton-scattering spectrum to the energy of the incident gamma ray because of this continuous distribution.

A gamma ray with an energy of at least 1.022 MeV can create an electron-positron pair when it is under the influence of the strong electromagnetic field of a nucleus. The electron and positron from pair production are rapidly slowed down by losing kinetic energy, and the positron combines with an electron in an annihilation process releasing two gamma rays with energies of 0.511 MeV each. These lower energy gamma rays may interact further with the absorbing material or may escape from the detector medium altogether.

Contributions from these multiple processes makes the gamma ray energy spectrum much more complicated, and difficult to interpret, than that of a charged particle.

We have described how radiation interacts with the atoms of the detector material and the associated energy transfer. The energy gained by the detector material is manifested in different ways. In direct conversion type detectors, the deposited energy results in the production of electrical charge pairs. Indirect conversion type detectors emit a burst of photons and additional detection apparatus is required to convert it into an electrical signal. The choice of the detector type depends on the application, available technology, and cost considerations. For example, measuring the energy of gamma rays with reasonable efficiency requires a detector volume of several cubic centimeters. One can choose an expensive High Purity Germanium (HPGe) crystal detector to get high energy resolution or settle for a scintillation detector using Sodium Iodide or Cesium Iodide, depending on the application and financial budget. There is a wide range of organic and inorganic

scintillation materials available, and among them, NaI and CsI crystals are widely used due to their comparatively low cost, even though the energy resolution is much poorer than HPGe detectors. In our work we have mainly focused on Planar Silicon PN junctions for alpha particle detection and Cesium Iodide crystals coupled to a PN junction for gamma detection.

The amount of energy required to create a charge pair depends on the detector material. For silicon detectors, the energy required to create an electron-hole pair is around 4 eV. For gases around 30 eV is required to create an electron-ion pair. However, this is a statistical process and the variance reduces with the total number of charge pairs created. This implies that for a given incident energy, materials requiring lower energy per charge pairs create a larger number of charge pairs and give better energy resolution.

In order to collect the charge, an electric field needs to be applied across the detector material. The resistance of the detector material should be extremely high to reduce the idle current. In the case of Germanium detectors, the High Purity Germanium crystals are kept at liquid nitrogen temperature to reduce the idle current. A highly cost-effective solution is to use the depletion region of a reverse-biased planar geometry PN junction as a detector. It is widely used for charge particle detection. The depletion region is thick enough to stop most of the charged particles, due to the high reaction cross-section. For a detailed description of this topic, visit the lecture notes by Helmuth Spieler [27].

1.2.2 The Pre-Amplifier

The amount of charge generated by the detector by the arrival of a decay product is minuscule and is only a small fraction of a pico Coulomb. It is much smaller than the charge induced when you wave your hand near the pre-amplifier input terminal and handling this minute signals makes the electrical shielding and grounding very important. Since the amount of charge generated is proportional to the energy deposited, charge sensitive pre-amplifiers are used. A charge sensitive pre-amplifier integrates the collected charge across a capacitor to generate a voltage signal. The output of a charge sensitive pre-amplifier is a pulse with a fast rise time and a slow fall time, with a sharp top. The rise time depends on the detector characteristics, and the fall time is decided by the RC time constant of the pre-amplifier circuit. The output pulse amplitude is proportional to the charge deposited

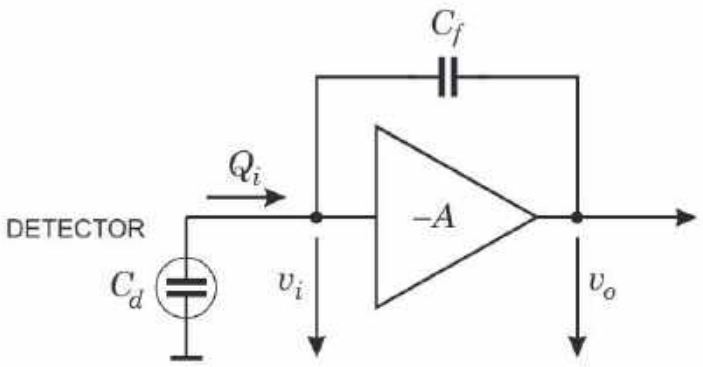

FIGURE 1.2: Block diagram of Charge Sensitive Pre-Amplifier[28]

The working principle of the charge sensitive pre-amplifier can be explained using the figure 1.2. The charge produced by an event is distributed between C_f and the input capacitance of the amplifier C_i, as per the equation

$$Q = C_i V_i + C_f(V_i - V_o)$$

Substituting V_i with V_o/A gives

$$Q = -V_o/(C_i + Cf)/A - V_o C_f = -V_o C_s/A + C_f(1 + 1/A)$$

When $A >> 1$, it becomes

$$= -V_o(C_s/A + C_f)$$

Re-arranging and applying the condition $C_f >> C_s/A$ gives,

$$V_o = -\frac{Q}{C_f}$$

The above equation implies that if we can make $C_f >> C_s/A$, the output voltage will depend only on the charge input and the value of the feedback capacitance. But C_f cannot be increased to meet this condition because it will reduce the output voltage. Increasing gain and reducing the input capacitance are the possible options. The input capacitance can be minimized by placing the detector very close to the amplifier input.

1.2.3 The Shaping Amplifier

To understand the necessity of the shaping amplifier, we need to look into the nature of the pre-amplifier output. It is mentioned that the statistical nature of the production of charges results in some variance in the signal output. In addition to this, the baseline of the pre-amplifier output also fluctuates due to external interference and inherent noise sources like thermal noise in resistors and shot noise in the semiconductor elements. The presence of this noise also contributes some random error to the pre-amplifier output. One method of reducing the noise is to limit the bandwidth of the circuit using an integrator circuit, which is a low pass filter. This will reduce the noise but also the rise time of the pulse. The rise time is chosen to be compatible with the measurement time.

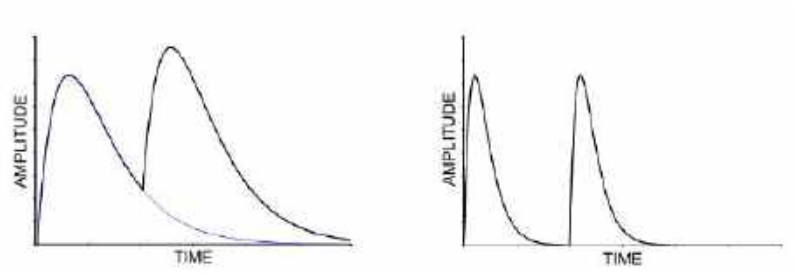

FIGURE 1.3: Reducing overlapping by differentiating the pre-amplifier output. The left side shows the pre-amp output after integration. The right side image is after reducing the long tail by differentiation.[27]

The pre-amplifier output pulse also has a very long fall time that may result in the outputs of two incident radiations overlapping with each other. This long tail can be reduced using differentiating circuits, as shown in figure 1.3. The shaping amplifier is a combination of integrating and differentiating circuits to achieve the two goals - reduce noise, and decrease the pulse width. A differentiation stage followed by a couple of integration stages results in a Gaussian-shaped pulse output. The time constants are chosen according to the detectors used and the expected maximum rate of measurement. The smooth top of the Gaussian pulse is also better suited for digitization. The final implemented circuit also needs to take handle many other aspects like baseline restoration and pole-zero compensation, and these will be discussed later. An elaborate description of this topic can be found at [27].

1.2.4 The Digitization system

The function of this part of the electronics is to digitize the height of the pulse outputs. A threshold detector is used to avoid digitizing noise spikes which are unrelated to input radiation events, and are present in every circuit. When the pulse height crosses a certain threshold, peak sensing and holding circuits are triggered. After a programmed time interval, the height of the pulse is digitized. These functions are generally implemented by dedicated logic circuits and analog to digital converters. The digitized data is stored with the help of a computer or micro-controller. In the case of a single detector, a simple Multi-Channel Analyzer (MCA) that generates the energy spectrum of the incident radiation suffices for digitization. For systems having multiple detectors, more complex analysis options like the time correlations between the pulses from different detectors are also available. We have developed various digitizing systems using micro-controllers and analog to digital converters.

1.3 Instruments Developed

The previous section explained the general features of the common subsystems of a radiation detection system. The purpose of this research is to develop affordable instruments for radiation detection and analysis using the latest advances in technology and also to identify low-intensity radioactive sources for performing nuclear physics experiments for teaching. This has been achieved with the development of a set of instruments and validating their performance by conducting and documenting several experiments using them. All of them are affordable, compact, portable, and USB powered. Several institutions are currently using designs we have developed and refined into finished products for spectroscopy.

Each of these require different types of subsystems. For alpha and gamma, the detectors are different, and the pre-amplifier and shaping amplifier specifications also differ. Another challenging part was designing a mechanical assembly that satisfies vacuum as well as electrical shielding requirements. Reducing the electrical noise to get the maximum possible energy resolution required several rounds of prototyping and testing. The following sections briefly introduce each of the instruments developed, followed by a more detailed description in the subsequent chapters.

1. 1024 and 4096 bin Multi Channel Analyzers(MCA): Independent USB powered multi-channel analyzers with List mode and histogram mode data acquisition options,
2. Alpha Spectrometer: A compact USB powered instrument for acquiring Alpha Particle Spectra with a 10 MeV range, 1K MCA, and vacuum chamber. A detector array was also developed
3. Gamma Spectrometer: Portable USB powered Gamma Ray Spectrometer with 3 MeV full-Scale range.
4. A gamma-gamma coincidence detection system. Two gamma detector outputs are fed to some logic circuits and the data is accepted only when both the detectors receive radiation within a specified time window.
5. Data Acquisition and Analysis software to use the instruments mentioned above.

Some advanced equipment development efforts made have also been mentioned, even though they have not reached the level of a final product.

1.3.1 Multi Channel Analyzers

The function of a Multi-Channel Analyzer(MCA) is to digitize the shaping amplifier output pulses and generate a histogram of pulse height distribution. The height of each input pulse is compared with a threshold DC voltage configurable by a digital to analog converter(DAC) or a potentiometer, and the process of digitization is started only if the pulse amplitude exceeds the threshold. The resolution of the MCA is determined by the number of bits of the Analog to Digital Converter (ADC) used for digitization. For example, a 10-bit ADC has 1024 possible outputs. A memory block of 1024 words is required to store the output, where the width of each word determines the maximum number of counts that can be recorded in it before an overflow event occurs. Digitization of a pulse results in a number between 0 and 1023 and that particular memory location is incremented. The final output is a pulse height distribution. It can be referred to as an energy spectrum after calibration using a radioactive source with known energy.

Two models of MCAs differing in resolution have been developed, having 1024 and 4096 channels each. Both employ a PIC24E series micro-controller. The 1024 channel

version uses the 12 bit ADC built into the microcontroller, and the 4096 channel MCA uses AD977, an external 16bit ADC. A 12 bit Digital to Analog Converter is used for setting the threshold in both designs. The main design considerations were linearity, conversion time, power consumption, and size. The differential non-linearity of the ADC is taken care of by using an ADC of higher resolution and discarding several least significant bits. The 1024 channel MCA uses a 12 bit ADC and the 4096 channel one uses a 16 bit ADC. Fast ADCs having a conversion time of several microseconds is chosen so that the throughput is not restricted by the conversion time. The major components are the threshold detector, sample and hold circuit, the Analog to Digital Converter, the logic circuits and a micro-controller coordinating the activities and providing the computer interface. The required bipolar DC power supplies are derived from the USB output using charge pumps, regulators, and filter circuits.

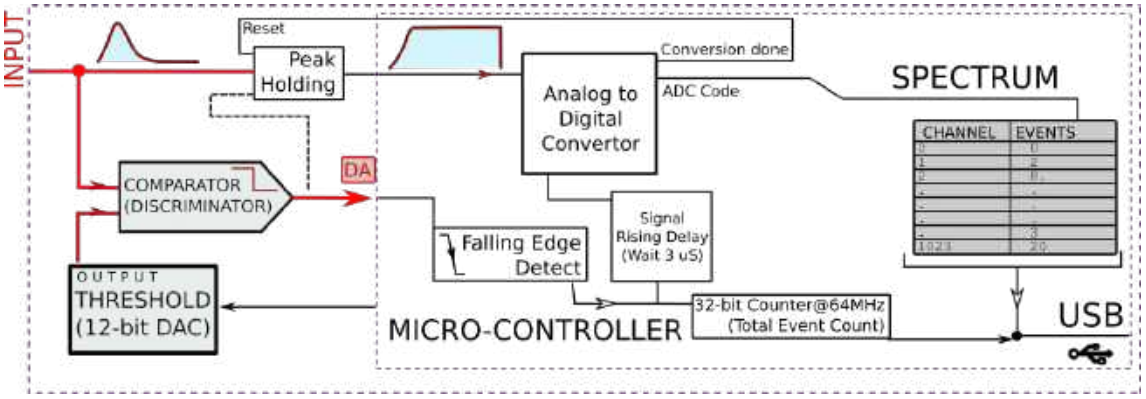

FIGURE 1.4: A flow diagram of our multi-channel analyzer [1]

The 1024 channel MCA design is incorporated into the Alpha and Gamma Spectrometers with different form factors. The PCB layout and firmware running inside the micro-controller are slightly different, but the same software can be used for accessing it from the computer. The micro-controller's code has been primarily written in the C language except for some time critical parts implemented in assembly language. Code running on the computer collects data from the micro-controller over the USB interface and performs data analysis and visualization. This software was developed using the Python programming language which enables users to control and access the hardware plugged into the USB port. We have emphasized on the use of open-source tools here, and the final software has been published[14] under open source terms on Github. It has been named CNSPEC and is common for all the instruments mentioned above. Much of

the software/applications written for these instruments span thousands of lines of code. Single-click installers are also been provided for Linux as well as Windows.

1.3.2 Alpha Spectrometer

Alpha spectrometers are devices that measure the energy of incoming alpha particles and generate an energy spectrum. The number of events at different energy intervals (counts) are plotted in the form of a histogram. It has applications in radio-chemistry, and in the screening of health physics and environmental samples. It is also an essential tool for nuclear physics research due to its ability to identify isotopes based on the energy of alpha particles emitted from them. Alpha Spectrometers are commercially available from several international vendors. For example, the model A-576 A-PAD from EG&G Ortec claims an energy resolution of 20 eV and costs several lakhs INR. The silicon surface barrier detector used in this system costs more than one lakh INR by itself.

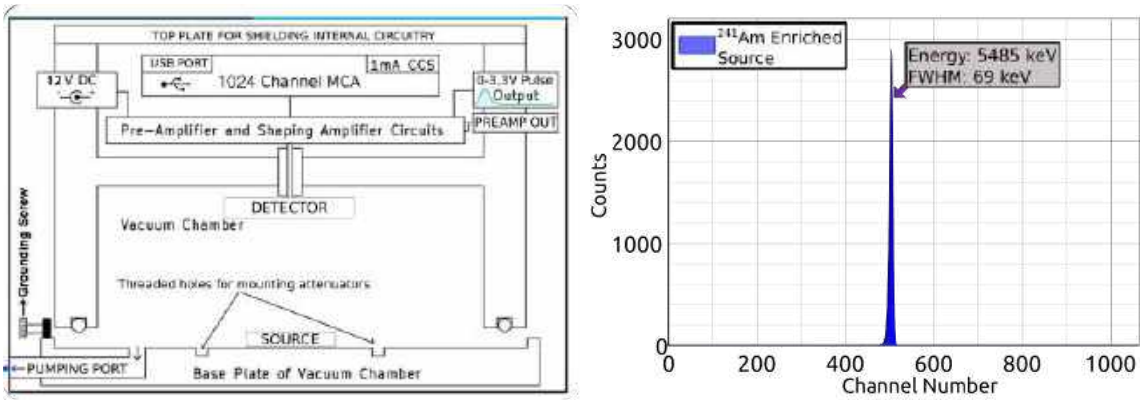

FIGURE 1.5: On the left is shown a schematic of an Alpha Particle Spectrometer consisting of the vacuum chamber containing the detector, the associated signal processing electronics. The figure on the right is an energy spectrum from ^{241}Am alpha source.

We have developed an Alpha Spectrometer that is affordable and very compact (110mm diameter and 73mm height). The vacuum chamber with a detector and all the electronics circuits are packed in a small metallic enclosure to reduce electrical noise. A Planar Silicon Diode detector is fixed inside the vacuum chamber with an 8mm collimator. The pre-amplifier, shaping amplifier, and the digitization circuits are all enclosed in another metallic cavity on top of the vacuum chamber. The computer interfacing and power supply is via the USB bus. Even though the built-in 1024 channel Analog to Digital Converter is

capable of giving the resolution at par with the commercial units, the energy resolution of our system is limited to around 70 eV (measured using the 5.485 MeV peak of ^{241}Am alpha source) due to the detector used. The Planar Silicon Diode was chosen over other options such as a Silicon Surface Barrier(SSB) detectors, to make the total cost of the system low. It is possible to use the electronics with an SSB detector to obtain a higher resolution but this is out of budget for most undergraduate labs. The vacuum chamber is designed in such a way that the radioactive source can be kept on the base plate with the detector mounted on the ceiling of the chamber facing down towards it. Fixtures are provided to place sheets of material between them in order to study energy loss characteristics.

1.3.3 Portable Gamma Spectrometer

Gamma ray spectrometers currently available for teaching labs use NaI scintillation detectors coupled with photomultiplier tubes, that require a high voltage DC power supply. The cost of such units which include the signal processing electronics and a multi-channel analyzer ranges from 3 to 7 lakhs INR. Lack of maintenance support is a major issue as per the feedback from the users.

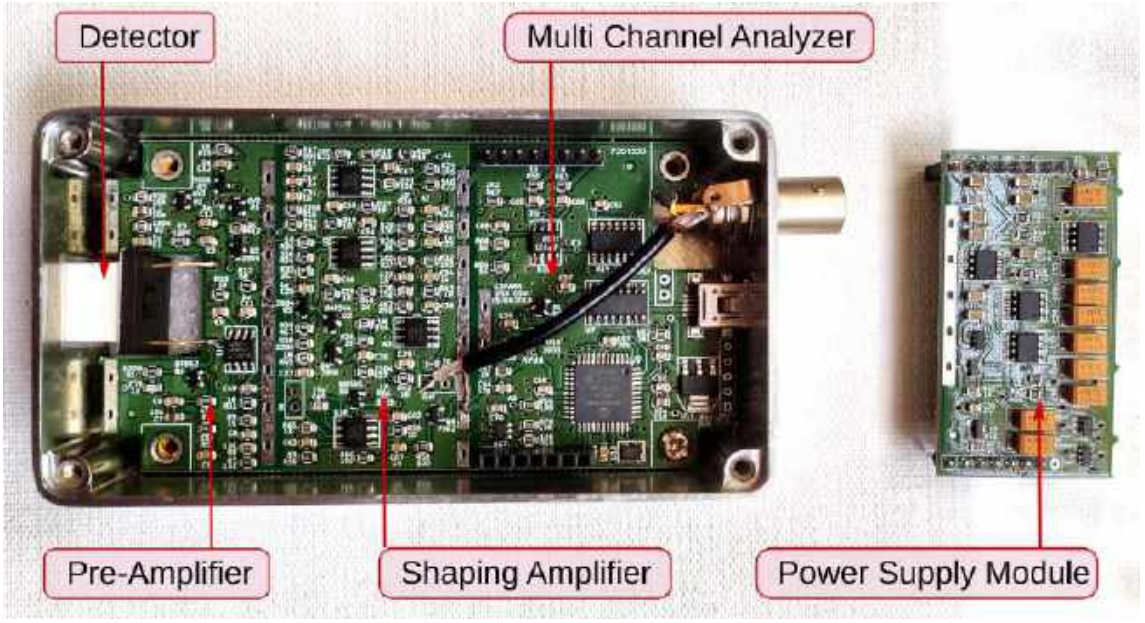

FIGURE 1.6: Components of the portable gamma spectrometer with an integrated 1024 channel MCA. The power supply module is unplugged and shown separately.

The second instrument in our list of developments is a compact, USB powered gamma ray spectrometer that weighs only a couple of hundred grams. The detector and all the required electronics are packaged inside a 112x60x31mm^3 aluminium enclosure, and can essentially be termed as a hand-held device. A 1024 bin multi-channel analyzer is also integrated, and all the required voltages are generated from the 5V USB supply by means of charge pumps and filters.

In the case of charged particle detectors, all the particles entering the detector volume will generate an electrical signal, but that is not the case with gamma detectors. The detector efficiency is defined in different ways. Intrinsic efficiency is the ratio of the number of pulses recorded by the detector to the number of gamma rays hitting the detector. Photo-peak efficiency is the parameter associated with producing full-energy peak pulses out of all recorded interactions. Due to the nature of interaction between gamma rays and the detector material, increasing the detector volume results in increased photo peak efficiency. Being a low cost design, certain compromises were necessary with the following consequences as outlined below.

We have used a CsI scintillator crystal having 10mm*10mm*8mm dimensions, which is smaller than the commonly used 2" diameter NaI crystals. This results in lower collection efficiency but it can be compensated by increasing the collection time. The light emitted by the scintillator is then coupled to a photo multiplier tube or a planar PN junction to convert it into an electrical signal. Subsequent signal processing needs are somewhat similar to the alpha spectrometer, but involve much higher gains owing to the weaker signal. More information on scintillation detectors can be found at [27]

The design considerations for a Gamma spectrometer are different from that of an Alpha spectrometer. For the latter, simultaneously obtaining good vacuum and electrical shielding is critical. For the Gamma spectrometer, there is no need for a vacuum chamber, owing to the high penetrating power of gamma rays, however, the much smaller output signal available from the detector was a major challenge. The noise floor had to be reduced further to achieve the desired energy resolution. After adopting a different pre-amplifier design and detector biasing, we were able to achieve better than 80 keV FWHM for the 1332 keV peak from a ^{60}Co source, which is at par with that of commercially available NaI detector+PMT based systems. The difference in collection efficiency attributed to the smaller volume has been reported in a separate publication dealing with environment monitoring[3]

The instrument is compatible with Linux, MS-Windows and Mac computers. An android app has also been developed for this system, and it can be plugged into any recent android phone by means of an OTG cable to acquire spectra with no additional requirements, making this a truly portable plug and play unit. The power requirements are also drawn from the USB port (approx 250 mA), and this translates to a typical maximum running time of a couple of hours on most phones. If longer acquisition times are required, a specialized adapter to simultaneously charge the phone from an alternate power source may be required.

1.3.4 Gamma-gamma Coincidence System

Gamma-gamma Coincidence measurements have a range of applications in isotope analysis and medical imaging such as Positron Emission Tomography (PET). However, it is severely under represented in UG and PG labs due to the extremely high costs of such systems.

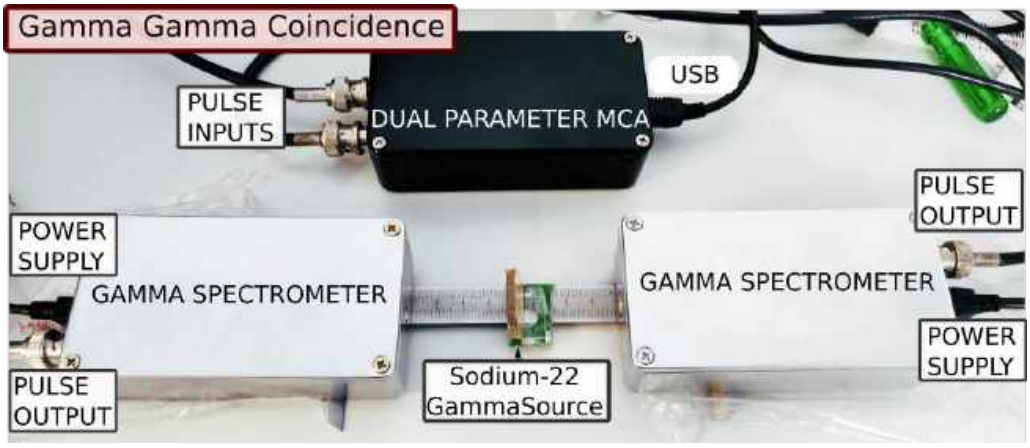

FIGURE 1.7: The gamma coincidence setup which includes two gamma spectrometers whose shaping amplifier outputs are routed to a dual parameter Multi Channel Analyzer

Development of a dual parameter Multi Channel Analyzer(MCA) was integral for detecting coincident events from multiple detectors. Towards this end, the existing 1K MCA design was augmented with coincidence logic, and mirrored to create a micro-controller based dual parameter MCA. The unit is enclosed in an aluminium chamber with two BNC ports fixed for input signals, and a USB port for communication and electrical power. The inputs accept 0-3.3 V Gaussian shaped signals with 3uS rise times, the shaping amplifier outputs of gamma spectrometer described earlier. Two high bandwidth

comparators with their reference inputs linked to 12-bit DACs were used to generate discriminator signals which are then interpreted by a micro-controller to detect coincident events. Digitization of pulse heights is carried out using built-in 10-bit Analog to Digital Converters of this micro-controller that has up to 4 analog inputs with simultaneous sampling by means of independent sample and hold circuits. Data is stored in a circular buffer in list mode which is periodically polled and uploaded to a connected computer.

Demonstrable results were obtained from ^{22}Na positron sources, and were further verified using angular correlation experiments. Positron annihilation phenomena results in two gamma rays with equal energies being emitted in diametrically opposite directions, and this makes it the easiest way to get introduced to coincidence experiments.

Various energy gates can be applied by the CNSPEC software to better understand this data. Several visualization options are available such as 2D histograms represented as Heat Maps, or as surface plots.

1.4 Other Developments

In addition to the instruments mentioned above, several other options pertaining to detector efficiency, design and fabrication were explored.

1.4.1 Single Crystal Diamond Detectors

The extremely novel properties of diamond used for nuclear detection are expected to provide far greater range and efficiency as compared to existing solutions, and specifically, it is being used in particle accelerators for in-beam, in-situ detecion applications due to its very high radiation hardness.

In comparison with PN junctions, diamond crystals exhibit significantly lower leakage current [29], and since they only respond to wavelengths in the mid ultraviolet and shorter, they are immune to background noise caused by the visible or IR light spectra . Once the artificial growth was successfully optimized and documented, research into exploiting the extremist properties of diamond grew exponentially in fields ranging from cancer therapy and diagnostics [30] and mammography [31], to high density and energy beam

monitoring for GeV range protons in particle accelerators [30]. The radiation hardness makes it an extremely suitable candidate for reliable operation under extremely harsh conditions, and it is being adopted for pixel detection, neutron detection, and for position sensitive measurements[32].

In collaboration with the dept of Physics, University of Delhi, single crystals were coated with gold and platinum electrodes using electron beam deposition, and contacts were made using wire bonding machines.

A few different samples were prepared, but reliable signals could not be obtained. While this could be attributed to the presence of nitrogen doping in the crystal, sufficient resources were unavailable for verifying the actual composition. This line of research was subsequently abandoned owing to the lack to resources to prepare purer diamond crystals with no dopants which act as charge trapping centres.

1.4.2 Array of Alpha Detectors

Since the single pixel spectrometer electronics had already been tested, the same was extended into a 3 x 3 array to be used for wider area detection systems.

1.4.3 Experiment Development

The objective here was to develop and document a range of nuclear physics experiments which adequately explain concepts. Including those which may currently not be covered by the limited curriculum owing to lack of equipment availability. Novel experiments have been designed as part of this research , and these have been elaborated in their respective chapters.

In particular, the Alpha Spectroscopy experiments involving Bismuth-212 have superb pedagogical value, and offer a refreshing deviation from the established practice of using commercial, enriched sources. One can explore branching ratios as well as measure the half life of the isotope.

For gamma spectroscopy, the identification of dominant isotopes in natural background is also a safer alternative to enriched sources, but comes at a cost of increased time requirement.

1.5 Impact of the research

All the equipment mentioned above have been made commercially available. Several universities and colleges have used them and given valuable feedback. This process has facilitated fine tuning of the design, as well as bug fixes. We were able to develop experiments as per existing curriculum, as well as introduce some new ones which were previously not included. Revenue thus generated has allowed investment in further research, and facilitated the development of new instruments.

1.6 Limitations of this research

As with any research, there are some aspects that have either not be attempted, or have been placed as stretch goals due to reasons ranging from paucity of funds to lack of time and facilities.

Scintillation crystal growth is out of scope of this research, and prefabricated scintillators of various geometries were procured from commercial entities. Very large scintillators and novel geometries were ruled out due to their associated costs.

Radioactive sources were limited to the ones already discussed in the previous section due to procurement constraints.

Source strengths did not exceed 1uC due to safety concerns, as well as safety regulations. However, the instruments were tested separately at specialized centres for their efficiency in dealing with count rates.

CHAPTER 2

Multi Channel Analysers

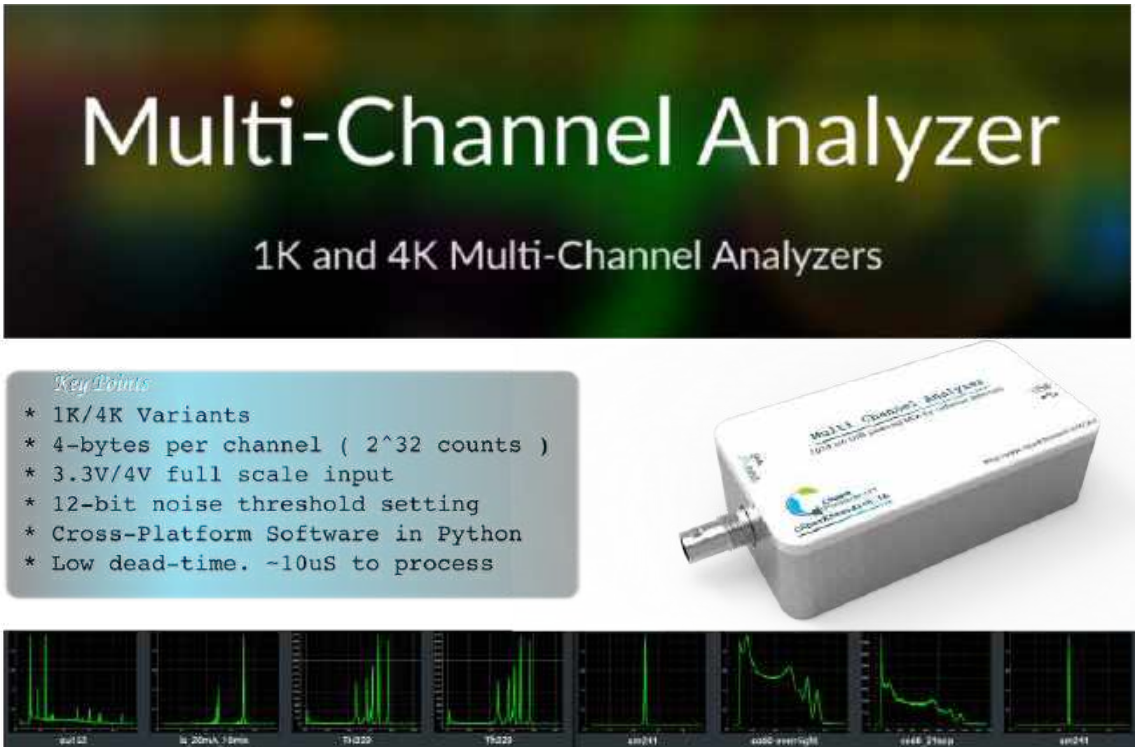

2.1 Introduction

Nuclear processes are studied by capturing and analysing the emitted radiation as a function of space and time. The radiation detectors are positioned strategically and the parameters of the captured radiation are recorded as a function of time. The nature of the nuclear

processes are generally inferred by analysing such data a number of detectors. In the case of a single detectors, this process could be as simple as measuring the energy of each incoming radiation and making a histogram plot that displays the prominent energies. The equipment performs that function is called a Multi Channel Analyser (MCA). The measured parameter, energy for example, is measured with some resolution that is indicated by the number of channels of the MCA. For example a 1024 channel MCA measuring in the range of 0 to 10 MeV, offers a resolution of around 10 keV(10000/1024), that can be increased to 2.5keV using a 4096 channel MCA.

The resolution of the measured parameter, energy for example, is not same as the resolution of the MCA. Due to the limitations of other parts of the measurement system, digitization results of same energy can fall in to nearby channels resulting in a Gaussian shaped peak after collecting large number of events. The energy resolution is measured from the Full Width at Half Maximum (FWHM) of this Gaussian peak. This is the frequently quoted figure indicating resolution of a measurement.

Even the data from a single detector can be recorded as function of time to provide some extra information. For example, the mean time between two consecutive emissions from a radioactive source should gradually increase, due to the finite half life and it can be studied by recording the events as a function of time. The explosive development of electronics makes it possible to have picosecond resolution time stamping. Even the low cost micro-controllers can give resolutions in tens of nanoseconds.

Recording the data from a single detector can be done in two different ways. One method is to generate the histogram into a block of memory inside the data acquisition hardware. This method requires less memory space and processing power but it is not possible to record any extra information, such as a time stamp. The other method is generally referred to as 'list mode' data acquisition, where the result of every measurement, sometimes along with a timestamp, is sent to a computer. Further analysis can then be carried out to generate different kinds of plots.

We have developed two single parameter MCAs having 1024 and 4096 channels respectively. A dual parameter MCA with 1024 channels also has been developed for coincidence measurements. The dual MCA implements list mode data acquisition from two separate detector channels. The following sections explain the hardware, firmware

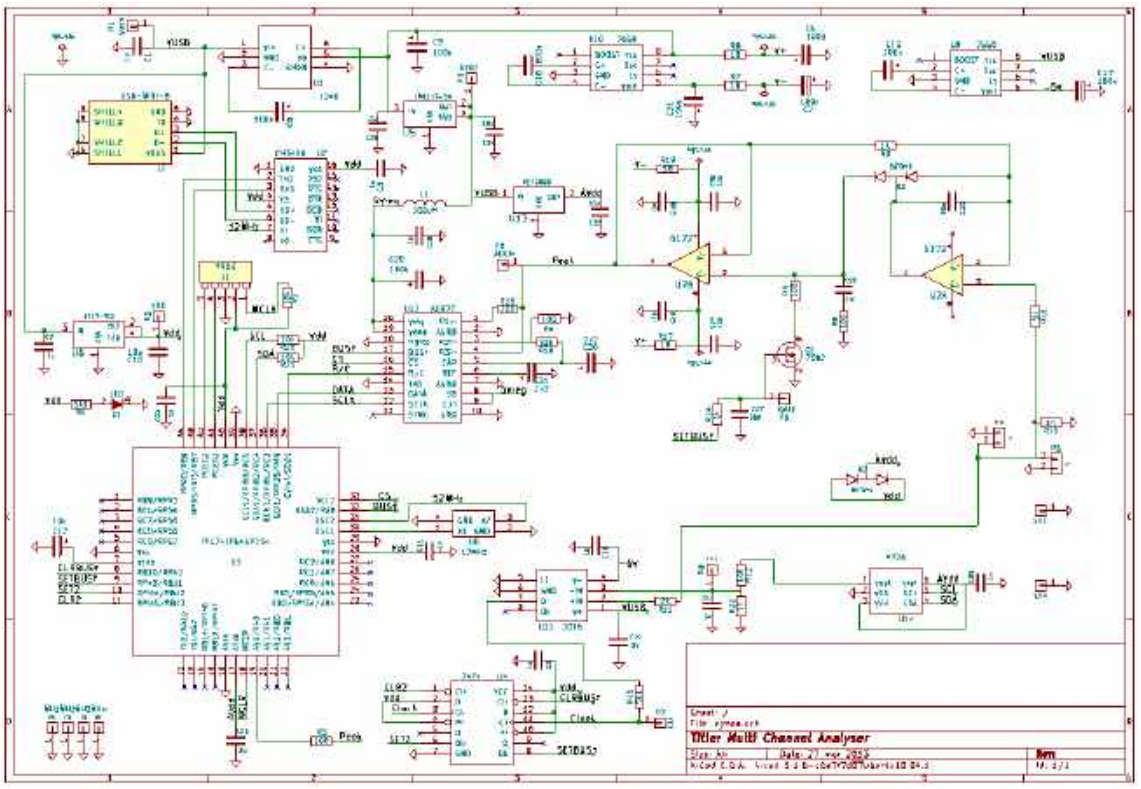

FIGURE 2.1: The circuit schematic of the single parameter Multi Channel Analyzer.

and software details of the single parameter MCAs. The dual MCA details are given in the chapter on gamma-gamma coincidence.

2.2 The hardware

The basic function of an MCA is to digitize the shaping amplifier output pulses and store the results to a block of memory and generate a histogram of the pulse height distribution. The height of each input pulse, above a threshold, is digitized and recorded to the corresponding channel.

A circuit schematic of the MCA circuit is shown in figure 2.1. The hardware mainly consists of a discriminator (U11), sample and hold circuit implemented using the op-amp(U7), an edge triggered flip-flop (U4), and a micro-controller (U3) and a USB to serial converter (U2). A PIC24E[33] micro-controller which includes a 12-bit analog to digital convertor (ADC) was used to build the 1024 bin MCA. A voltage reference of 50 ppm/^oC has been included in the design to minimize the effect of temperature drift in

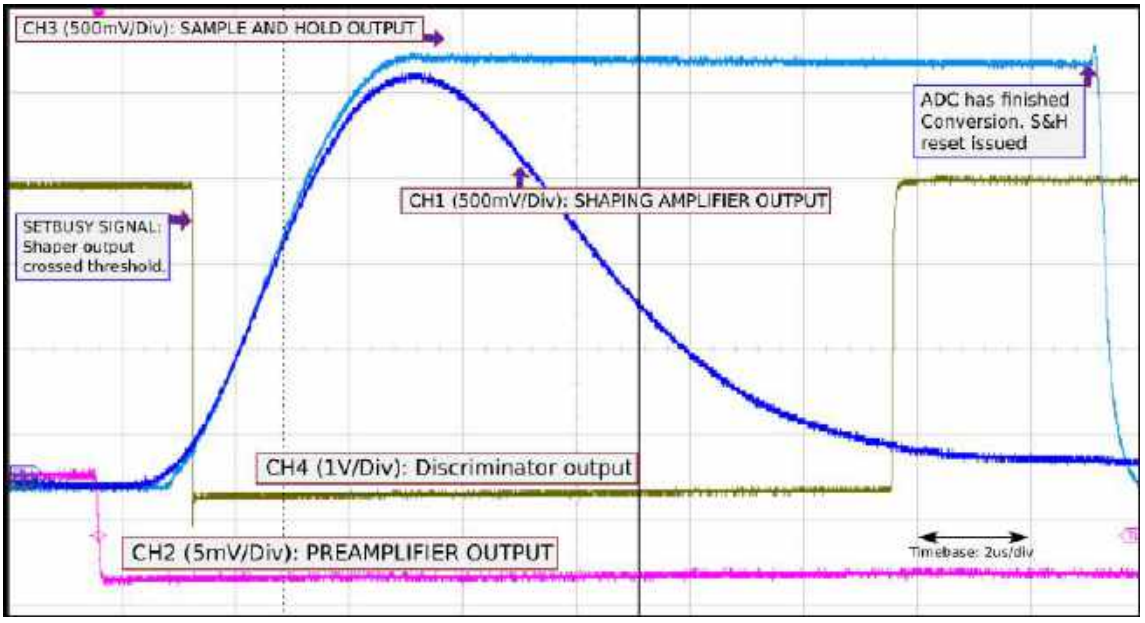

FIGURE 2.2: Timing digram for the 1K Multi Channel Analuyzer

the digitization process. An external flip-flop and a comparator in conjunction with the micro-controller are responsible for the digitization logic. Each pulse which crosses the threshold set by the comparator initiates an ADC conversion by means of a falling edge interrupt, prior to which a BUSY flag by the flip-flop is set to reject further input pulses till the conversion is complete. Post conversion, a short clear pulse(100ns) is output by the microcontroller which drains the sample and hold capacitor of the peak sensing circuit via a FET switch to ground, and prepares it for the next event. Figure 2.2 shows the various signals within the MCA recorded using a 4 channel oscilloscope. The input shaping amplifier signal is connected to CH3, and was configured to trigger the oscilloscope. CH2 shows the corresponding pre-amplifier input which was fed to the shaping amplifier, and is shown for additional clarity. The discriminator signal on CH4(SETBUSY) goes LOW whenever the shaper signal crosses the threshold set by the 12-bit DAC, and invokes the interrupt service routine linked to its falling edge. Post digitization, the sample and hold circuit is cleared using a FET based switch. The clear signal is not shown, but its position is at the falling edge of the CH3 signal.

The differential non-linearity of the ADC as per the datasheet [33] gives an idea of the number of least significant bits to ignore in order to get good performance. We have therefore shifted out 2 LSBs of the 12 bit digitized code, and the remaining 10-bits represent the maximum height of the shaped pulse scaled to a number between 0 and

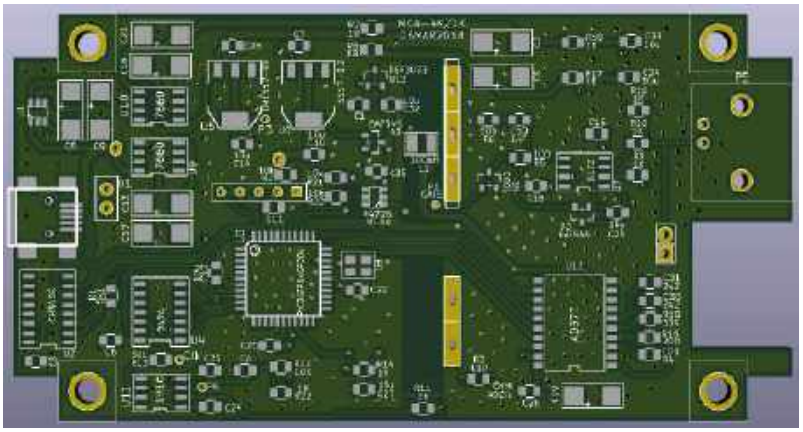

FIGURE 2.3: PCB of the 1K Multi Channel Analyzer .

1023. The MCA therefore has 1024 channel(1K) resolution, and an input voltage range of $0 - 3.3V$. The energy resolution can thus be calculated as $\frac{10MeV}{1023} = 9.7keV$. We also carried out a detailed performance review of the 12-bit ADC. A commercial voltmeter (Keithley Model 2000) was first interfaced with a computer using a Python script which can also read the value from the 12-bit ADC of the microcontroler. A 12-bit DAC was used to generate a slowly rising sawtooth signal, and both instruments were simultaneously recorded. The error signal of the ADC in its full range of 0 - 3.3 V showed a repeating sawtooth pattern with a maximum amplitude of 2 mV. This error is indicative of the differential non-linearity, and can only be corrected using techniques like sliding scale. Truncation of 2 LSBs could suppress the DNL. Each channel of the 1024 bin histogram generated by the MCA is allocated 4 Bytes which correspond to over 4 billion counts per channel, and an overflow event is very unlikely to occur.

Both the designs, 2014 channel and 4096 channel, are combined on the same PCB, but some components are not wired in the case of the 1024 channel version. The firmware, coded into the micro-controller, takes care of the differences. The 16 bit ADC (U12) is used by the 4096 channel version, truncating four LSBs. The 1024 channel firmware uses the internal ADC of the micro-controller. The 16 bit ADC is not wired in the 1024 channel models of the MCA.

The PCB of the MCA is shown in figure 2.3. It is a double layer board where the analog and digital sections are well separated with their ground planes connected at a single point. The circuit generates the various DC voltages to power the ADC and the op-amps from the USB supply using charge pumps and filters.

The PIC24E contains a 12-bit ADC with 8 channels. The 1024 channel MCA uses one channel to digitize the pulse signal. Other channels are used for various monitoring purposes such as power supply voltages and the voltage of the constant current source present in the alpha spectrometer MCA design. In addition, the PIC24E has various digital communication channels. The I2C channel is used to relay information to a 12-bit DAC (MCP4725) which is used as the threshold setting for the peak sensing circuitry. One UART communication channel is used to connect the MCA to a laptop running the CNSPEC software via a UART-USB bridge.

The MCA also has some additional features implemented for self-testing such as a square wave generator for generating short pulses which can be relayed through a 1pF capacitor to generate test pulses for the pre-amplifier.

2.3 The Firmware

The micro-controller at the heart of the MCA and it handles all the data acquisition and communication requirements. It is programmed to deal with the analog to digital conversion, threshold setting, as well as the communication bridge to a laptop via the UART-USB conversion. The firmware runs a state machine that listens to the commands from the computer, arriving over a USB communication link, while the randomly arriving detector signals are handled by an Interrupt Service Routine (ISR) that operates asynchronously. The single channel MCAs generate the histograms locally, managed by the ISR code itself. The histogram is transferred to the computer in response to a request. Firmware of the dual input version buffers the result of each digitization along with a time stamp and transfers it to the computer on request. The analysis, like looking for coincident arrival of signals on both the detectors, are done by the software using the timestamp information.

Firmware is coded in C language using the MPLAB-X IDE, available from Microchip Inc., for their PIC processors used in this MCA. The code is compiled using the C compiler (GCC from the GNU project), and uploaded using PicKit3, a proprietary tool created by Microchip Inc. for uploading code to their micro-controllers. We have used a PIC24E series micro-controller which is equipped with 32kB of RAM that is sufficient to store a 1024 word array for the spectrum where each word is 4 bytes. The PIC24E operates using a 12MHz external oscillator whose frequency is multiplied using Phase locked loop

circuits to generate an operating frequency of 128MHz. The clock speed is half of this, 64 MHz, implying a single cycle operation takes approximately 15nS.

2.4 The Software

The code running on the computer side receives data from the micro-controller via the USB interface and performs the data analysis and visualization functions. This software is written in Python programming language, and named CNSPEC. The Python programming language was chosen due to the availability of a wide range of libraries for data analysis and visualization. Python is cross platform, and can be executed on Linux/Windows/MAC. Since an MCA is an integral part of all the spectrometers developed during this research, the software has been designed to support all of them with minor instrument specific tweaks. It can automatically identify the connected device, and adapt the interface accordingly. A screenshot of CNSPEC GUI is shown in figure 2.4.

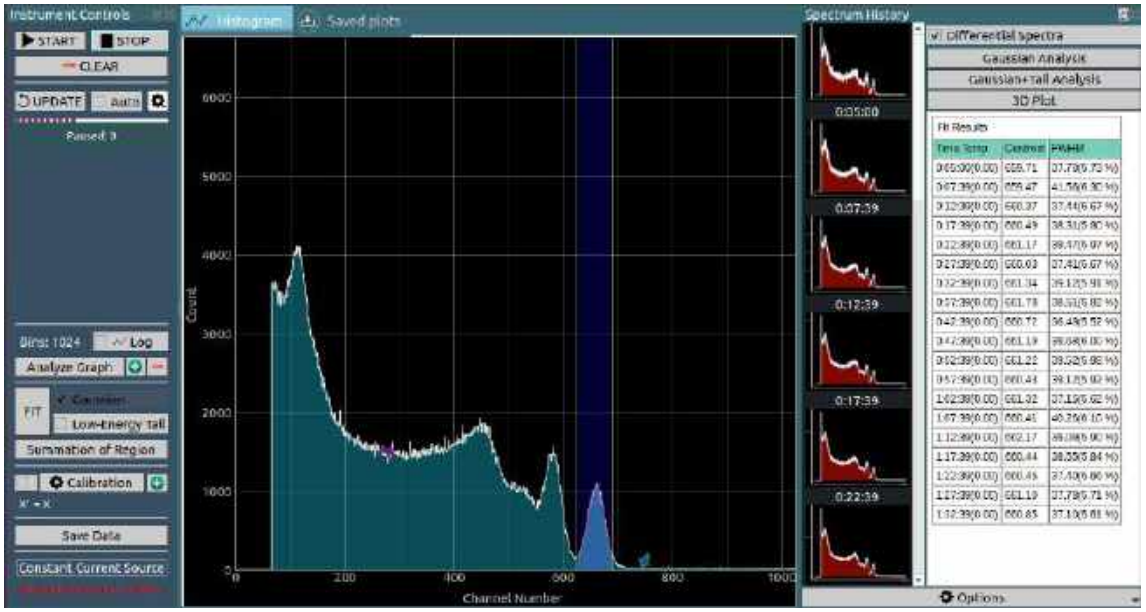

FIGURE 2.4: A screenshot of CNSpec. Shows acquisition of a ^{60}Co spectrum to study the temperature stability of the Gamma Spectrometer.

The following is a summary of the software and its salient features.

- Compatible with the Alpha Spectrometer, Gamma Spectrometer, standalone Multi Channel Analyzers, and the Gamma-Gamma Coincidence setup.

- It implements algorithms for curve fitting for extraction of centroids, half-lives, and drifts.
- Utilities for automatic data analysis at periodic intervals for purposes such as half life estimation in also a part of this.
- Visualization libraries for generating surface plots are also included.
- Has been open sourced and made available on Github.

A complete description of the software is documented in a separate chapter6 owing to its complexity and versatility which spans several different instruments developed during this research as well as their analysis and visualization requirements.

2.5 Linearity and Dead time Measurements

The various stages involved in interpreting the signals from a detector and generating a final spectrum have their own inherent offset and gain variations. It is therefore necessary to test the linearity of the instrument, not the MCA alone, across its full input range in order to properly understand whether one needs a single point calibration(Gain correction only), or a two point calibration (Gain and offset correction), or a polynomial correction (if the gain is not constant across the whole range).

The following parameters affect the digitized output corresponding to a given detector output.

- Offset and gain errors: Op-amps used in the pre-amplifier and shaping amplifiers have varying levels of offsets. Resistors used in the circuits have a tolerance of 1% , and when used in amplifier circuits, a corresponding error in the gain will be introduced.
- Pole-zero correction: The capacitors used in the CR-RC shaping circuits also have a 5% tolerance which can affect the shape of the output pulse. Each unit has to be inspected for undershoots in the shaping amplifier output and it should be corrected.

- Stability of the voltage reference for the ADC : The 3.3V reference chosen has a claimed 50ppm/C temperature stability. Within several degrees of change in temperature, contribution from this is smaller than the MCA resolution.
- Differential non-linearity of the ADC : This has already been discussed in detail, and it is solved by truncating several LSBs of the ADC.

Linearity tests were carried out using a pulse generator (Model PB-5 from BNC Inc.). A pulse frequency of 200Hz was set, and pulses of sequentially increasing heights were injected into the pre-amplifier via a charge terminator for fixed intervals. The series of resultant peaks from the Multi Channel Analyzer were used to check the linearity of the entire instrument excluding the detector as shown in Figure 2.5. After linearly fitting the input pulse heights as a function of their measured peak centroid channels , we found a maximum non-linearity of 0.6%.

To calculate electronic dead-time, the pulse frequency was systematically increased till a drastic mismatch in the measured and incident count rate occurred. This limit is reached when the shaping amplifier signal does not have enough time to restore to the baseline before the next pulse is incident, and as a result, rejects the next pulse. The difference in measured and applied count rate stayed within a 1% error until a frequency of 58 kHz was crossed, and we thus estimate an electronic dead time of 17.2 μs. Beyond 58 kHz, the count rate dropped precipitously as expected and was observed using an oscilloscope.

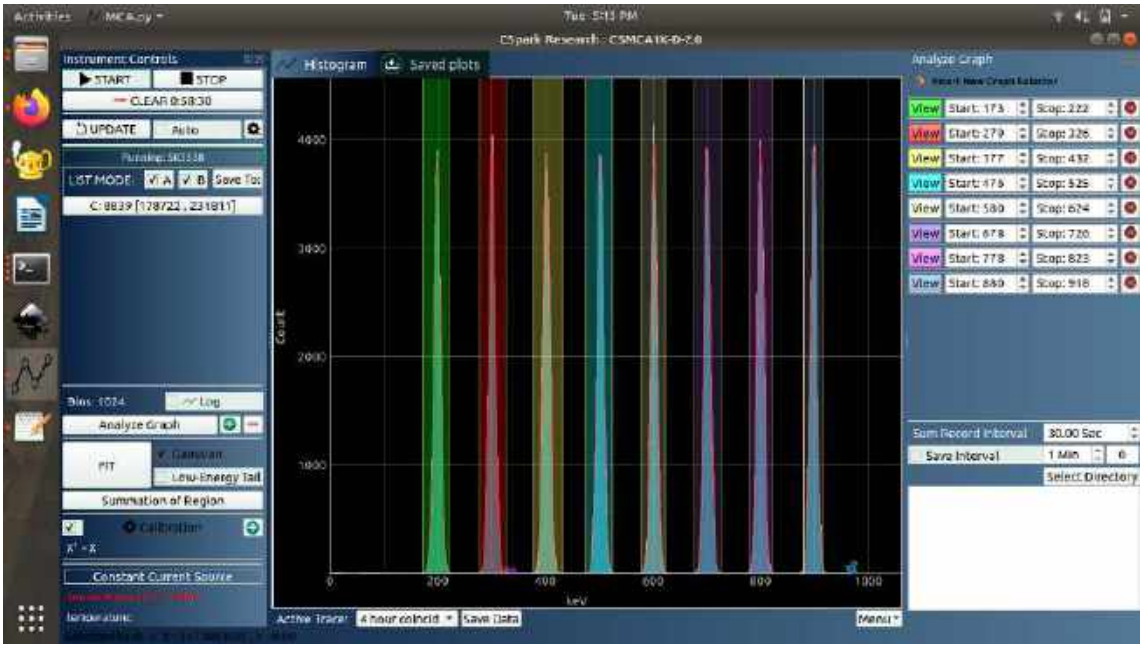

FIGURE 2.5: Results from Linearity testing. Pulses of varying heights were injected into the spectrometer electronics using a charge terminator, and the instrument's linearity was tested in the full range.

CHAPTER 3

Alpha Particle Energy Spectrometer

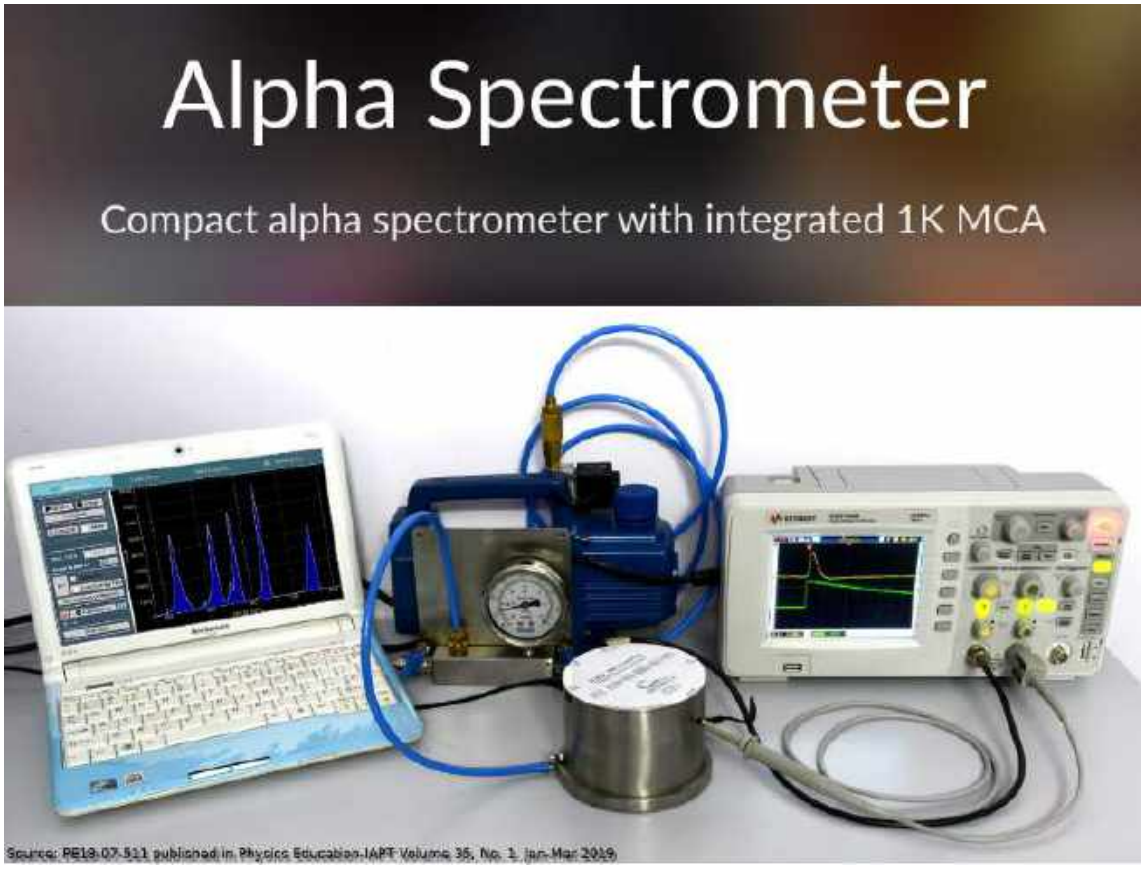

Publications

Title	Journal	Author(s)
Measurement Model of an Alpha Spectrometer for Advanced Undergraduate Laboratories	Physics Education-IAPT Volume 35: No 1. Jan-Mar 2019	Jithin B.P. , V.V.V. Satyanarayana, Swapna Gora, O.S.K.S Sastri & Ajith B.P.
Alpha Spectrum of 212-Bi Source Prepared using Electrolysis of Non-Enriched ThNO3 Salt	Physics Education-IAPT Volume 35: No. 1. Jan-Mar 2019	Swapna Gora, B.P. Jithin, V.V.V. Satyanarayana, O.S.K.S Sastri and B.P Ajith

FIGURE 3.1: Publications pertaining to the Alpha Spectrometer. It was featured on the cover of the Jan-Mar 2019 edition of the IAPT Physics Education journal.

3.1 Introduction

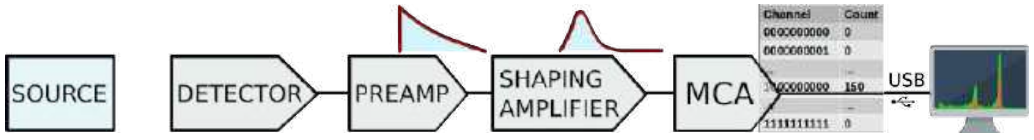

FIGURE 3.2: Schematic diagram for the alpha spectrometer

The building blocks of a radiation detection system in general has already been discussed in the introductory chapter, along with an overview of the alpha spectrometer. This section delves deeper into the development process of the Alpha Spectrometer, and the considerations followed during the design process. The building blocks of the developed system are shown as a flow diagram in figure 3.2.

Alpha particles travelling through air lose energy by colliding with the air molecules. This scattering phenomenon necessitates that, for energy measurement applications, the detector section must be kept inside a vacuum chamber wherein the presence of air can be minimized. Since the equipment is meant for educational purpose, it is also desirable to examine the output of each signal processing stage using an oscilloscope. Considering

these factors, it may appear that one can design the system as independent blocks connected by cables carrying signals from one stage to another, but such a system will be bulky and assembling and powering them will demand some amount of skill. If not chosen properly, the quality of the interconnecting cables could affect the reliability of the system. The cost considerations and our preference for a compact system also prevented us from taking such a route. The final design optimized the desired features within the technological and budgetary constraints. The following sections explain our approach to the design of each subsystem, namely - the Vacuum chamber, Pre-Amplifier, Shaping amplifier, DC Power supplies and the Multi Channel Analyser. Mechanical drawings were made and a 3D image, shown in the figure 3.3, was rendered before proceeding for fabrication.

FIGURE 3.3: Rendered image of the Alpha Spectrometer showing various components.

3.2 The Vacuum Chamber

We started with the design of the vacuum chamber because it's dimensions impose some constraints on the design of the other components. Stainless steel (grade 304) was chosen for it's mechanical and vacuum properties, also the chamber should be opaque due to the sensitivity of the detector to light photons. A cylindrical shape is chosen to reduce the number of weld joints. Vacuum tight welding requires special skills and a complicated

FIGURE 3.4: Top- Vacuum chamber with the detector and O-ring. Bottom - Base plate of the chamber showing the fixtures to place materials between the source and the detector.

geometry with sharp corners is not advisable. It was decided to have a base plate where the source can be kept on it's flat surface. Materials to be studied can be mounted above the source using fixtures. Threaded blind holes are provided for mounting those fixtures. All these can be handled conveniently because the base plate is accessible from all sides without any obstruction, by removing the top portion. The pumping port is incorporated on the base plate so that the vacuum pipes are not disturbed during a change in the experimental setup. The base plate surface is polished to mirror finish using diamond paste to ensure vacuum tight contact with the O-ring.

The cylindrical chamber is placed above this base plate. The lower edge of the cylindrical chamber has a groove for a Viton (synthetic rubber from Dupond Inc.) O-ring providing the vacuum sealing. The dimensions of the O-ring and the groove are chosen in such a way that not only the vacuum but electrical contact between the two sections are also established. This is a somewhat tricky optimization, a bigger diameter O-ring projecting from the groove guarantees the vacuum but prevents good electrical contact. Still, as a precaution an adjustable screw is provided to make an external electrical contact between the base plate and the chamber. However, it need to be used only if the signal appears noisy due to bad electrical contact. This condition can be easily detected by the excessive counts in the lowest channels of the spectrum.

The detector is mounted on the ceiling of the 30mm deep chamber facing downwards. To some extent, this prevents the detector collecting dust or getting damaged by any inadvertent physical contacts. The chamber is designed to have two compartments, the lower part under vacuum holding the detector and the upper portion housing the electronics. This approach eliminates the need of inter-connecting cables and associated reliability issues and also gives excellent shielding to reduce electrical noise. The detector leads are connected to the top compartment using a wire running through a 4mm diameter ceramic bead, giving a connection with low capacitance. Vacuum sealing of this connector is obtained using the Araldite adhesive and a layer of Loclite EA-1C hysol Epoxy resin having better than 1×10^{-10} mBar l/s leak rates. The top compartment is further partitioned to isolate the analog and digital electronics sections. The chamber has openings for monitoring the Pre-amplifier and Shaping amplifier outputs, for the USB connector and also for a 10mA constant current source output.

3.3 The Detector

Energy resolution, size and cost were the main deciding factors in selecting the alpha detector. Silicon Surface Barrier (SSB) detectors are commonly used for alpha detection and available commercially. The specified energy resolution is about 20eV, for example the A-series SSBs from EG&G Ortec, but they were ruled out due to their high cost (more than US$1000/-).

We have found the planar geometry PN junctions as an affordable option to detect alpha particles. PN junctions having an area up to 10mmx10mm are available commercially. We have tested products from several vendors but some were not suitable for alpha detection due to their high dark current values, increasing the noise level. After several trials we could achieve 70eV energy resolution, for the 5.486 MeV peak of ^{241}Am alpha source, using a 10mmx100mm PN junction. The model that we used is having junction capacitance of around 150pF at a bias voltage of 10 volts.

The performance of the PN junction as a detector depends on the applied reverse bias voltage. The thickness of the depletion region increases with the bias voltage. Increased thickness of the depletion layer results in lower capacitance and hence a lower noise level. We have restricted the bias voltage to 10 volts due to the following reasons. Measurements showed that increasing beyond that level did not reduce the noise further, and the thickness of the depletion region at this voltage is found to be sufficient to stop alpha particles up to 9 MeV. Another reason was to avoid the extra circuits needed to generate higher voltages from the USB supply voltage of 5 volts.

The alpha particles falling on the edge of the detector may not result in a full charge collection, and the result would be reduced energy resolution. This was remedied by placing an 8 mm diameter circular aperture in front of the detector. The aperture is actually a printed circuit board that also acts as a holder for the PN junction detector. Small area detectors provide finer resolution, but lower count rates due to solid angle limitations. Large area detectors are suitable for weak sources due to higher collection efficiency, but their high capacitance values reduces signal strength which results in a poorer signal to noise ratio. The geometry should be selected depending upon the application.

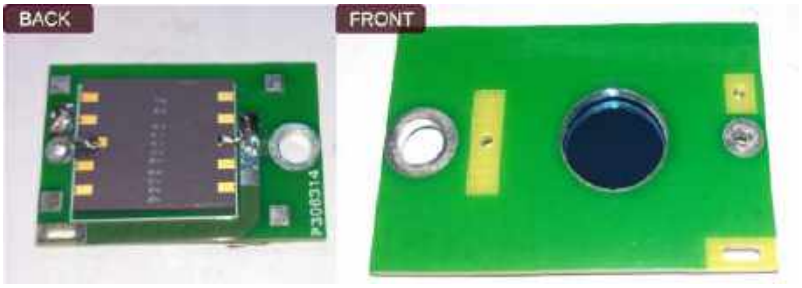

FIGURE 3.5: The Detector mounted on the PCB which serves as a support and also as a collimator

3.4 The Pre-Amplifier

The function of the pre-amplifier is to collect the charge generated inside the detector by the incident radiation and generate a voltage output. The commercially available models like ORTEC 142 series [34] are routinely used charge sensitive pre-amplifiers. Different pre-amplifier schematics have been tested during this work, and the best noise performance so far has been obtained from a combination of a current feedback Op-amp, and a FET as shown in the figure 3.6.

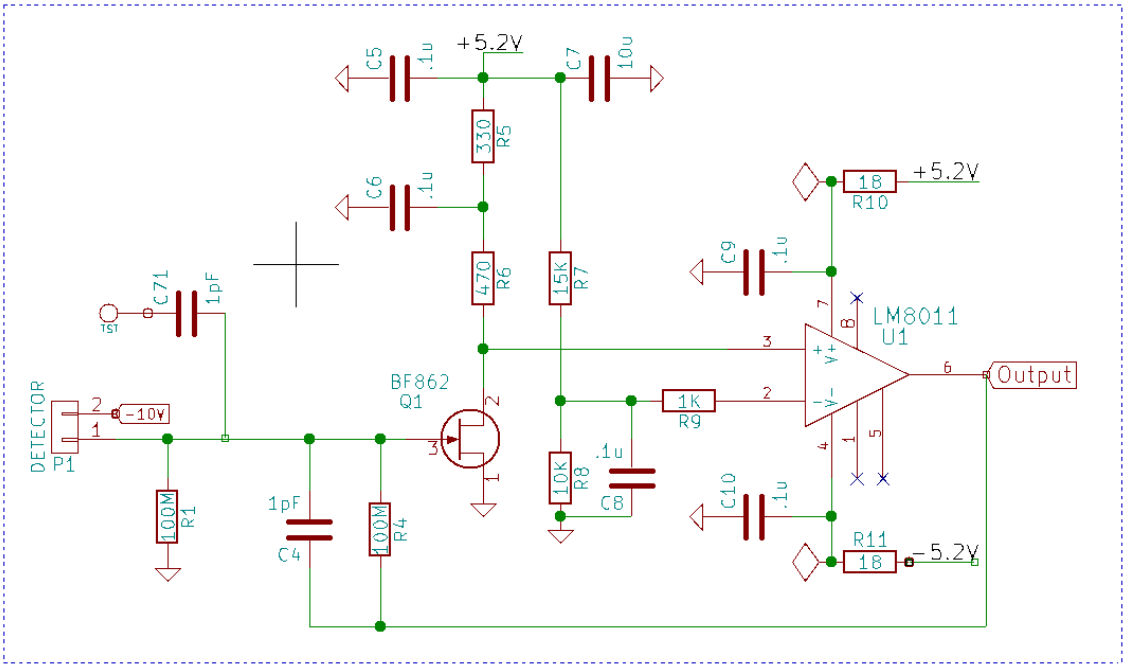

FIGURE 3.6: Circuit Schematic of the Pre-Amplifier

The preamplifier rise times are determined by the detector capacitance and input impedance of the FET, and is around 50nS. The fall time and gain is the function of the feedback RC , and is tuned to approximately 100uS, thereby giving it a distinct sawtooth appearance..

The DC operating point is set by the potential divider formed by the resistors R7 and R8. Any charge arriving at the gate of the FET results in a current through it's Source-Drain path and the voltage at the non-inverting terminal of the op-amp changes accordingly. The feedback is provided by a 1pF capacitor and a 100 MΩ resistor in parallel. The RC value decides the gain, noise level and the fall time of the output pulse. In this design the detector is connected between the bias supply and the input of the amplifier. Configurations where the detector connected to ground were implemented first but they were replaced due to the reduced noise levels of this design.

The same configuration has also been used, with additional gain stages, for amplifying signals in the gamma spectrometer described in the next chapter.

3.5 The Shaping Amplifier

The basic function of the shaping amplifier is to convert the pre-amplifier output pulse into a shape that is suitable for digitzation. It also improves the signal to noise ratio by filtering out the high frequency noise. The long tail of the pre-amplifier output also is reduced by RC differentiation, thus reducing the overlapping of signals from two consecutive events. There are several commercial modules available for this purpose, like the EG&G model 570 Spectroscopy amplifier. Most of them incorporate a lot of features like adjustable gain and shaping time, polarity selection etc. but they are bulky and expensive. Our objective was to develop a compact and inexpensive one that satisfies the energy resolution requirement. Since the detector choice is fixed, there is no need to change the shaping time. The gain is set to give a full scale reading for 10 MeV alpha particle. A circuit schematic of the shaping amplifier is given below and the features are explained with reference to it.

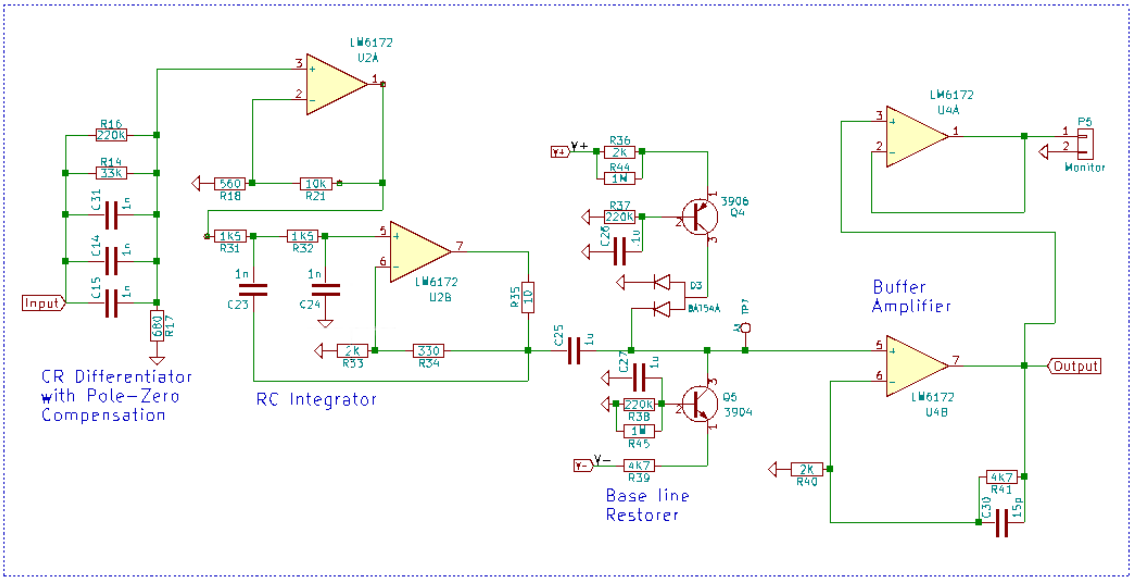

FIGURE 3.7: Circuit Schematic of the Shaping Amplifier

In order to measure the energy of the alpha particles, one must accurately determine the maximum height of the pulses from the detector output which is proportional to it. However, we must first alter the shape to a more gradual Gaussian-like appearance for proper digitization. The shaping amplifier circuitry's function is to do this precisely, and the width is chosen based on the capabilities of the measurement equipment further down the line. An FWHM of a few microseconds is typical.

The input to the shaping amplifier is a fast rising and slowly falling positive pulse. The three 1pF capacitors (C14,C15,C31) in parallel and the 680 Ohm resistor (R17) differentiates the input signal. After that it is buffered and integrated. This simple CR-RC circuit produces an undershoot as the amplifier pulse attempts to return to zero. The problem can be alleviated by use of a pole-zero cancellation network. The Pole-zero compensation resistor is placed in parallel with the capacitor and it can be adjusted to cancel the undershoot. The common practice is to use a variable resistor but we have found out the required values by trial and error and used fixed value resistors, R14 and R16 in parallel. All spectroscopy amplifiers incorporate a pole-zero compensation circuit (the term pole-zero comes from the mathematical representation of the circuit, the resistor 'cancels' a pole in the expression).

Another important section is the baseline restorer. Since the energy measurement is done by measuring the pulse height it is important to prevent any shift in the baseline. In

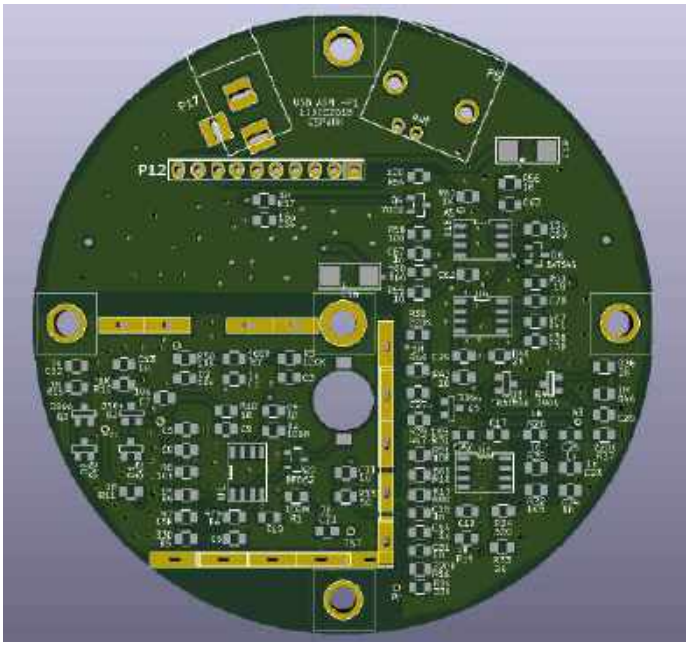

FIGURE 3.8: Alpha Spectrometer bottom side PCB. The analog sections of the electronics are implemented on this.

the absence of any signal, the two arms of this circuit (D3 and Q5) makes the voltage at the input of the next section zero. Finally, the signal is again buffered before feeding to the MCA input. Another buffered output is provided on a BNC socket for external monitoring with an oscilloscope or a separate MCA. The maximum height of output pulses has a range of 0-3.3V, where 0 indicates the absence of a pulse, and 3.3V indicates an incident alpha particle with energy close to the maximum permissible value of 10MeV. The peak value of this pulse is to be sampled and digitized. The shaping time is configured to be close to 3uS using the CR-RC filter circuit and the output available for monitoring shares the same width. The linearity of gain is an important consideration, gain should be same at all signal levels. The errors that can arise from the gain compression of the Op-amps is minimised by keeping the maximum output signal much smaller than the supply voltage.

The pre-amplifier and shaping amplifier circuits are implemented on the same PCB, circular in shape to match the vacuum chamber, shown in figure 3.8. The pre-amplifier part has provision for extra shielding using copper foils. A BNC connector provides monitoring the shaping amplifier output while the pre-amplifier output can be monitored using oscilloscope probe. It is not advisable to connect the monitoring probe during data acquisition, to prevent injection of noise. The typical signal outputs are shown in figure 3.9

FIGURE 3.9: Oscilloscope displaying signals from the pre-amplifier(green trace) and the shaping amplifier(yellow trace).

3.6 Power Supply Module

The electronics circuits of the alpha spectrometer requires a range of DC power supplies,as listed below.

1. +9V and -9V for the operational amplifiers
2. +5V and -5V for the threshold detector
3. +3.3V for powering the micro-controller
4. -10V for biasing the detector

All required voltages are generated from the USB power supply of 5 Volts by means of charge pumps followed by low pass filters for removing the switching noise. The ICs used are TC7660 for inverting voltages, and 1240A for doubling voltages. Both these ICs are connected to 100uF Tantalum capacitors which have low ESR essential for the fast switching speeds of approximately 6 KHz. 10Ω-100uF RC filters are attached to all outputs to filter any residual ripples. The schematic of the final version is shown in figure 3.10.

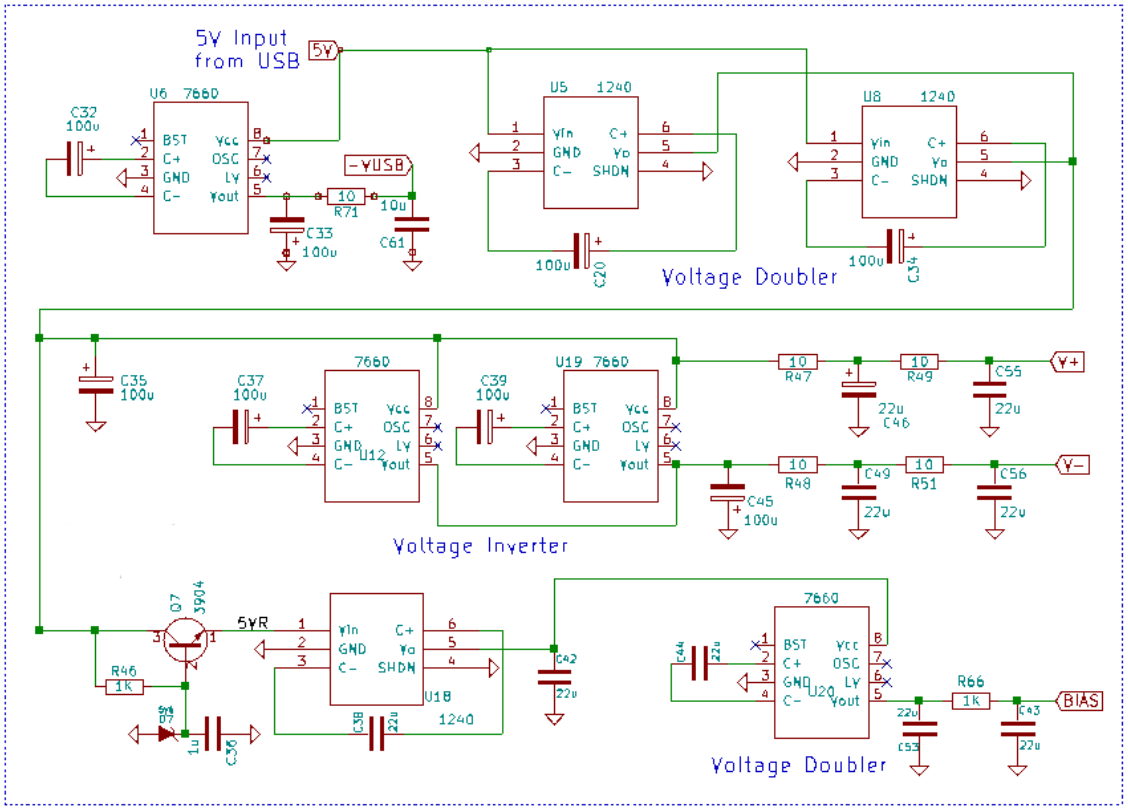

FIGURE 3.10: Circuit schematic of the DC power supply module. From the 5V USB input, this circuit generates the $\pm 9V$, -5V and -10V outputs using charge pumps and RC filters.

3.7 Multi Channel Analyser

The details of the MCA are already explained in the previous chapter. The same design is incorporated into the alpha spectrometer in a different form factor. The 16 bit ADC portions are not used.

The MCA and the DC power supply modules are implemented on the same PCB as shown in figure 3.11. A 10 mA constant current source circuit is also provided on the same PCB, for preparing alpha sources from a solution of thorium nitrate by electrolysis.

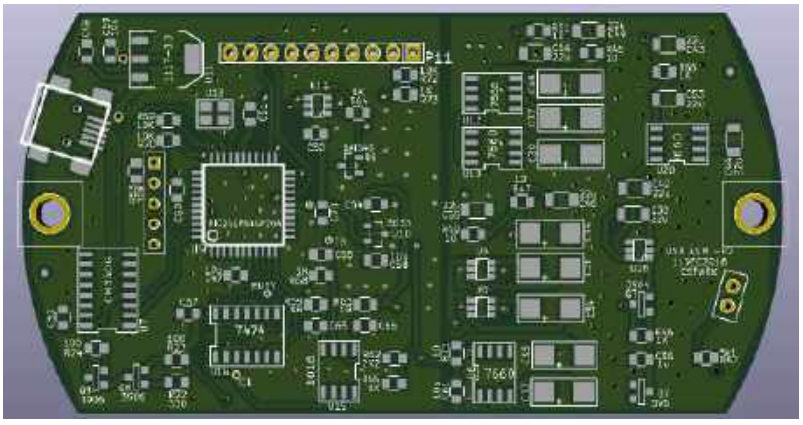

FIGURE 3.11: Alpha spectrometer top side PCB. The MCA, DC power module and the USB interface are implemented on this

FIGURE 3.12: The final assembly of the electronics circuit boards mounted inside the upper part of the cylindrical chamber. The detector mounting inside the vacuum chamber is shown on the top right.

3.8 Pumping System

A small rotary pump capable of creating a vacuum down to 1 mbar is sufficient to reduce scattering by air molecules to a negligible level. Since the chamber volume is only around

half a litre, a 50 LPM pump commonly available for evacuating refrigerants from air-conditioning systems before refilling them was chosen. Since it caters to a wide market, the costs are low. The electronic vacuum gauges and vales were found to be very expensive and we decided to use simple dial gauges and ball valves available in the local market. A stainless steel manifold with two valves and one dial gauge was designed to meet the requirements. Threaded holes were made on the manifold to fix the gauge and valves as shown in the figure 3.13. The arrangement is sufficient for the vacuum required to study alpha particles at this energy resolution. Under the level of vacuum achieved, changing the distance between the source and the detector did not change the measured energy.

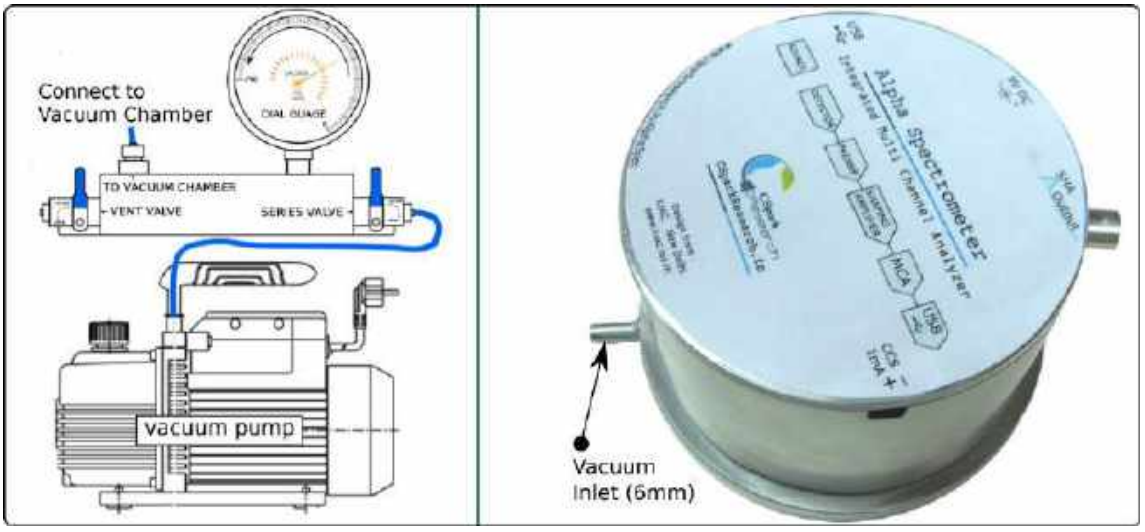

FIGURE 3.13: The Vacuum system schematic.

The inlet of the manifold is connected to the rotary pump via a series valve. The chamber is connected to the manifold. To evacuate the chamber, first the vent valve should be closed and the series valve should be opened slowly. The dial gauge should indicate the change in pressure. After the reading stabilizes experiment can be started. To vent the chamber, close the series valve and gradually open the vent valve. To check for leaks, evacuate the chamber and close the series valve. Without pumping if the vacuum degrades rapidly, it indicates a leak. The O-ring should be checked and vacuum grease should be applied if needed.

3.9 Test Results

The gain of the shaping amplifier was chosen to give a 10 MeV range. This is verified by using the 5,485 MeV alphas from an ^{241}Am enriched source. The energy resolution is measured and the instrument is tested for long term temperature stability. The gain linearity testing is done using the multiple alpha energies from a ^{229}Th enriched source. Further, ^{212}Bi was extracted from thorium nitrate salt, as described in Swapna et al.[4], and its branching ratio as well as half life was reliably estimated using this instrument.

3.9.1 Calibration with ^{241}Am

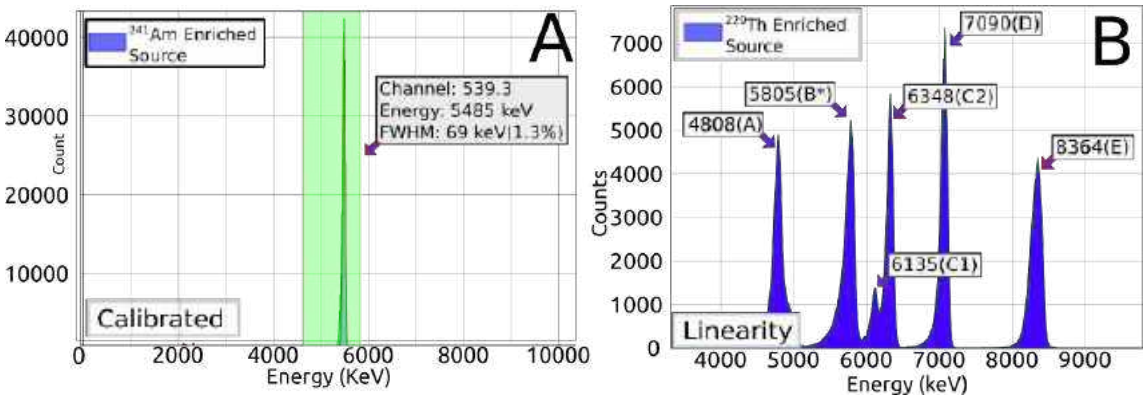

FIGURE 3.14: a) Alpha spectrum of ^{241}Am obtained under 50mBar vacuum the sourced placed 2cm from the detector . b) Spectrum of ^{229}Th with physical conditions identical to (a). [2]

The spectrum obtained by placing ^{241}Am at a distance of 2 cms at a pressure of 50 mBar is shown in Figure3.14(a). Using a least square fitting using a standard Gaussian function, the position of this peak was estimated at 496 channel number. Since the energy of this peak from ^{241}Am is known to be 5485 keV, the following calibration polynomial involving just the slope can be derived

$$Energy = \frac{5485}{496} \times channelnumber \tag{3.1}$$

The FWHM of this peak was found to be 81 keV from the fitting function applied to the calibrated peak. Single point calibration has a major drawback, in not being able to

TABLE 3.1: The decay chain of ^{229}Th showing dominant(Intensity > 5%) alpha energies have been compiled from ENSDF. Peak positions have been identified in Figure 3.14B and are labelled against their $E\alpha$ values. The % errors have also been calculated [2]

Parent	Daughter	$E\alpha$(Actual)	$I\alpha$	$E\alpha$ (Measured)	$\%error$	$t_{\frac{1}{2}}$
^{229}Th	^{225}Ra	4845.3(A) 4814.6	56.2 9.3	4808 -	0.76 -	7340y
^{225}Ra	^{225}Ac	β	-			14d
^{225}Ac	^{221}Fr	5830 (B*)(5817) 5732 5790.6 5792.5	50.7 8 8.6 18.1	5805	0.25	10d
^{221}Fr	^{217}At	6126.3(C1) 6341(C2)	15.1 83.4	6135 6348	0.14 0.11	4.9m2
^{217}At	^{213}Bi	7066.9(D)	99.9	7090	0.32	32.3ms
^{213}Bi	^{209}Tl	5869	93			45.59m
^{213}Bi	^{213}Po	β	-			45.59m
^{213}Po	^{209}Pb	8375.9(E)	100	8364	0.143	4.2us
^{209}Tl	^{209}Pb	β	-			2.2m7
^{209}Pb	^{209}Bi	β	-			3.25h14

account for offset errors as detailed in the previous section. This can be sorted with multi point calibration. We have used ^{229}Th enriched source for this purpose. But it can also be done using the two distinct peaks of ^{212}Bi, that can be prepared from thorium nitrate.

3.9.2 Linearity tests with single point calibration

In order to check if the calibration remains valid over the entire range of 10MeV, it is essential to use a source with multiple energy emissions spanning the range. ^{229}Th is a good source since it has alpha decay products with multiple energies from 4Mev to 8.7MeV as shown in Figure Figure3.14(b). The relevant emission energies are listed in Table 3.1 .

A ^{229}Th disc source was placed at a distance of 20 mm from the photodiode, and the data was recorded under vacuum. The Peak labelled $B*$ in Figure 3.14 corresponds to four values shown in Table 3.1. Their promiximity to each other and the limited resolution

of our instrument cause them to be recorded as a single peak, and we have therefore considered a weighted average of 5817keV to represent all four.

The peaks correspond to their expected energies with an accuracy better than 1%, sufficient for educational purposes.

3.9.3 Linearity testing with 2 point calibration

Two distinct peaks from the spectrum of ^{229}Th were chosen to calibrate the spectrum including offset correction. In Figure 3.15, ^{221}Fr and ^{217}At marked A and B have known energies of 6341kev and 7066.9keV, and Gaussian fitting of their peaks revealed centroids at 572.8 and 639.9. The corresponding calibration polynomial is 10.83 x + 137.30.

Decay energy data from commonly used sources have been included in the software, and a feature has been implemented to show their positions in the spectrum so that users can identify isotopes more quickly. In Figure 3.15, these markers have been enabled, and the positions of the peaks after calibration has been applied can be viewed against the actual positions for comparison.

TABLE 3.2: Linearity analysis using 2 point calibration with ^{229}Th source. Calibration has been applied using the decay peaks of the highlighted rows, and the % errors are calculated for the remaining peaks.

Parent	Daughter	$E\alpha$(Actual)	$E\alpha$ (Measured)	$\%error$
^{229}Th	^{225}Ra	4845.3(A) 4814.6		0.27 -
^{225}Ac	^{221}Fr	5830 (B*)(5817) 5732 5790.6 5792.5	5808.2	0.15
^{221}Fr	^{217}At	6126.3(C1)	6134.5	0.13
^{221}Fr	^{217}At	6341(C2)	-	-
^{217}At	^{213}Bi	7066.9(D)	7090	0.32
^{213}Bi	^{209}Tl	5869	-	-
^{213}Po	^{209}Pb	8375.9(E)	8314	0.74

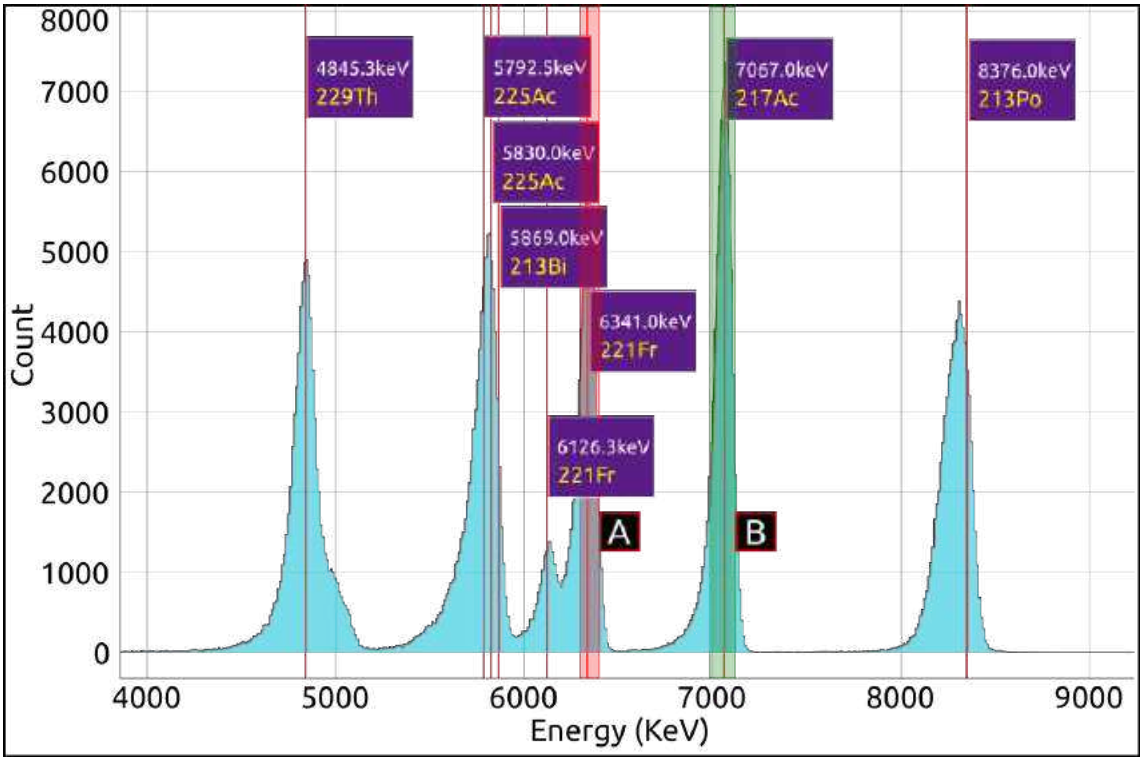

FIGURE 3.15: 229Th spectrum calibrated with known energies of 221Fr(A) and 217At(B) decays. Energy markers for daughter products of the 229Th chain have been enabled for visualization purposes.

3.9.4 Testing with non-enriched sources

One of the difficulties in teaching nuclear physics in high school or college, is the limited availability and tight regulations on sources, and high prices of detectors. It happens because of the special care for handling and storage, being subject to a high level of regulation in some countries. These difficulties can be overcome by using naturally available sources, such as ^{232}Th progeny, present in lantern mantles and in thoriated welding rods used extensively in industries, or the measurement of ^{220}Rn half-life collected in a suitable adsorbent material from the emanation of the lantern mantles, or naturally radioactive sands. These practices will enable wide access to either college or high-school didactic laboratories, and has the potential for the development of new teaching activities for nuclear physics.

The extraction procedure of ^{212}Bi from ^{232}Th Nitrate salt solution via electrolysis immensely reduces waste generation[4]. The short half life of ^{212}Bi provides excellent teaching value, and also can be safely disposed within a day after ensuring that the activity has depleted to negligible levels. The solution can be reused after storing it for several months to allow regeneration of depleted isotopes, however this must handled and stored carefully.

This section summarises work carried out by Swapna et al.[4] using this alpha spectrometer. Key developments involve preparation of an un-enriched source of ^{212}Bi from Thorium Nitrate salt extracted via electrolysis. They report on the branching ratio, as well as half-life calculations of this isotope.

Thorium nitrate salt is commercially available and after several months of storage it will have the decay chain products of ^{232}Th. The decay series results in alpha, beta and gamma radiation. For usage as an alpha source, an electrolytic process has been fine tuned in order to extract one of its daughter products, ^{212}Bi, in a thin film form. This prepared source has then been used in a variety of experiments with very interesting results which are otherwise difficult to carry out using commercial sources due to the short half life of ^{212}Bi.

The publications include spectra acquired from ^{232}Th nitrate salt under different conditions. The results validate the usability of the system for undergraduate laboratories. Some of the data is shown in fig 3.16 and 3.17.

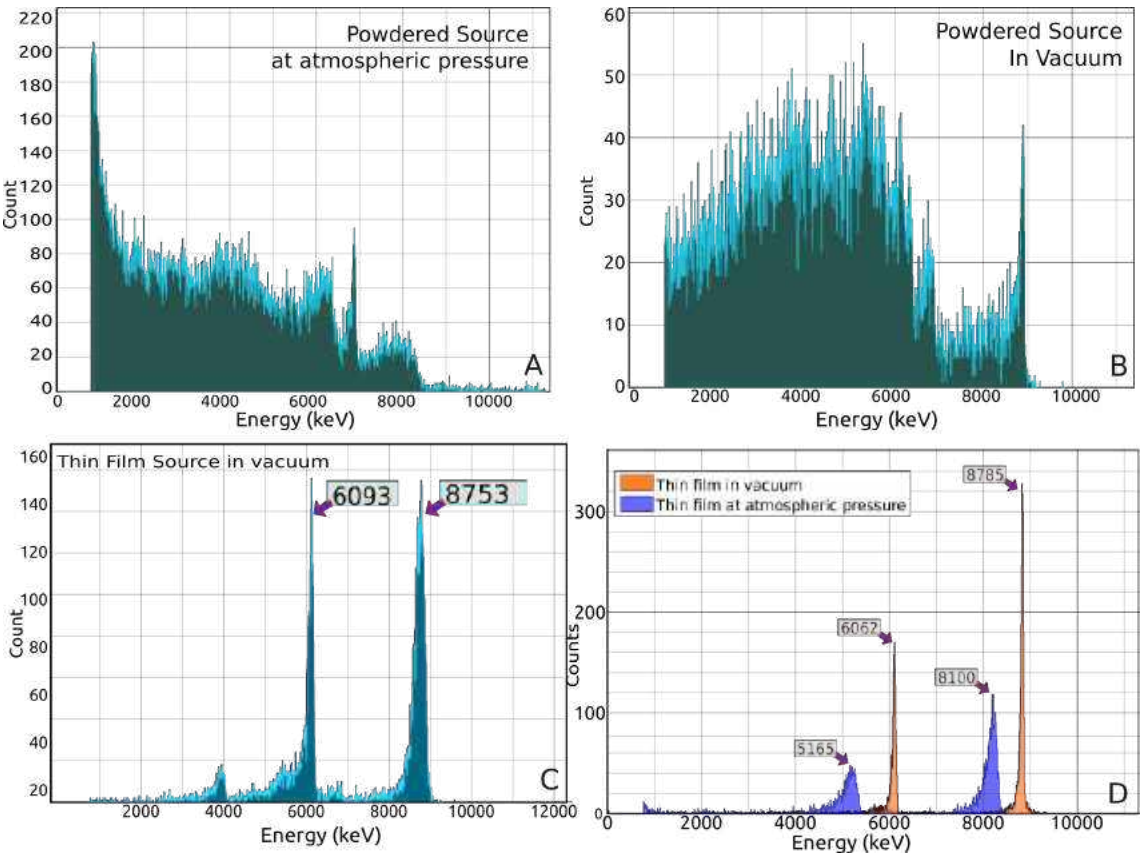

FIGURE 3.16: Spectrum from radioactive sources with different attenuating conditions a) Alpha spectrum of ThNO3 salt; b) The same sample recorded under vacuum; c) ^{212}Bi thin film spectrum under vacuum; d) Comparison of the ^{212}Bi spectrum obtained under 1 mbar vacuum, and at 1 Bar atmospheric pressure. [Data acquired by Swapna Gora [4]]

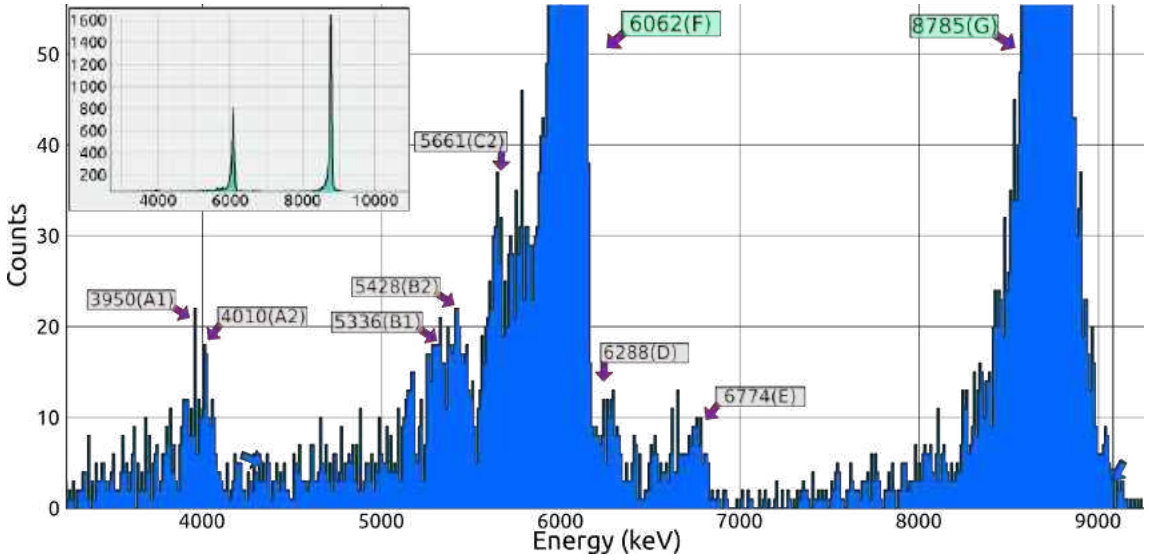

FIGURE 3.17: Spectra showing peaks associated with the alpha decay chain of 232-Thorium [4]

3.9.4.1 Results from ^{212}Bi

In order to extract Bismuth, 3.5gms of Thorium Nitrate($ThNO_3$) salt was dissolved in 5gms of water, and 20mA current was passed via lead foil electrodes for 10 minutes through this solution. This yielded a greyish film on both electrodes. Spectrum from the anode film was recorded. It was noted to contain two distinct peaks with centroids at 6081 keV and 8685 keV as shown in Figure 3.18 after a single point calibration was applied using ^{241}Am. These values corresponded closely with the known energies from the decay chain of ^{212}Bi which are 6062keV and 8785keV [4] with percentage errors of 0.31% and 1.13% respectively, further validating the linearity of the electronics. The higher energy peak formed around 8685keV was used for half-life calculations, and requisite algorithms for exponential fitting was simultaneously implemented in the CNSPEC software. Half-life was determined and reported to be 60.3 minutes with an uncertainty of 2.4 minutes. This agrees with the expected value of 60.5 minutes to an accuracy of 0.33%.

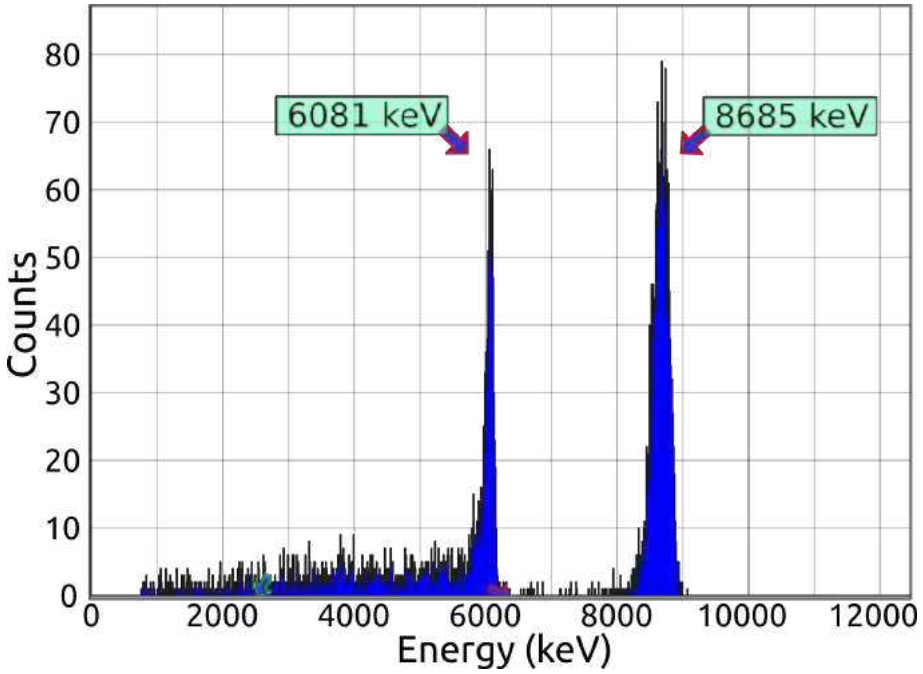

FIGURE 3.18: ^{212}Bi Spectrum

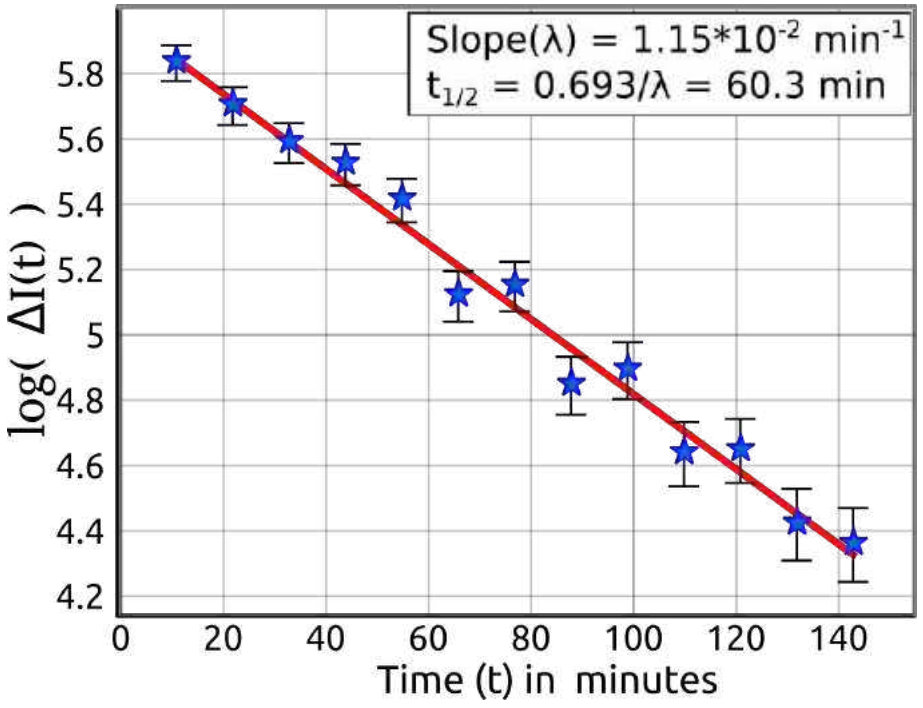

FIGURE 3.19: Activity of ^{212}Bi decreasing as a function of time. The events are in Log base 10 units, and have been used to calculate the decay constant, and subsequently the half life of the isotope

3.10 Array of Alpha Particle Detectors

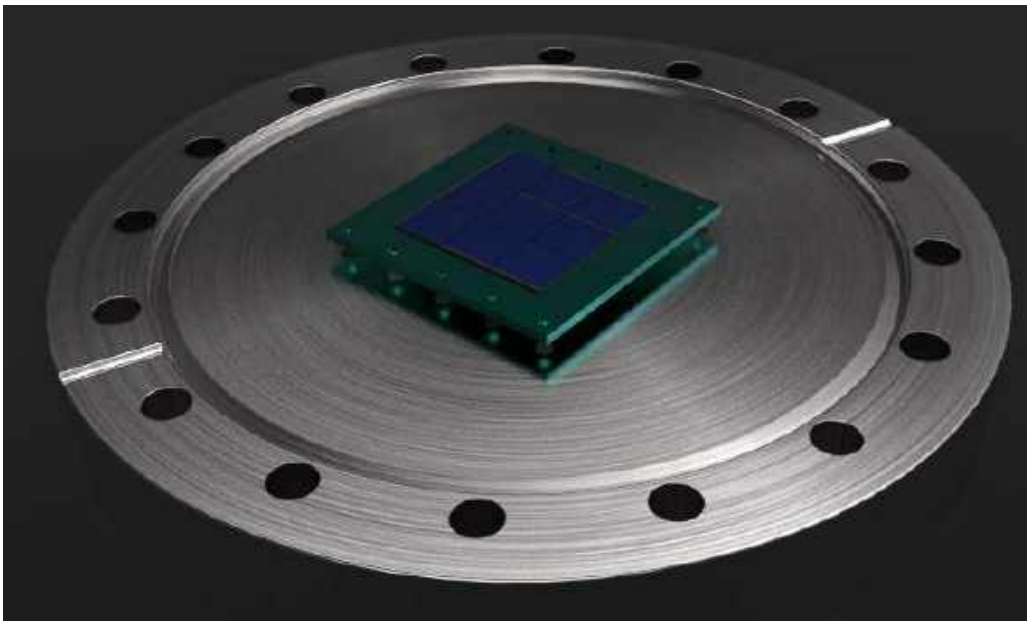

FIGURE 3.20: A 3x3 matrix of alpha detectors mounted on a PCB and fixed on a flange that is part of a vacuum chamber

We have already developed the electronics for an alpha spectrometer. However, the dimension of each detector is 10mmx10mm only, and this is inadequate for capturing radiation from extremely weak and large area sources such as soil samples. Attempts were made to wire multiple detectors in parallel, but the increased capacitance increased the noise and adversely affected the resolution. Up to four detectors were wired in parallel as shown in Figure 3.21. However, even with two detectors, the FWHM increased by a factor of two.

FIGURE 3.21: Four detectors wired in parallel for making large area detectors

A solution for this is to independently develop the processing electronics - preamplifier , shaping amplifier - in order to keep the detectors separate. This configuration can also be used to obtain spatial distribution of incoming radiation. Large area detectors are commercially available, but the price difference is almost a factor of twenty. Detector arrays are also commercially available from vendors such as Hamamatsu, but we have made an attempt to develop the array as well as the electronics ourselves. The challenges lie in making the electronics more compact and simultaneously preventing cross talk between channels.

A prototype setup with nine detectors mounted on a stainless steel KF100 sized flange, that can be mounted on a vacuum chamber with the same sized port, was designed and fabricated. A separate PCB was made for soldering and mounting the detectors. The back-plane of the detectors is used as the signal input, and the thin gold contacts along the edge of the top side are either grounded, or negatively biased depending on the circuit design adopted. The detectors mounted on the flange are shown in figure 3.20

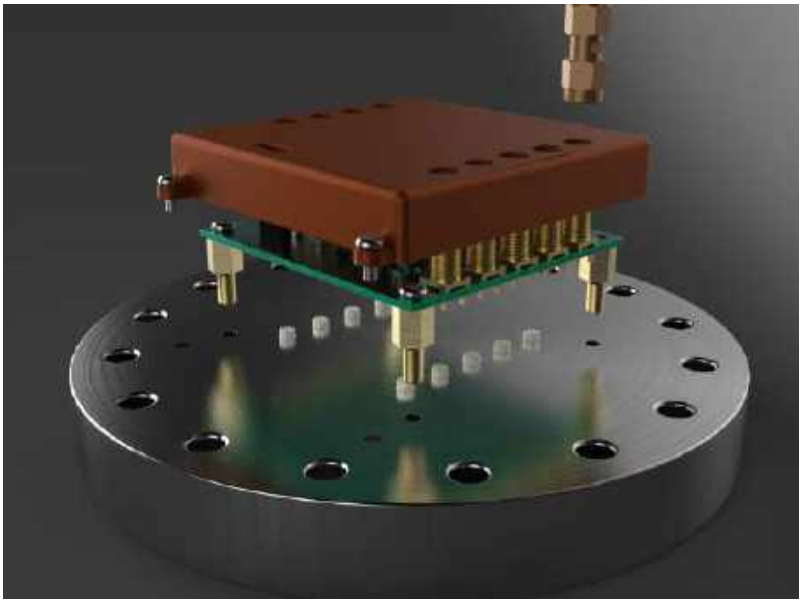

FIGURE 3.22: The pre-amplifier board mounted on the CF100 flange. Render made with CAD software and KiCAD

3.10.1 The Pre-amplifier

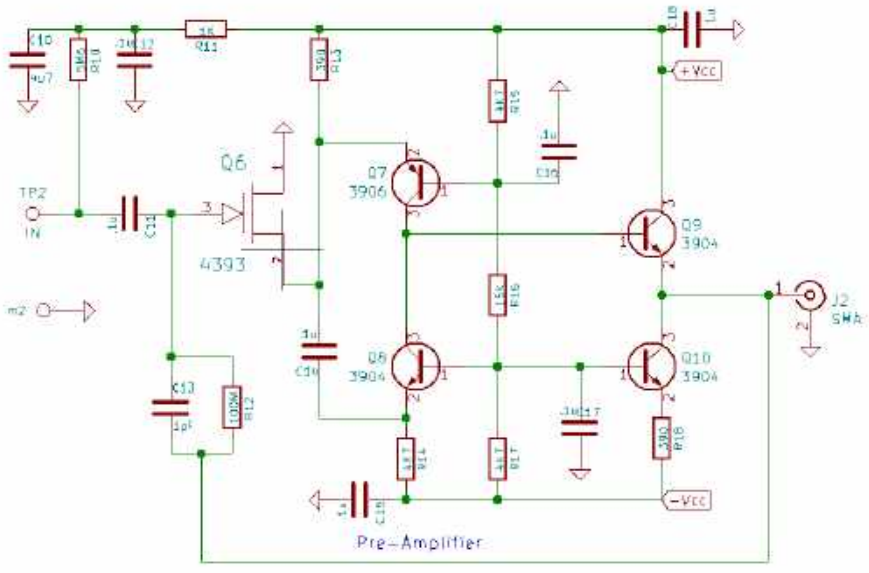

FIGURE 3.23: Schematic for the pre-amplifier. Nine identical units are assembled on the same board, one for each detector. Outputs are available on SMA connectors.

The first pre-amplifier design we used is available In open source hardware [35]. It consists of a MOSFET at the input in cascade with a bipolar junction transistor (BJT) . A 1pF capacitor in the feedback path decides the gain/charge-sensitivity. A high value resistor (typically $100M\Omega$) is connected in parallel to the capacitor. The circuit schematic of a single unit is shown in figure 3.23 and a 3D render of a PCB having nine pre-amplier channels is shown in figure 3.24.

The pre-amplifier should be kept very close to the detector to reduce the noise pickup, and the circuit board was mounted on the other side of the flange, that is outside the chamber and at atmospheric pressure. The connections are made through ceramic beads inserted inside the holes drilled on the flange. Vacuum is secured by sealing the joints with Araldite adhesive and a layer of Loclite EA-1C hysol Epoxy resin with low outgassing properties. The pre-amplifier outputs are made available on SMA connectors for further processing.

Due to the electrical noise sensitive nature of the initial preamplifier design used, we also developed a second board based on the op-amp design used in Gamma spectroscopy and later adopted for alpha spectroscopy which has better noise performance. For this design, the top side contacts of the detectors are wired in parallel and negatively biased at 10 Volts. The back plane is used for tapping the signal.

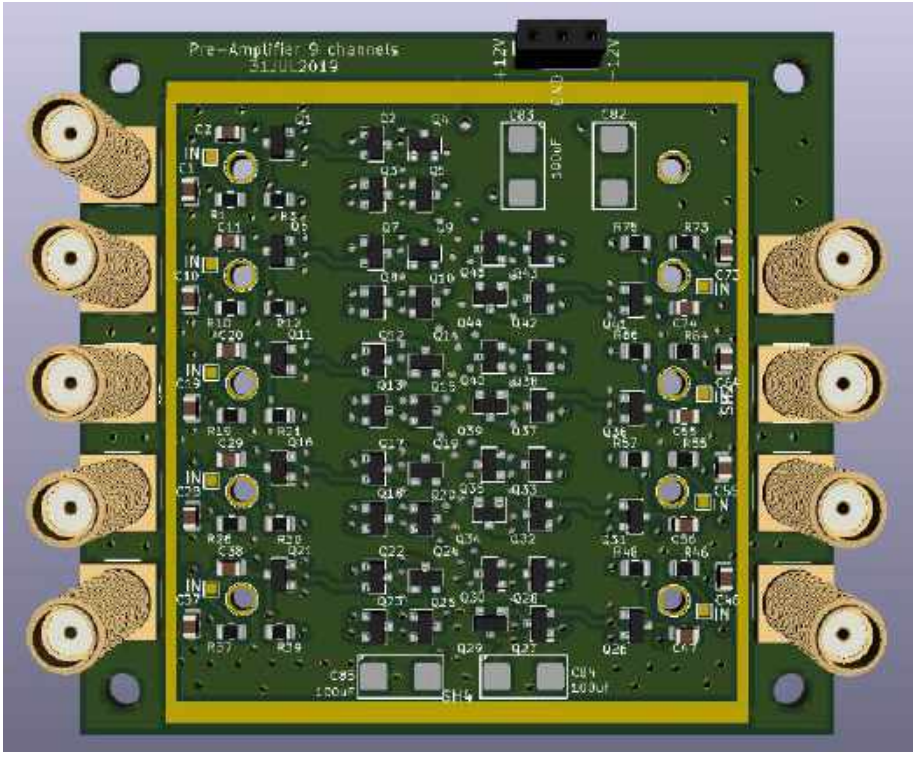

FIGURE 3.24: Schematic for the pre-amplifier. Nine identical units are assembled on the same board, one for each detector.

3.10.2 Electronics testing and Characterisation

One channel from each design was wired and tested. The circuits were tested with a pulser for rise time characterisation. We injected pulses via a charge terminator, and studied the rise time of the preamplifier circuit.

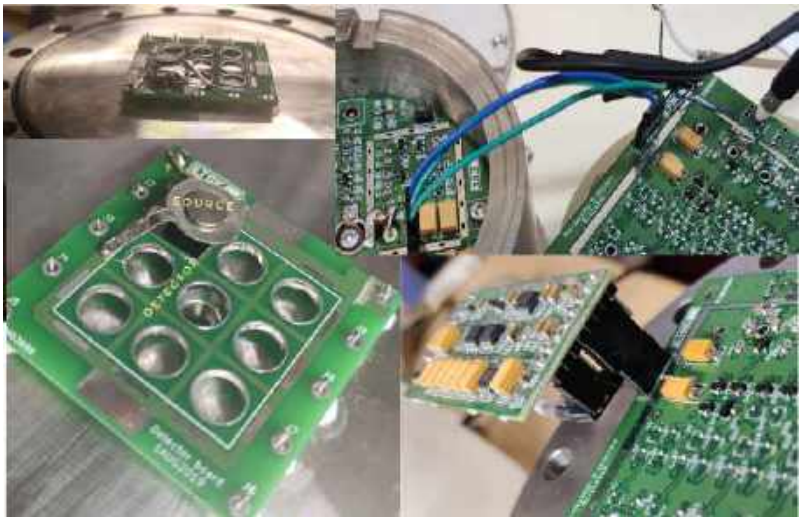

FIGURE 3.25: A single pre-amplifier is wired and tested using a test pulse input. External DC power supplies were used.

FIGURE 3.26: Pre-amplifier testing screenshot from an oscilloscope. The yellow trace shows a series 400mV tall input pulses, and the pink trace is the output signal from the pre-amplifier showing a decay time of $200\mu S$

CHAPTER 4

Gamma Ray Spectrometer

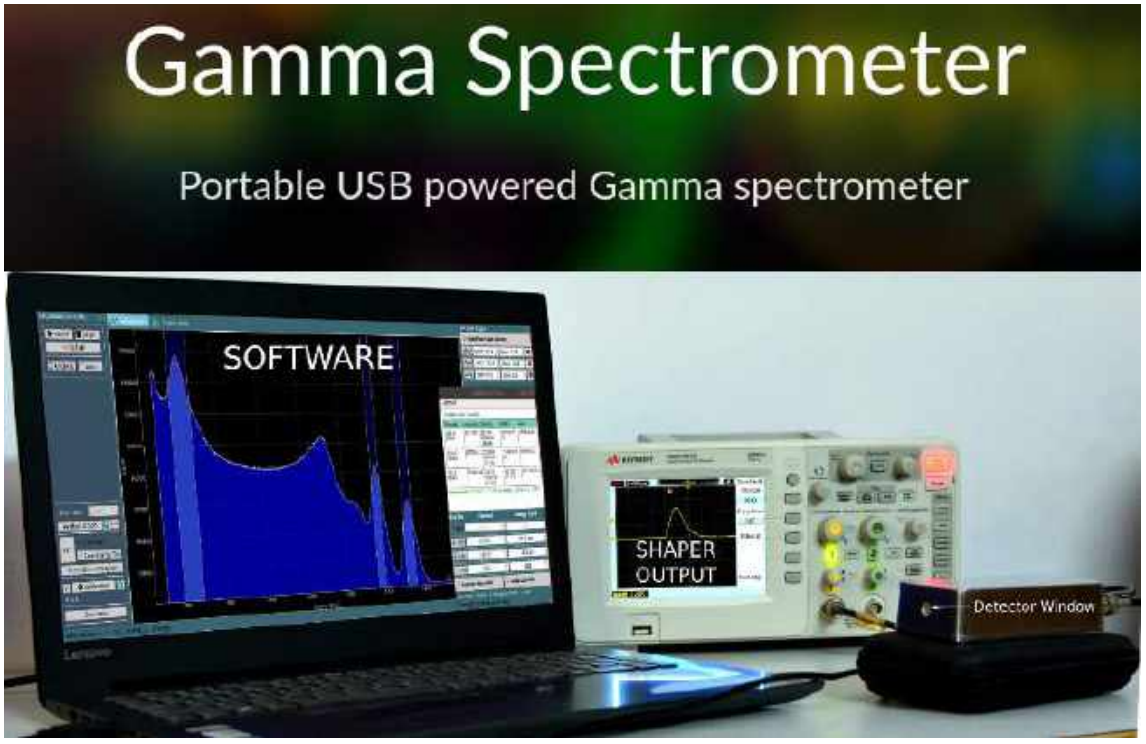

4.1 Introduction

After the successful completion of the Alpha Spectrometer, it was felt that there are several reasons to pursue the same for gamma detection. As per the radiation safety regulations, acquiring enriched alpha sources require trained radiation safety personnel in

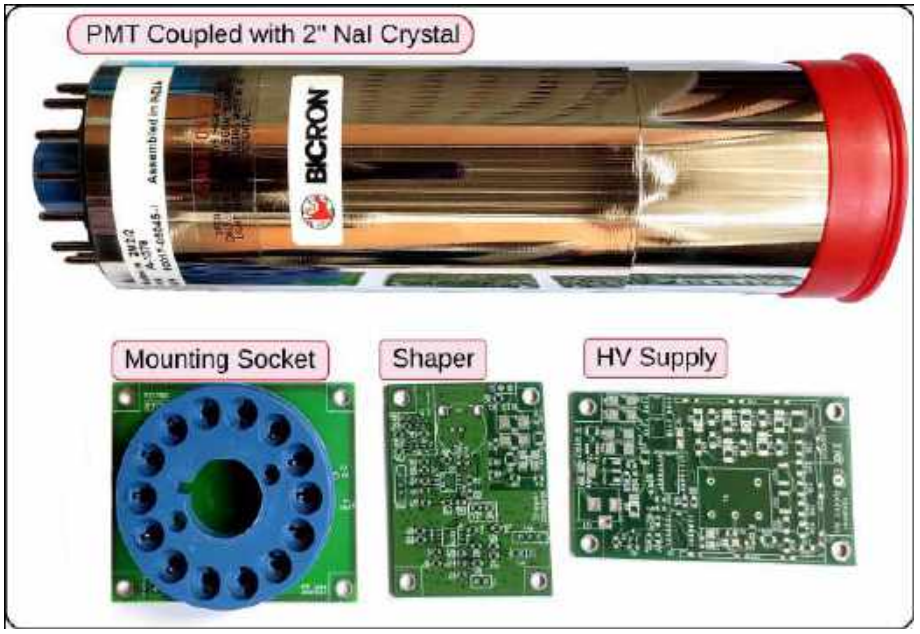

FIGURE 4.1: NaI scintilltion crystal coupled with photo multiplier tube. Circuit boards for the base, shaping amplifier and high voltage are also shown

the laboratory. We could overcome this hurdle by preparing weak sources from thorium nitrate salt and documenting experiments with excellent teaching value using them.

On the other hand, gamma sources are sealed, and the low-intensity ones do not require a person trained in radiation safety to be present. This has enabled a large number of colleges to acquire gamma sources along with basic Geiger-Muller counter setups for their nuclear physics labs. Spectrometry is rarely found because a gamma spectrometer costs several lakhs. An affordable instrument to measure the energy of gamma rays would enable the inclusion of much better experiments in lab courses using their existing sources. Due to the larger penetrating power of gamma rays, a vacuum chamber is not required and this makes the equipment easier to handle. Gamma detection requires a larger volume of detector material but developing big crystals of scintillators or semiconductors is impossible without major facilities and expertise. The better option was to search for cost-effective detectors from commercially available sources and develop the requisite electronics.

4.2 NaI Scintillator with Photo Multiplier Tube

The gamma spectrometers based NaI scintillation crystals coupled with photomultiplier tubes are available from several sources, costing around 5 lakh INR. As part of the initial foray into gamma ray spectroscopy, we procured a 2" NaI crystal coupled with a photomultiplier tube from M/s St.Gobain, manufactured by Bicron. The cost of the detector assembly itself was around 1 Lakh INR. High voltage circuits and necessary adapters were also designed and fabricated in order to develop a gamma spectrometer. The work done in this direction is shown in figure 4.1. We also realised that it is not possible to develop a cost-effective instrument following this method, due to the high cost of the detector itself.

4.3 CsI Scintillator with PN Junction

The high cost of the NaI+PMT detector was the main motivation to look for other options, and one that stood out was a scintillation detector coupled to a planar photo-diode similar to the one used for alpha detection. Given that we had made good progress in digitizing signals from photodiodes, this made much sense. Crystals of CsI scintillation material having different dimensions were procured for testing. They were coupled with the PN junction detectors used for alpha detection.

The main challenge involved in this method is to effectively transfer the photons generated inside the scintillator to the photo-diode, and minimize the two dominant modes of signal losses. One, the generated scintillation photons may escape from all the six faces of the crystal but the detector diode is fixed only to one face. Reflective coating must also be applied on all other five sides to reduce these losses. Second, the optical coupling of the crystal to the photo-diode is also very important. The refractive index of the mating glue should have a value matched closely to the refractive indices of the two materials to prevent losses due to total internal reflection. The detector must also be coated to protect from humidity due to the slightly hygroscopic nature of Cesium Iodide.

The assembled detectors, shown in figure 4.2, were characterized using a ^{60}Co source by measuring the counts obtained in the full energy peak. The results showed that the photo-peak efficiency increases with the volume of the crystal as expected. However,

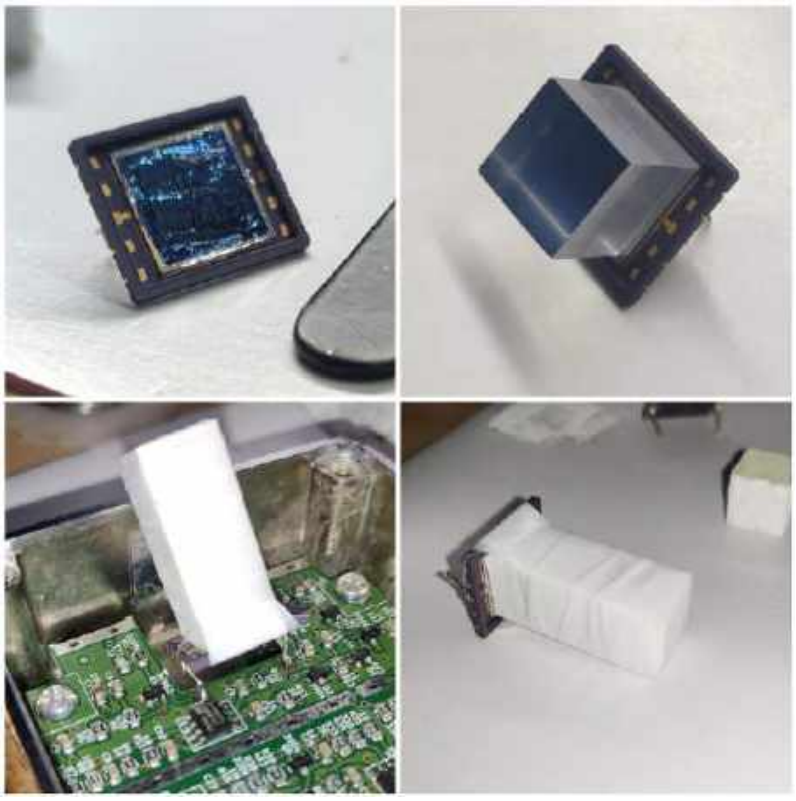

FIGURE 4.2: Fabrication of custom gamma detectors by coupling CsI scintillator crystals to Planar photo-diodes.

crystals with identical volumes also gave slightly different values, due to the variations in the light coupling and the reflective coating. The scintillator is painted on five sides using highly reflective paint in order to bounce maximum photons into the detector. However, there are bound to be variations in the reflectivity while comparing a set of detectors. Reflective losses at the surface that couples the scintillator with the photo-diode, using optical grease, also showed minor variations. The ratio of counts in the 662 keV peak from cesium 137 to the total count improved from 30% to 36% when optical grease was used at the interface. Windowed photo-diodes need to be procured in order to get better results. The windowless photo-diodes currently in use are easily damaged by optical grease. The work was continued by procuring some assembled units, having 10mmx10mm photo-diode coupled with a 10mmx10mmx8mm CsI crystal. The output from these devices were found to be very small and developing the electronics that could give an energy resolution at par with the commercially available NaI+PMT detectors took several rounds of prototyping. Major steps of the development process carried out are explained below.

4.4 Electronics Development

The sequence of electronics required is the same as that of the alpha detector but the gain must be made high, to compensate for the low detector output. The low signal level makes the reduction of electrical noise extremely critical. Special care must be taken in the PCB designing and shielding. Since the major focus was on noise reduction by optimising the PCB layout and providing shielding, we will discuss more on the changes made to the PCB design, shielding, and layout of the subsystems.

4.4.1 The first prototype

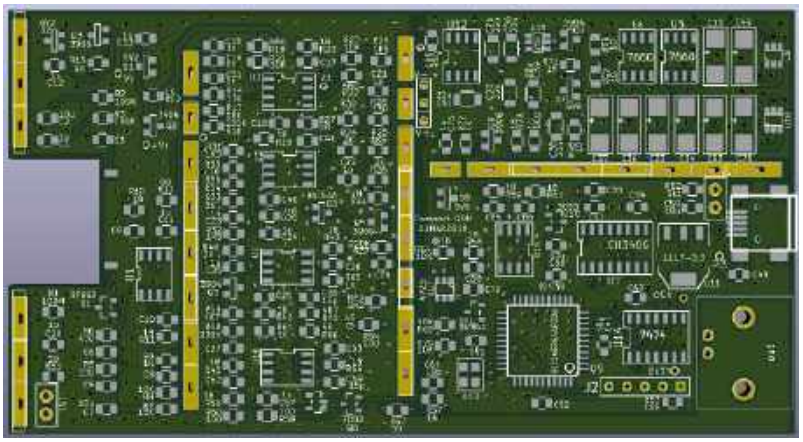

FIGURE 4.3: First prototype PCB with Gamma detector, pre-amplifier, shaping amplifier and MCA on a single PCB. The ground strip with slots between sections are for providing extra shielding using copper foils.

The PCB layout of the first prototype, developed along the same lines as the alpha spectrometer, is shown in figure 4.3. It is a double layer PCB. The rectangular slot on the pre-amplifier section is for placing the detector. The shaping amplifier and the analog part of the MCA are in the middle section. On the right side, the digital and the power supply circuits are fabricated. The different sections were separated by ground areas with plated through-holes so that shielding could be inserted to isolate them electrically.

The circuits were assembled and tested. The measured FWHM of the 1332 MeV peak of ^{60}Co was found to be more than 100 eV, around 20% higher than that of the commercially available NaI+PMT systems. The two possible reasons could be the lack

of a perfect shielding and the noise from the switching circuits getting coupled with the low-level analog signal stages. In order to identify the exact reason, it was decided to assemble the analog sections of the circuit on a separate board, and test using an external MCA.

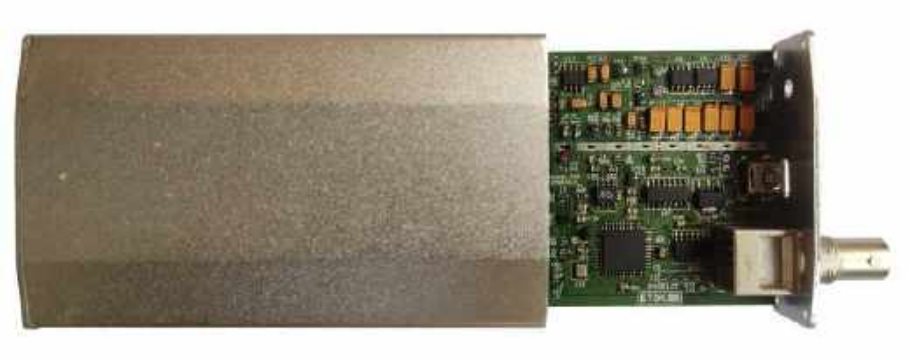

FIGURE 4.4: First prototype which includes a 1K MCA assembled and inserted in an aluminium enclosure. There were several problems mostly triggered by light leaks in this box design, as well as electrical noise coupling from the power supply.

4.4.2 The second prototype, without MCA

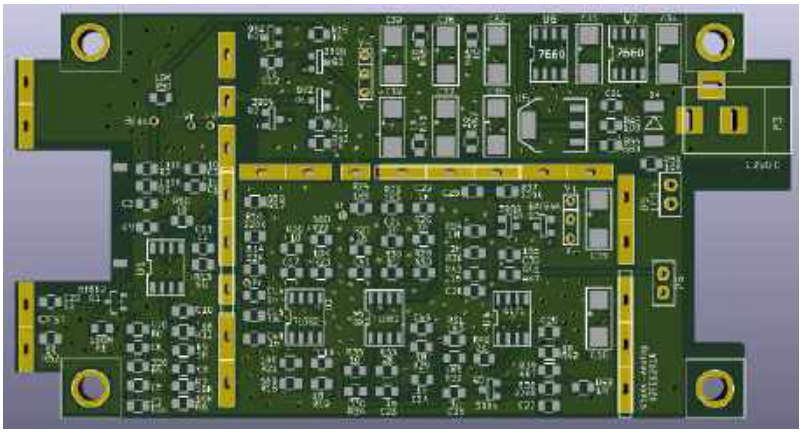

FIGURE 4.5: PCB of the pre-amplifier and shaping amplifier for gamma detector. Circuits to generate $\pm 9V$ from 12V DC input are also included. 12V DC input connector is at the top right corner.

The second prototype containing only the analog part of the required electronics was made. It consists mainly of the pre-amplifier and shaping amplifier. It is powered by an external 12V DC supply and the $\pm 9V$ supplies for powering the shaping amplifier is generated using

charge pumps and filter, as explained earlier. The $\pm 5.2V$ supplies for the pre-amplifer were generated using regulator circuits. The shaping amplifier output is made available on a BNC connector. The PCB layout is shown in figure 4.5.

FIGURE 4.6: Second prototype, without the integrated MCA, assembled inside a moulded aluminium box. Powered by external 12V DC.

This PCB was assembled into a moulded aluminium box that provides better shielding. The shaping amplifier output, from the BNC connector, was analysed by an external MCA. The measured energy resolution, an FWHM less than 80 eV for the 1332 MeV peak of ^{60}Co, found to be at par with the results from the commercially available NaI+PMT systems. The detector efficiency is lower due to the smaller size of the scintillator crystal but it does not pose a problem for teaching labs. Better statistics could be obtained by taking measurements for longer duration.

The desired energy resolution was achieved, but the equipment consisted of three pieces, the detector plus analog electronics, the multi channel analyser and the 12V DC adapter. The next step was to make it truly portable by eliminating the 12V DC supply and combine everything into a single enclosure.

4.4.3 The final version

We have already achieved the desired energy resolution and reliable operation and the following steps were taken to make the instrument more compact and portable. We

switched to a four layer PCB design, with one layer dedicated for the ground plane. The ground plane is covered with as much copper area as possible, and helps isolate the switching noise from the analog electronics. Ground connections between layers are made using plated vias.

Almost all parts are of the surface mount type since this reduces the board size and makes the design more suited for large scale manufacturing. Most passive components such as resistors and capacitors are 0805 size(2mm x 1.2mm), and ICs are of the SOIC package. The micro-controller is a TQFP package that has pins on all four sides. BGA type packages would have allowed for preparing more compact circuit boards, but they are unsuitable for hand assembly during the prototyping stages and have therefore been avoided.

The four layer PCB is shown in figure 4.7 The power supply board that contains a lot of switching circuits was made on a separate PCB. This is then attached to the main analog board using Berg type connectors. The physical spacing between the noisy power supply board and the sensitive analog board helps isolate electrical noise.

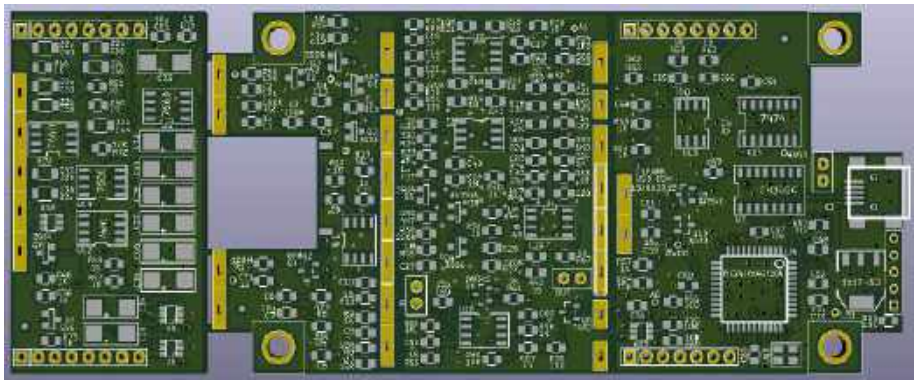

FIGURE 4.7: The 4 layer PCB of the gamma spectrometer with an integrated 1K MCA. The power supply module shown on the left side will be stacked above the MCA section during assembly.

Separating the power supply module and increasing the number of PCB layer to provide a better circuit ground improved the performance considerably. Details of the power module are shown in figure 4.8.

Similar to the Alpha Spectrometer electronics, the power supply requirements are ±5.2 V for the pre-amplifier, ±9 V for the shaping amplifier, ± 5 V for the discriminator,

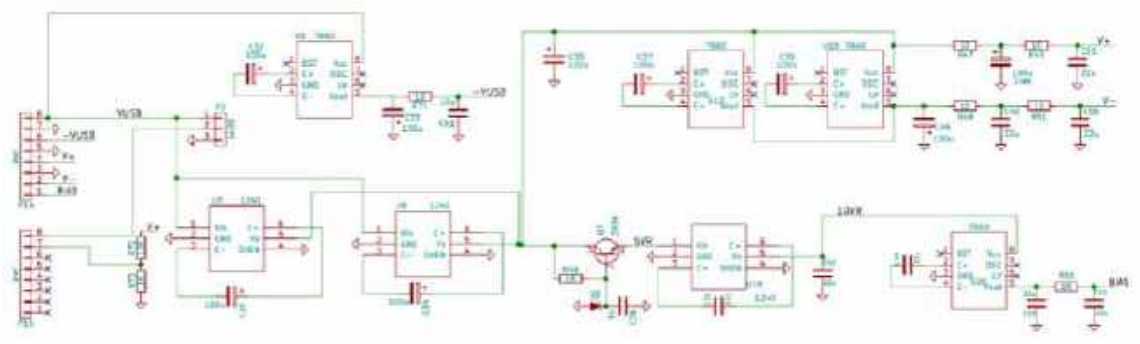

FIGURE 4.8: Circuit schematic of the power supply module. Due to the highly noisy charge pump circuits, this section is assembled on a separate board.

and -10 V for the photo-diode bias. All required voltages are generated from the 5 V USB power supply using a series of charge pump circuits and low pass filters. The power supply board also contains LM35 sensor to monitor the temperature inside the instrument. These are fabricated on a separate PCB that is then coupled onto the signal processing PCB by means of berg connectors. The physical distance between the two was planned in order to prevent the fast switching signals in the power supply charge pumps from interfering with the delicate analog signals.

A photograph of the assembled unit, with top lid removed, is shown in figure 4.9. An 8 mm hole is provided in front of the detector. This is sealed with a thin aluminium foil to protect the components from moisture. Gamma rays enter the detector through this foil. Silicon RTV compound is used for sealing the gaps around the USB connector. The part housing the detector and pre-amplifier is provided with an extra copper foil shielding.

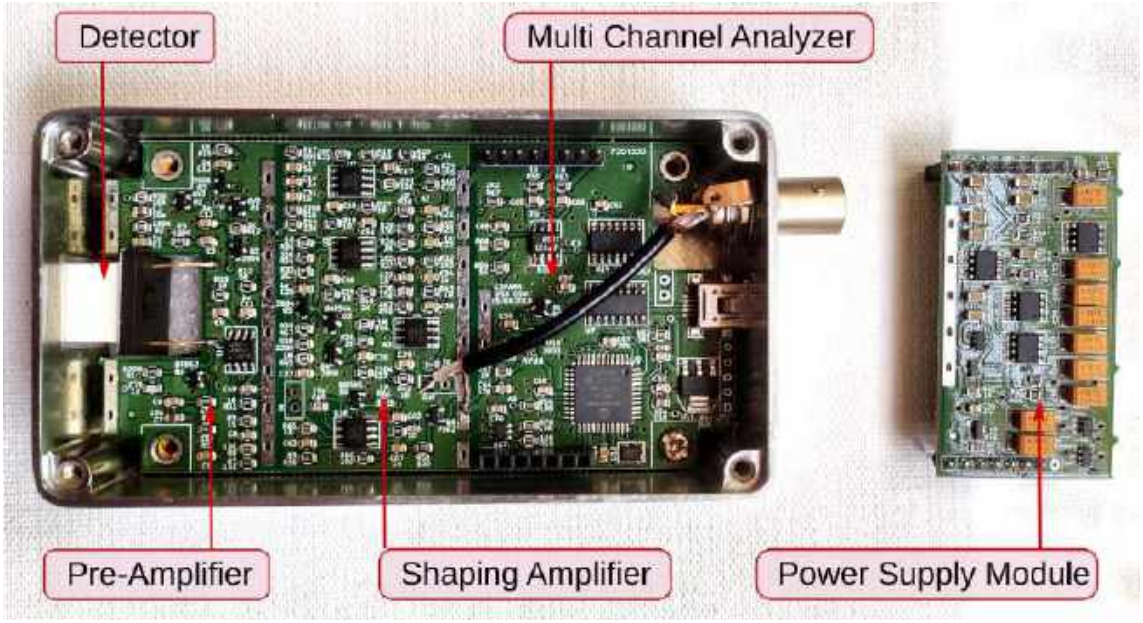

FIGURE 4.9: Components of the portable gamma spectrometer with an integrated 1K MCA. The power supply module has been removed and shown outside separately for clarity.

4.5 Final Product and Specifications

Traversing through several iterations, we have arrived at a product that is schematically represented by figure 4.10. The pre-amplifier and shaping amplifier designs were optimized to get the desired gain and energy resolution. A compact form factor has been achieved by a careful design of PCB and the shielding enclosure. The specifications of the final design are given below.

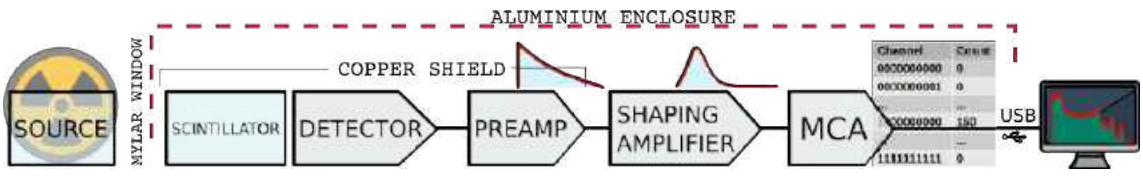

FIGURE 4.10: Schematic diagram for a compact gamma spectrometer that is being developed

Analog Electronics		
Preamplifier	Gain	10-20mV/MeV
	Rise Time	<100 nS
Shaping Amplifier	Gain	100x
	Rise Time	3 uS
Threshold Setting	Resolution	12-bit
	Range	10-512 Channels
Power Supply	Voltage	5 Volts
	Voltages Generated Internally	-10V, -9V, +9V, -5V

TABLE 4.1: Specifications of the analog signal processing stages

Specification	**Value**
Dimensions	112mm * 60mm * 31mm
Weight	200 grams
Resolution	80keV FWHM @ 1.33MeV centroid
Full Scale Range	3 MeV
Multi Channel Analyzer	1024 Channels. 16 million counts per channel.
ADC Resolution	12-bit. 2LSB are rejected, and 10-bits are used.
Noise Threshold	Adjustable via 12-bit DAC. Typical 65 Channels/1024
Power Consumption	<200mA typical
Power Supply	USB Powered
Communications Interface	USB
Software	CNSpec : Developed In-House. Compatible with Windows/Linux
Signal Output	Shaper output available via BNC for external monitoring

TABLE 4.2: Overall specifications of the developed instrument

4.6 Test Results with Gamma sources

For testing the functionality of the developed instrument, it is first calibrated with a source with known photopeak energies, and is then used to measure the photopeak position of a different source for verification. For linearity testing, sources with energies spanning the entire range must be used. The electronics and the Multi-Channel analyzer have already

been tested for linearity, and results have already been included in an earlier chapter on the Multi-Channel Analyzer 2.

4.6.1 Curve Fitting and Calibration

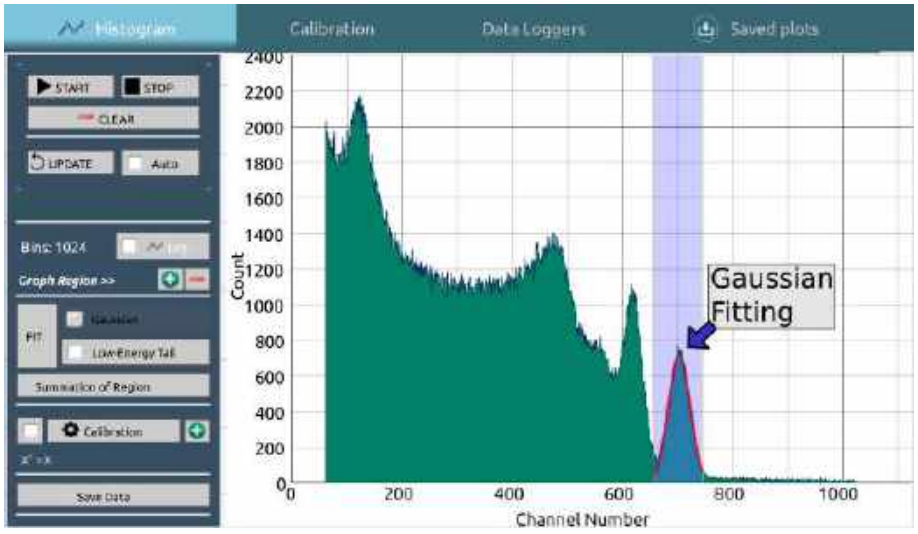

FIGURE 4.11: Screenshot of Gaussian Fitting being used to calculate the centroid channel number of a photopeak from a 60-Cobalt gamma spectrum. The extracted centroid channel numbers from the two peaks, and their known energies of 1173keV and 1332keV are used to generate a calibration polynomial

As can be observed from the spectrum shown in Figure 4.11, ^{60}Co has two photopeaks to the right of the spectrum and their associated Compton edges and backscatter peaks.

Using a gaussian fitting algorithm, the centroids of the photopeaks are first calculated in channel number units. Since the decay energies corresponding to these peaks are known to be 1173 keV and 1332 keV respectively, a linear calibration polynomial consisting of a slope and an offset parameter can be calculated.

The backscatter peaks associated with these photopeaks have energies at 183.6 keV and 197.5 keV but will be merged into a single peak as shown. This is due to limitations in the resolution of the instrument.

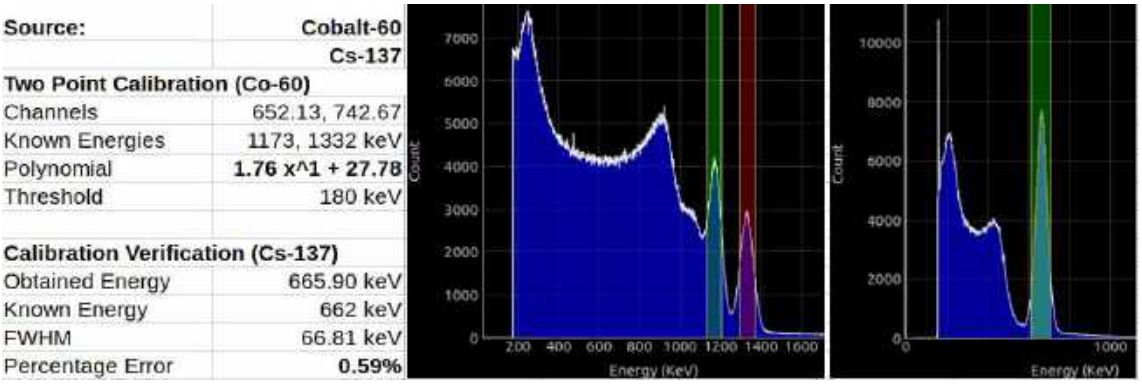

FIGURE 4.12: Two point calibration and verification

In Figure 4.12, the known photopeak positions of 60-Cobalt are used to obtain a calibration polynomial. Following this, the spectrum is cleared, and a third source, 137-Cesium, is analyzed. Since the photopeak energy of 137-Cs is known to be 662 keV, and the energy obtained for the same using the calibration polynomial calculated before was 665.9keV, a percentage error of 0.59% is observed.

4.6.2 Stability characterisation

Long term stability of the instrument is critical for accurate measurements. If a photopeak appears with a certain channel as the centroid, then this value must not change during continuous data acquisition in a stable instrument. In order to verify this, the 1.33MeV peak from a 60-Cobalt source placed in front of the spectrometer was marked with a region selector, and the auto-update interval was set to 5 minutes.

The spectrum history tool was then used to obtain a differential spectra for each five minute update as in Figure 4.13, and the centroid position was monitored for a total acquisition period of 1 hour and 30 minutes. The value did not fluctuate by more than 2 channels from the mean position, and this indicates a variation within 0.2% of the full range.

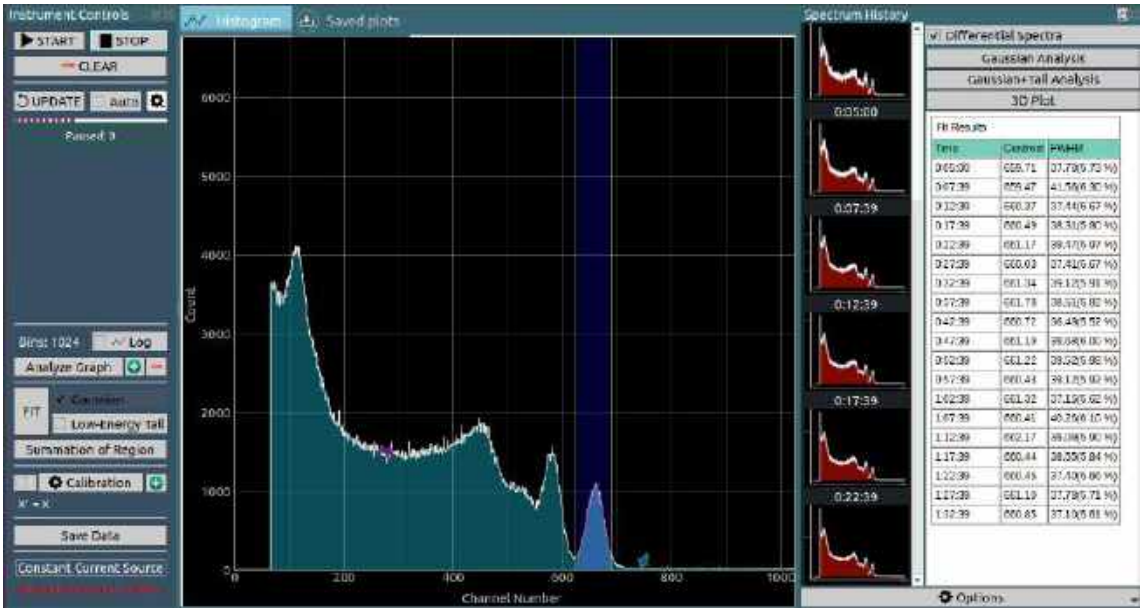

FIGURE 4.13: Cobalt spectrum being acquired for drift measurement of the position of the 1.33 MeV decay peak.

4.7 Study of naturally radioactive sand

The highly portable, low-power consumption design allows the instrument to be carried around by researchers surveying the natural background radiation in various parts of the country.

Indian Rare Earths Ltd (IREL), a govt owned lab in Manavalakurichi, Kanyakumari expressed interest to use our spectrometer in addition to the dosimeter based geotagged surveying of the country that they are already involved in. For characterization purposes, the results from our system were compared with a 3" x 3" NaI scintillator based system available with them. The purpose was to check the relative efficiency of high energy peaks which depends on the scintillator volume.

The source for this comparative study was Monazite, collected from the sand found in the beaches of Kanyakumari, India. The activity of a one gram sample is approximately 300 Bq of 232Th and 30Bq of 235U in secular equilibrium with daughters. The low activity requires long acquisition times to get a spectrum.

A paper comparing the spectrum from 1gm Monazite Sand with Thorium Nitrate salt in order to validate the usability of our gamma spectrometer for radiation safety applications was communicated to Physics Education. It has been accepted for Publication[3]. This publication also compared the performance of our instrument with a commercial one using thorium nitrate salt as a test source. This work is presented in the next section.

Thorium nitrate salt is a non-enriched radioactive sample composed of thorium nitrate ($Th(NO_3).5H_2O$) in powder form which has ^{232}Th and its various daughter products in secular equilibrium via decays associated with alpha and beta emission. De-excitation of daughter products from these decays are accompanied by emissions of gamma rays. The paper shows a side by side comparison of the level scheme of ^{232}Th as shown in Figure 4.14, with the actual data acquired from the salt.

The various peaks are reliably identified, and one can appreciate the potential of the non-enriched, naturally radioactive Monazite sand as a safer alternative to enriched sources. A comparison between the CsI scintillator+photodiode detector and the NaI+PMT was also made in order to estimate the efficiency difference caused by the scintillator sizes.

4.7.1 Performance Comparison with a Commercial Detector

The intention here was to make a comparison between the small scintillator based GammaSpec unit which we have developed, and a commercially available gamma spectrometer with a 3" Scintillator.

$20gm$ of Thorium Nitrate powder was placed in front of a 3" NaI scintillator attached to a PMT detector manufactured by Ortec. The obtained spectrum from 2 hours of data collection is shown in Figure 4.15.

The same sample was placed in front of our GammaSpec device, and data collected for a period of 3.5 hours is shown in Figure 4.16.

The total counts obtained by each detector is a function of various parameters such as the source-detector distance, geometry of the detector, and the detector efficiency itself. But since were are interested more in the efficiency as a function of energy, and the consequences arising from smaller scintillator size, we compute the normalized efficiency. This ratio of counts in a particular photopeak region to the total incident peaks indicates a

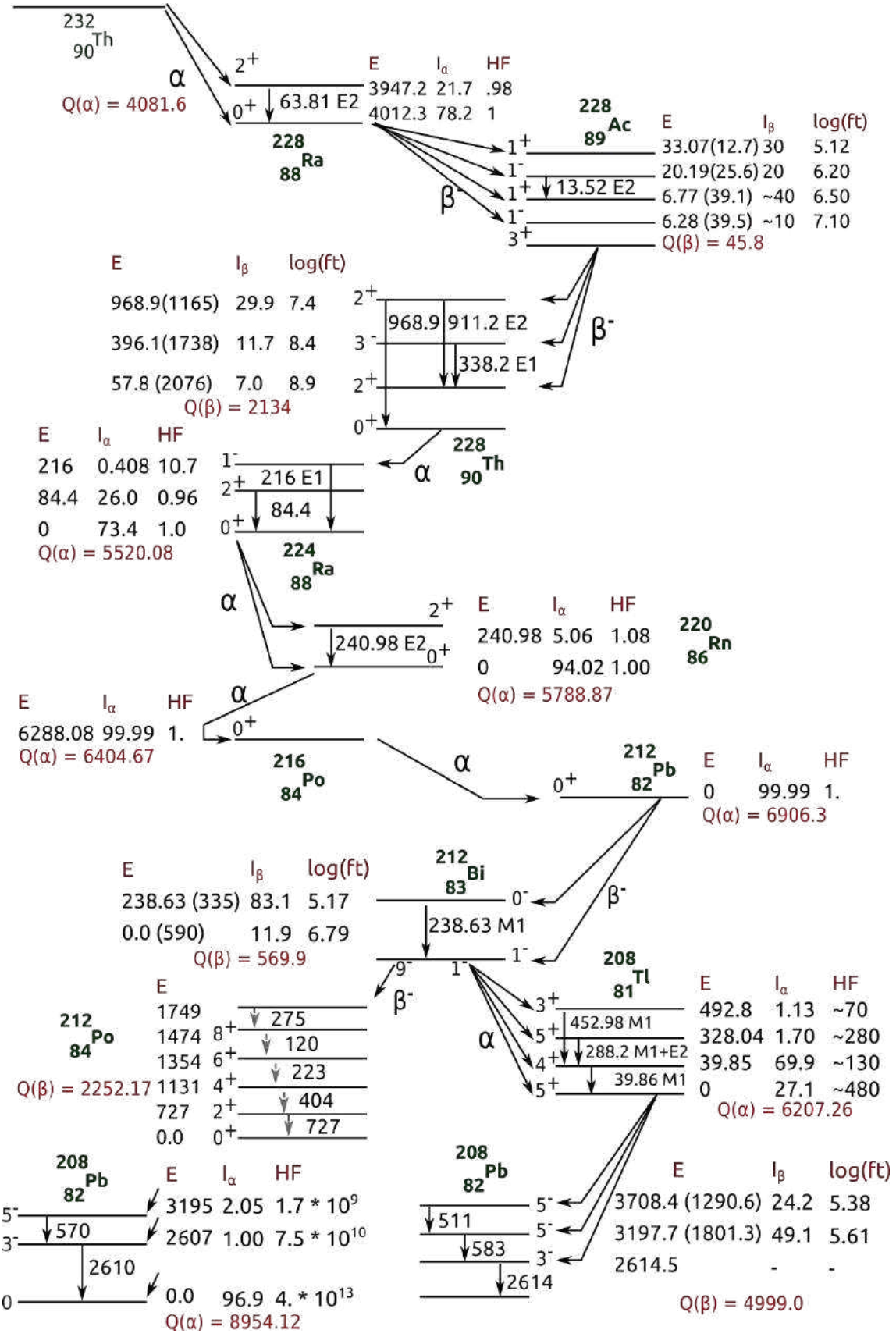

FIGURE 4.14: The decay chain of ^{232}Th highlighting the level structures of daughters that result in > 10% gamma intensities.[3]

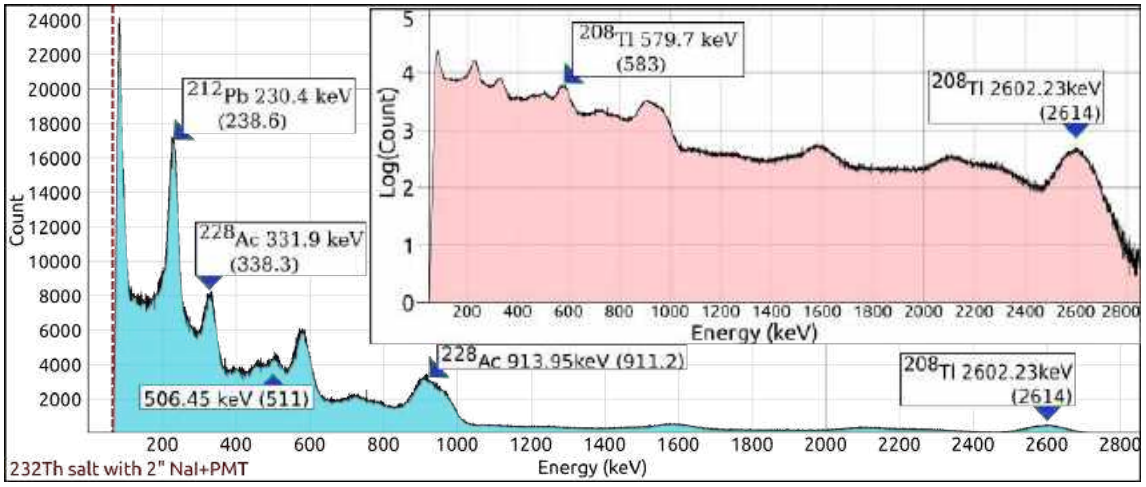

FIGURE 4.15: The Gamma spectrum of $ThNO_3$ powder obtained with a commercial PMT from Bicron with 2" NaI scintillator and a 4K MCA.[3]

Expected (in keV)	238.6	338.3	511	583	911	968.9	2614.5
2" NaI(tl) + PMT	230.4	331.9	506.5	579.7	913.95	Unclear	2602.2
10mm CsI(Tl)+ Photodiode	235.6	339.0	508.5	580	913.6	966.6*	2607.2

TABLE 4.3: Comparison of peak centroids obtained from 20gm $ThNO_3$ sample from the two different detectors used. *Peak appears as a shoulder peak, and has been identified manually.[3]

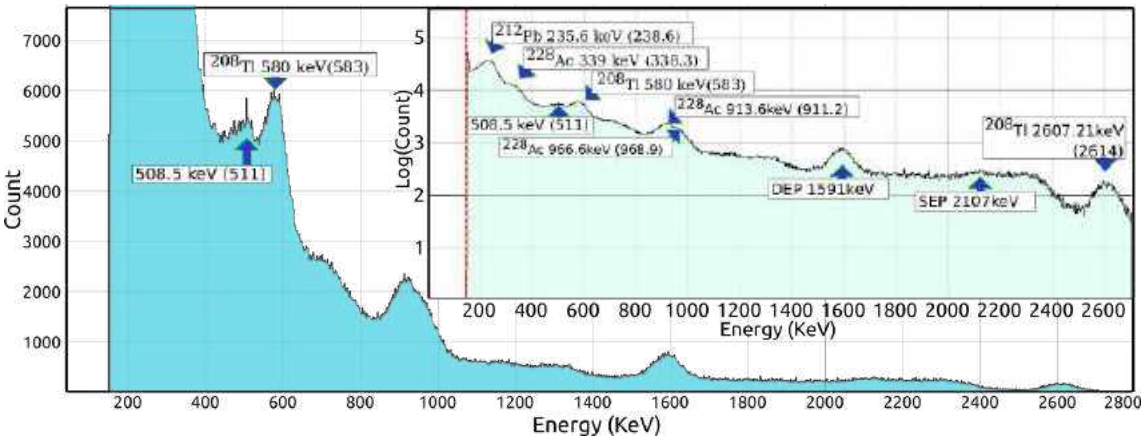

FIGURE 4.16: The Gamma spectrum of $ThNO_3$ powder obtained with GammaSpec1K spectrometer with CsI scintillator having volume $10mm * 10mm * 8mm$.

Detector	Total Counts	Energy(keV)	Energy Interval(keV)	N_E	$\frac{N_E}{N}$
2" NaI(Tl) With PMT	6768879	230.4	194.71-265.22	1079108	0.159
		913.95+968.9	840-1030	5443016	0.08
		2602.2	2516.83 - 2689.34	73771	0.01
10*10*8mm CsI(Tl) with Photodiode	2914071	235.6	201.26 - 270.11	856272	0.293
		913.6+966.6	840 - 1030	122310	0.04
		2607.2	2521.05-2693.18	2521.05	0.0024

TABLE 4.4: Determination of normalized efficiency for various energy peaks[3]

normalized efficiency which can be used to compare the different detectors as long as the source is the same. The results are presented in Table 4.4.

It can be seen that at higher energies (particularly the 2.6MeV peak from 208-Tl), the smaller scintillator has much lower normalized efficiency due to the gamma interaction lengths being a function of energy. This can however be compensated by acquiring data over a longer duration.

4.8 Elementary Gamma-Gamma Coincidence demonstration

A rather simple technique was explored in order to study coincident events recorded from multiple detectors. This was facilitated by the fact that the Multi-Channel Analyzers have been developed from scratch by us. Since the Multi-Channel Analyzers record information when a level changing discriminator signal triggers an interrupt in the microcontroller, we could modify the program to detect more than one discriminator input. One spectrometer is designed to generate a gate signal(A short pulse) whenever it records an event, and this signal is relayed via a coaxial cable to another spectrometer which considers it along with its own input. The coincidence logic, which involves comparing both signals, can be easily completed during the 3uS wait time wherein the shaper signal rises to its maximum. Figure 4.8 shows the configuration of this setup, and we were able to obtain good results from a positron source.

A ^{22}Na point source was placed at the center of the two spectrometers facing each other with a 10cm distance between the two detectors as shown in Figure 4.8. After a 40-minute acquisition duration, the spectra from the regular spectrometer as well as the gated spectrometer are shown in Figure 4.17. Both spectra were calibrated using the annihilation

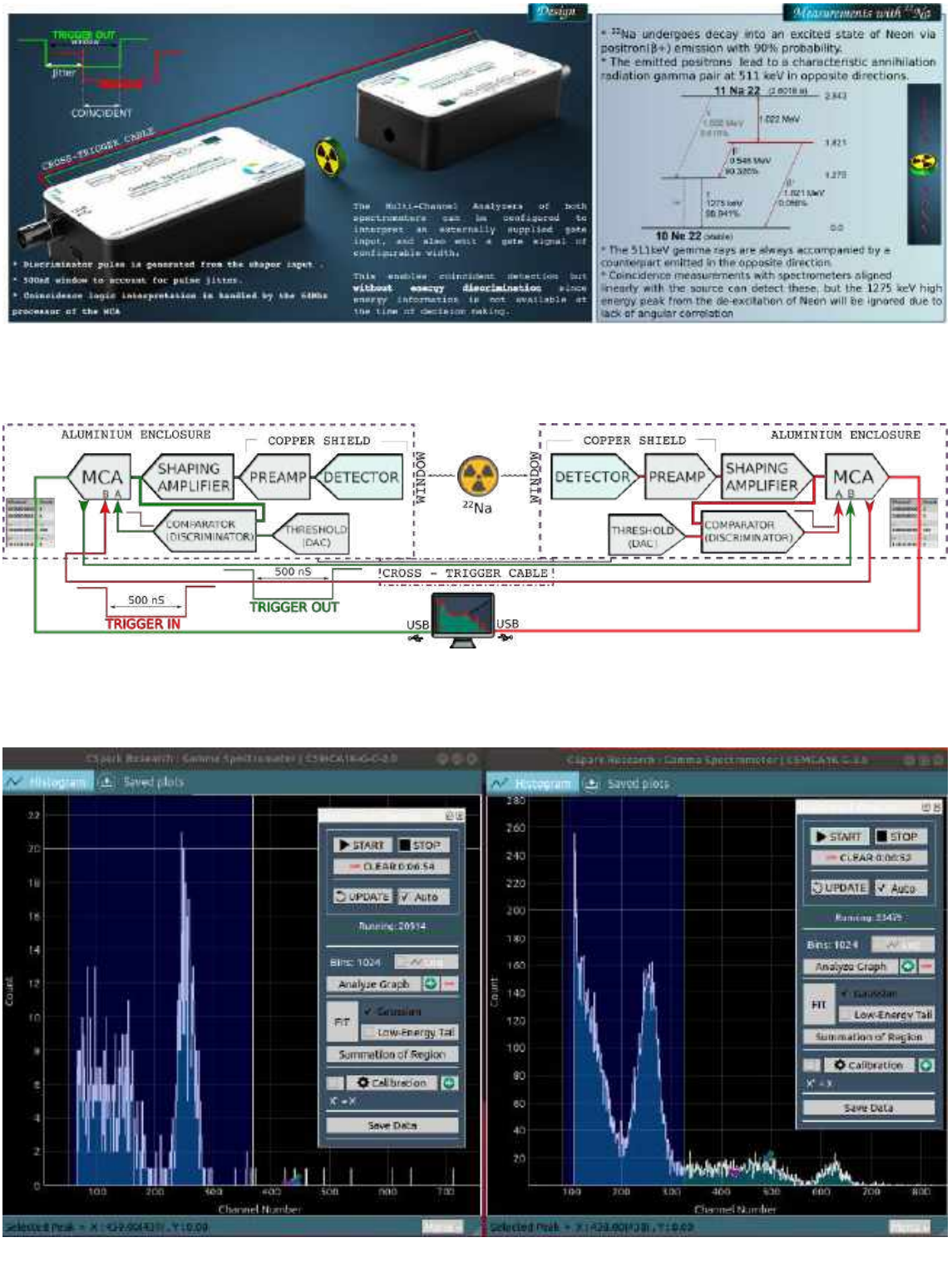

FIGURE 4.17: On the right is the full gamma spectrum from Na-22 which includes peaks at 1275keV, 511keV and their associated Compton portion. On the left is the spectrum from a gated MCA configured for coincidence measurements

peak at 511keV, and the attenuation of the high energy peak in the gated spectrometer was observed. Detailed results have been published in [1].

This rather simple approach can be quite useful from an instructional point of view but is rather limited in terms of experimental value which demands record keeping of the energy of the event responsible for the gate signal for each coincident event also. This allows detailed analysis for isotope identification and also helps rule out stray coincident events triggered by noise or background. Since digitized pulse height(Energy) value is not available at the time of decision making, signals from two separate events may often be recorded erroneously as coincident. These limitations led us to develop a dual parameter MCA setup which is elaborated in a separate chapter.

4.9 Android App

An Android app was written to make this a truly portable system. Android devices above API level 14(Android KitKat) support USB OTG. This allows plugging in peripheral devices such as keyboards, mice, storage devices etc. via a special OTG cable. The MCA of the Gamma Spectrometer uses a CDC-ACM chip for communications, which is also recognized by android phones when connected.

A simple application was coded in Java using Android Studio and tested on my Redmi Note 7 phone. The usb-android-serial library was used for handling communications. The app can auto-detect a plugged in spectrometer, and acquire basic spectra. The proof of concept is successful and further development work can be carried out if sufficient requirement is made out for the same.

The circuit can be integrated into a compact back panel to make a portable radiation surveying device. Combined with the features of the modern smartphone such as GPS, communications, and processing power, it can be a powerful tool at a low price.

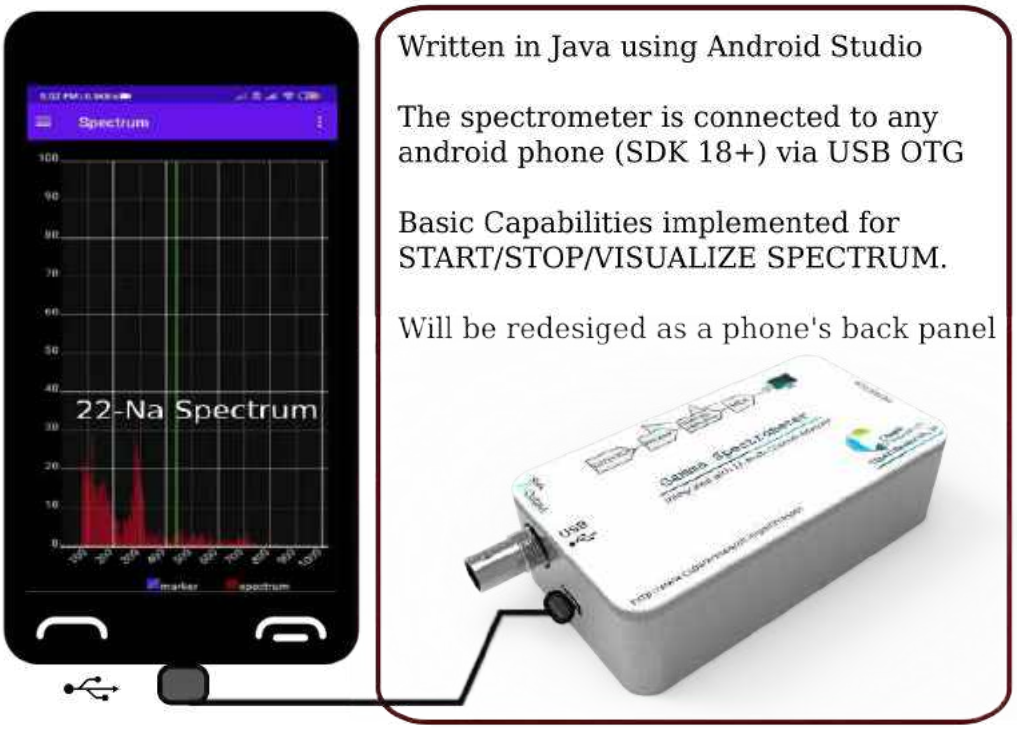
Spectrum
22-Na Spectrum
Written in Java using Android Studio
The spectrometer is connected to any android phone (SDK 18+) via USB OTG
Basic Capabilities implemented for START/STOP/VISUALIZE SPECTRUM.
Will be redesiged as a phone's back panel

CHAPTER 5

$\gamma - \gamma$ Coincidence Measurement System

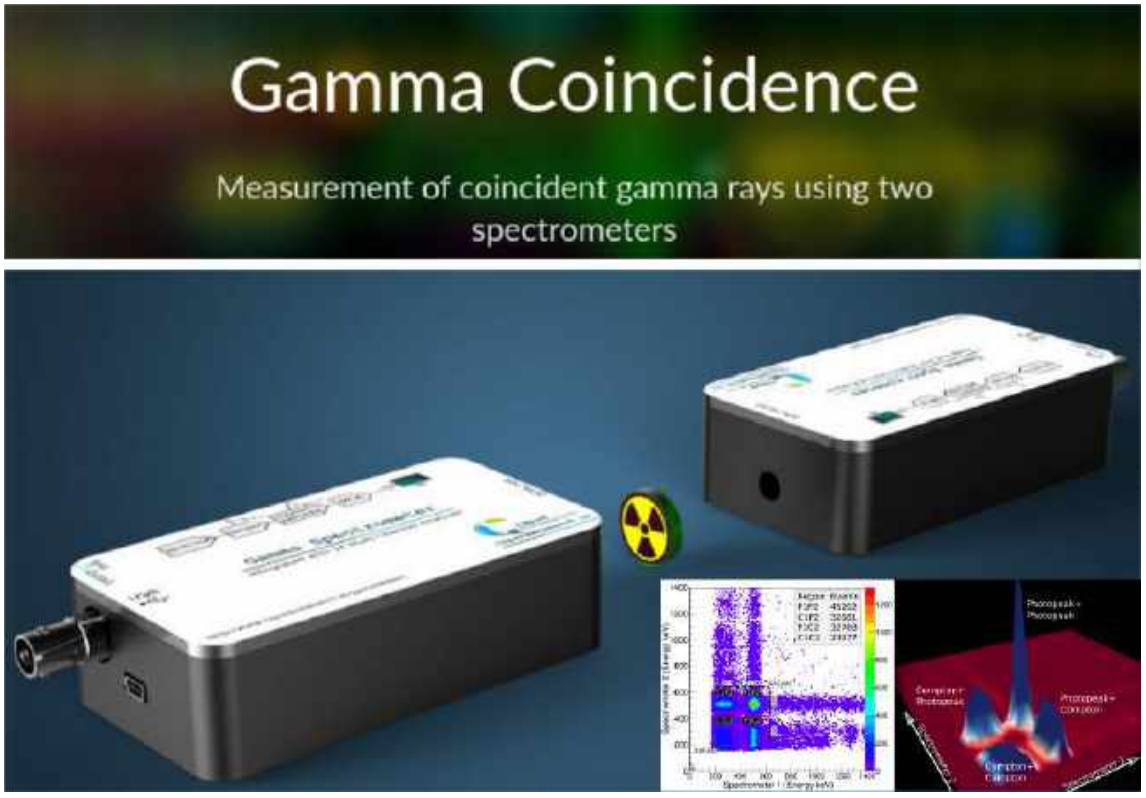

5.1 Introduction

In many nuclear physics experiments the number of signals from the detection system will be very large but all of them does not contain relevant information. Setting logical

conditions based on the expected physical processes reduces the time and resources wasted on on collecting the irrelevant signals. One such example is the Compton suppression in Gamma detector systems, where the signals resulting from Compton scattering are identified by detecting the simultaneous firing of the HPGe detector and the Compton shield and such events are rejected. Correlating the data from more than one detector helps in identifying the physical processes better.

Some nuclear processes produce two photons simultaneously, while other processes produce two or more photons in quick succession. In processes like positron annihilation the emissions occur simultaneously. The case of a beta emission followed by a gamma emission, by the daughter nucleus, also may come under this category when the two decays happens within a time period shorter than the time resolution of the detection system. In such cases, it is possible to study the angular correlations between the two photons by setting up a coincidence detector system. In nuclear physics applications, coincidence systems are used to detect and identify weak detection signals or to distinguish a relevant signal from background signals. In high-energy physics detection systems consisting of thousands of detectors and electronics channels, data is collected only if the predefined coincidence conditions are met.

The angular correlation between the emitted photons can also be studied to identify the physical processes involved. One such instance is the positron-electron annihilation processes in a source such as ^{22}Na which emits two 511 keV gamma rays in exactly opposite directions, to conserve momentum. A coincidence configuration of the the detectors will be used for de-convolution of peaks and reduction of background, allowing for more precise characterization of complex spectra. Gamma-gamma coincidence has the advantage of virtually eliminating all background peaks that do not exist in coincidence with other peaks, significantly improving detection limits.

Multiple detectors with cross-linked electronic triggers can be used to identify such events by considering only those events which trigger both detectors simultaneously. The schematic for a typical setup is shown in Figure 5.1 taken from [36]. This approach involves complex electronic circuitry where separate timing signal outputs, delay blocks and logical gating circuits are employed.

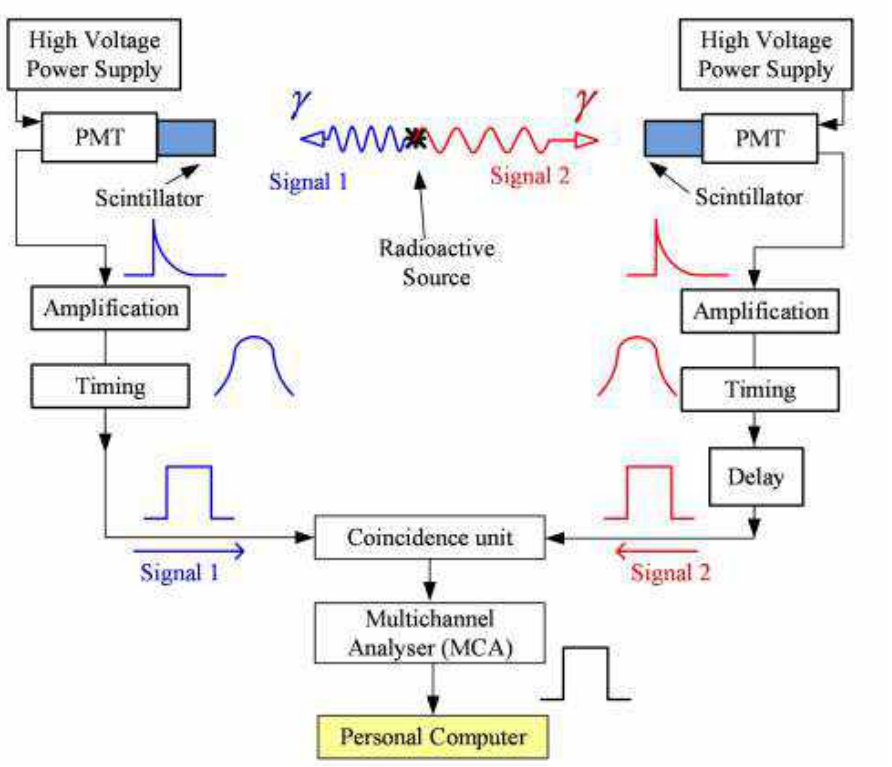

FIGURE 5.1: Schematic diagram of a typical gamma-gamma coincidence setup, wired using commercially available gamma detection systems and logic modulesHKU2015

5.2 The Coincidence setup, using a dual parameter MCA

The previous chapter described a method to perform coincidence measurements by coupling two gamma detector systems simply by using a gate signal relayed from one to the other via a cable. In that method, no energy specific gating is possible, and noise spikes and background signals result in false coincident events being recorded.

These drawbacks were remedied by developing a proper coincidence detection system, implemented using a dual parameter MCA. The Dual parameter MCA is essentially a list mode data acquisition system that can collect the data of two input channels(parameters) along with a corresponding timestamp. Shaping amplifier outputs corresponding to two detectors are the inputs for this instrument. Two identical sets of discriminator, sample and hold circuitry and ADC are handled by the logic implemented in the firmware.

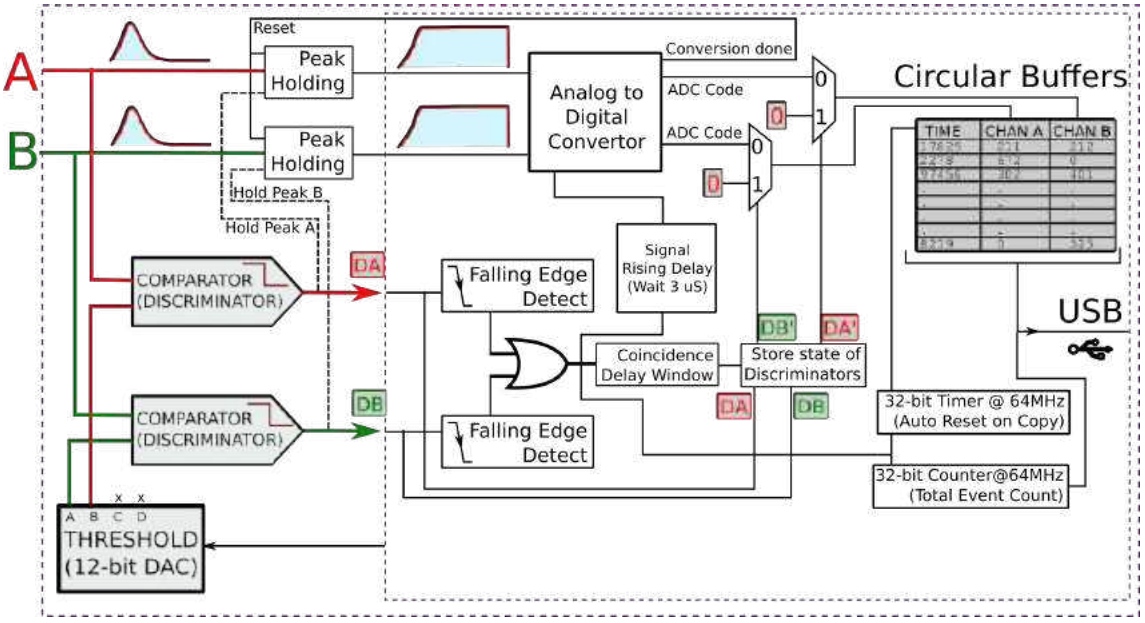

FIGURE 5.2: Control flow diagram of the two parameter MCA

The flow diagram in Figure 5.2 illustrates the implementation of this setup. This technique has now been published in Nuclear Instruments and Methods in Physics Research A [1]. When either input crosses the threshold, the discriminators send a rising edge signal to the microcontroller, causing the interrupt service routine to be activated. This function waits briefly for a predefined coincidence window which is typically 500nS wide, and then records the state of both discriminators. After a further delay of 3uS to account for the rise time of both signals, the 10-bit ADC is used to digitize both of them via parallel sample and hold circuits. If either of the discriminators were FALSE during the coincidence window, the value is discarded and overwritten with 0. If both are TRUE, it is a coincidence condition, and the peak values are recorded for both. The coincidence window is software configurable, starting from 100 ns and increasing in steps of 15 ns.

5.2.1 List mode data format

The list mode data is a multi-column circular buffer containing the timestamp and the ADC outputs from both inputs. The limited buffer size requires a connected computer to continuously transfer its contents to the software which has access to much larger storage space. Each column is a separate circular buffer with a position index shared across all three. The first column is used to record the time elapsed since the last recorded event.

Recording time difference instead of absolute timestamps from the start of acquisition allows us to reduce the bandwidth required for data transfer. A 32 bit timer running at 64MHz is used to keep time, and the corresponding step size is approximately 15 nano seconds. At this speed, the timer will overflow only when no event occurs for a duration exceeding 67 seconds, a possibility that is very remote due to the presence of the source or even otherwise wherein cosmic background radiation will trigger either detector every couple of seconds. The timestamp value is shared if the coincidence condition is met, and otherwise only one of the detector values will be non-zero. The acquisition software calculates the cumulative sum of the timestamps to obtain the absolute timestamp. It also polls the circular buffer continuously in order to prevent overflows which can cause data to be lost.

The CNSPEC software was augmented with features for data acquisition , analysis, & visualization for list mode data from the new MCA. It can plot the coincidence data as a 2D histogram data, or as a surface plot. Certain analytical tools for applying energy gates on either detector data, and studying the effect on the other were also implemented as described in the Software chapter. Experiments were performed with ^{22}Na to confirm the usability of the new setup.

5.3 Circuit schematic of two parameter MCA

. The circuit of the dual parameter MCA is shown in figure 5.3. It consists of two identical units of the discriminator, sample and hold and ADC chain. The first one is implemented by U2, U3 and Q1, and the second channel by U7,U8 and Q2. The two channels of the flip-flop (U6) implements the BUSY flag and the thresholds are set by the DAC (U10). The sample and hold outputs are fed to different ADC inputs of the microcontroller. The DC power module is not included in the schematic because the same PCB developed for the Gamma spectrometer is reused, through the connectors P9 and P10.

The PCB design of the dual parameter MCA is shown in figure 5.4. The circuit is implemented on a double sided PCB and enclosed in an aluminium enclosure with two BNC connectors from the inputs. DC power and computer interfacing is through USB. Technical specifications are given in the table 5.1.

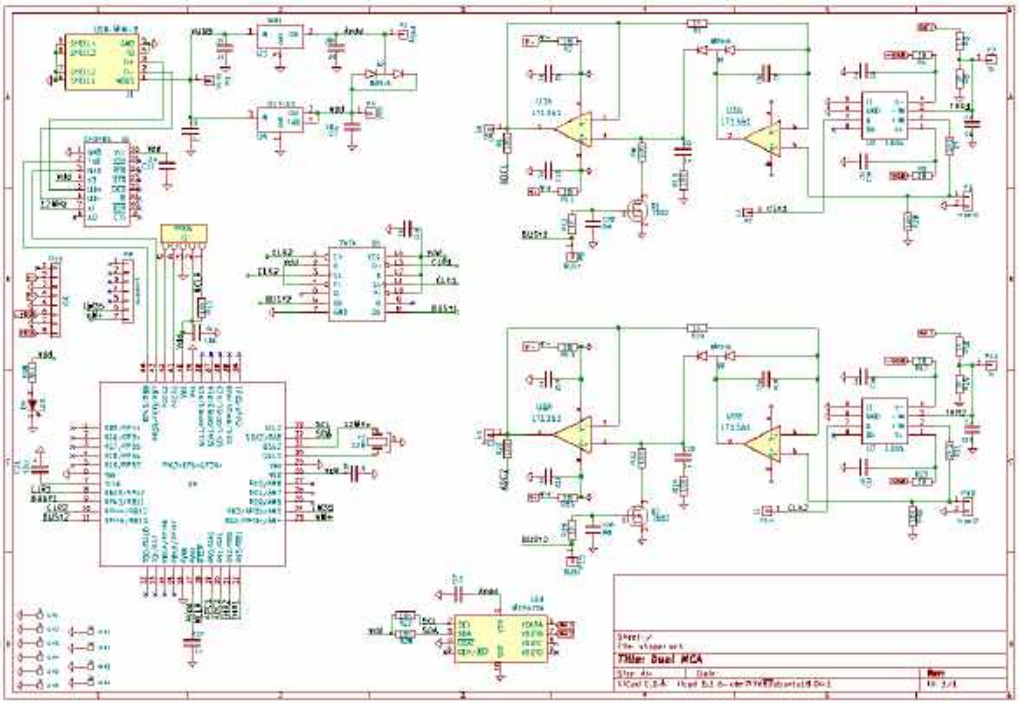

FIGURE 5.3: Circuit schematic of the two parameter MCA

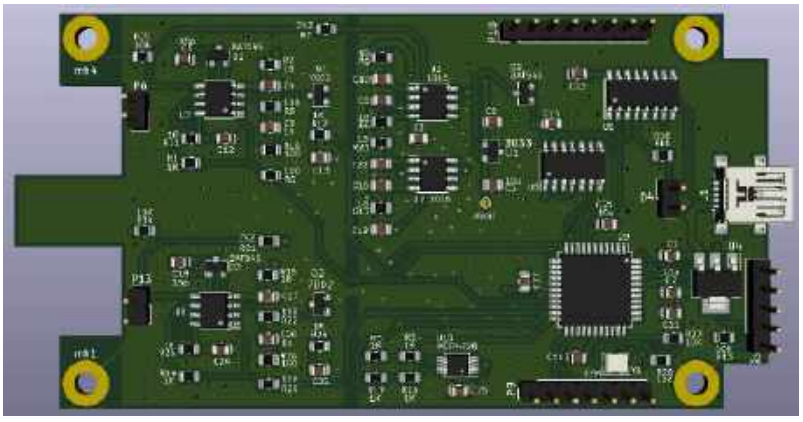

FIGURE 5.4: PCB of the two parameter MCA. Input pulses are connected to P6 and P13.

5.4 Test Results

Figure 5.5 shows the configuration used to validate the coincidence setup using a positron source. The spectrometers are connected to the dual parameter MCA as shown. A ^{22}Na positron source is placed at the center, and is at a distance of 4cms from each detector on

Dual Parameter MCA : Technical Specs		
Total Inputs	2	BNC Female Type
Input Rise Time	3uS	0-3.3 Volts
Clock Speed	64MHz	
Timestamp Resolution	15nS	
Threshold Setting	2 Channel, 12 Bit	
Circular Buffer Size	1000 Points	10-512 Channels
Dead Time	8 uS	
Communications	USB	

TABLE 5.1: Specifications of the dual parameter MCA [1]

either side of it. This was to confirm that under coincidence conditions, the 1275keV high energy gamma ray is only recorded as random coincidence events. The ratio of events in the 511keV gamma ray region(photopeak + Compton of high energy) to the high energy photopeak events was calculated with and without the coincidence condition enabled, and results are discussed below. Data was acquired over a 5 hour 30 minute period, and analyzed.

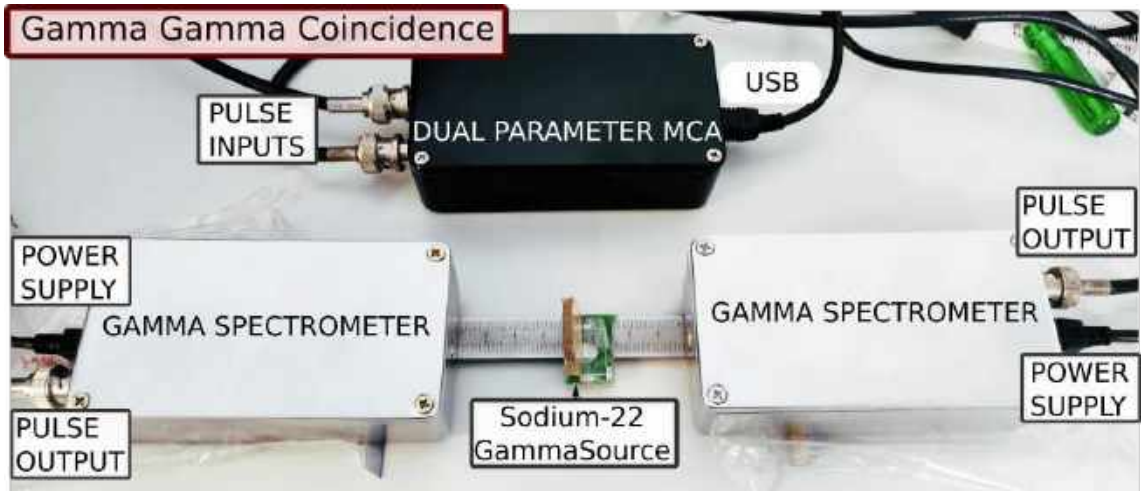

FIGURE 5.5: Configuration for testing the coincidence setup with the dual parameter MCA

5.4.1 Visualization of multi-parameter data

Typically, two parameter data is visualized as a heat map wherein the counts in a 2D dimensional histogram plane are represented by colours. We used the most popular analysis tool CERN-ROOT[37] to create this image as shown in Figure 5.6, but also implemented the same in CNSpec using PyQtGraph. Each pair of energies recorded in the

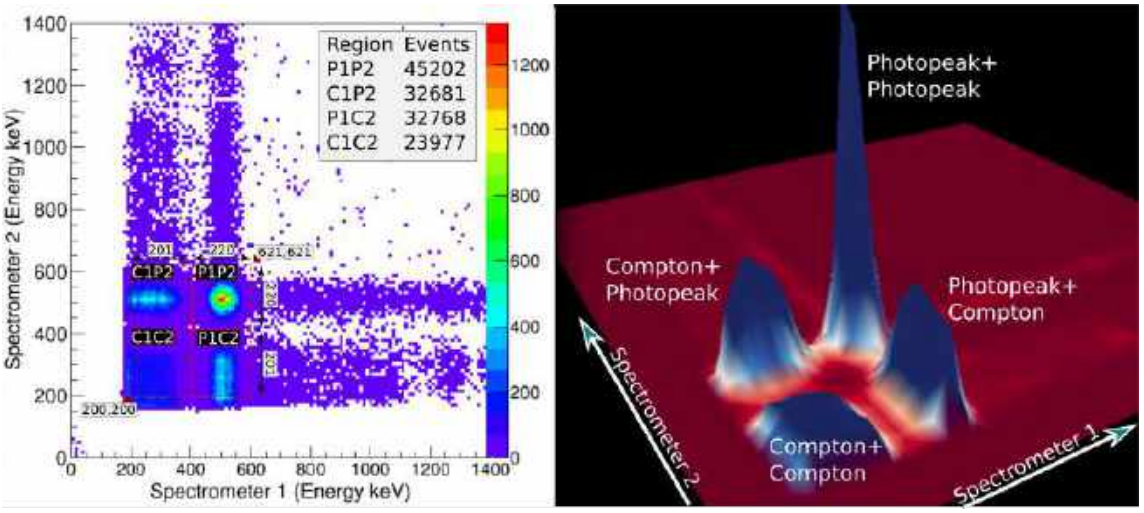

FIGURE 5.6: Left - heat map showing the coincidence spectra for data acquired over 5 hours and 30 minutes. Right - Surface plot representation of identical data. [1]

list mode data is essentially the XY coordinate on the heat map which must be incremented by a factor of one to record it. If either of the events is zero, it is counted along one of the axes, and is not considered coincident. These are ignored, and only those events with both coordinates non-zero form the heat map. The prominent features such as peaks and plateaus are better visualized in a surface plot which we have implemented in CNSpec. In case of positron annihilation spectra, four distinct peaks corresponding to the four possible combinations of photoelectric or Compton interactions in either detector are formed. A quantitative analysis of the total events recorded in each of these regions is shown as an inset in Figure 5.6. Prefix P stands for photopeak, and C stands for Compton. The Photopeak region is selected between energies 401 and 621keV symmetric about 511keV. The corresponding channel range for Spectrometer 1 is 153 to 237, and for spectrometer 2 is 140 to 218. Similarly, the compton range is 200-401keV, and the channel numbers are 70-140 and 77-153 respectively. The difference in channel numbers is due to slight variation in the gain of each spectrometer arising from difference in component tolerances, but has been compensated by appropriate calibration.

5.4.2 Analysis of multi-parameter data

The first step is to locate the centroid channel of the 511keV peak to be used as a reference in spectrometer A. A Gaussian fitting function estimated this to be at 179.6 channel with an FWHM of 22.5(12.1%). It was observed that by channel number 220 this gaussian function

Gate Applied	(A) 511 keV Counts Photopeak (421-601keV)	(B) 511 keV Total Photopeak+Compton (175-601 keV)	Ratio (A) to (B) (Signal Quality)
Full Spectrum Gating	3952	8089	48.9 %
511 keV Gate (421-601keV)	44654	79016	56.5 %
1275 keV Gate (1200-1350keV)	281	476	59 %

TABLE 5.2: Relative effectiveness of the full spectrum gating and 511keV gating method via the dual list mode method. The 511 keV photopeak quality obtained with both methods is compared.

becomes negligible. This reference channel of 220 was used to divide the spectrum into two segments in order to study the effects of application of a coincidence gate. These segments as shown in Figure 5.7 are :

- The high energy segment on the right: channels 220-1023 which can contain only contributions from the high energy gamma, or neglibigle contributions from pile-up or background.
- Low energy and Compton segment: channels 0-220 contain events from the 511 keV gamma and only Compton events from the high energy gamma.

In the absence of any coincidence conditions, the ratio of A to B was measured as 1830285:358067. This can also be termed as segment B containing 16.36% of all recorded events.

Once the coincidence condition with spectrometer B was enabled, this ratio was measured to be 165215:5534, or 3.24% of all recorded events. The random coincidences recorded here are not incredibly small, but can be explained by the large solid angle subtended by the $10mm * 10mm$ detector due to the source being only 4 Cm away from it.

In Figure 5.7, the effect of the gate is more pronounced, and one can see that the high energy contribution to the spectrum has disappeared, and has taken its Compton plateau with it.

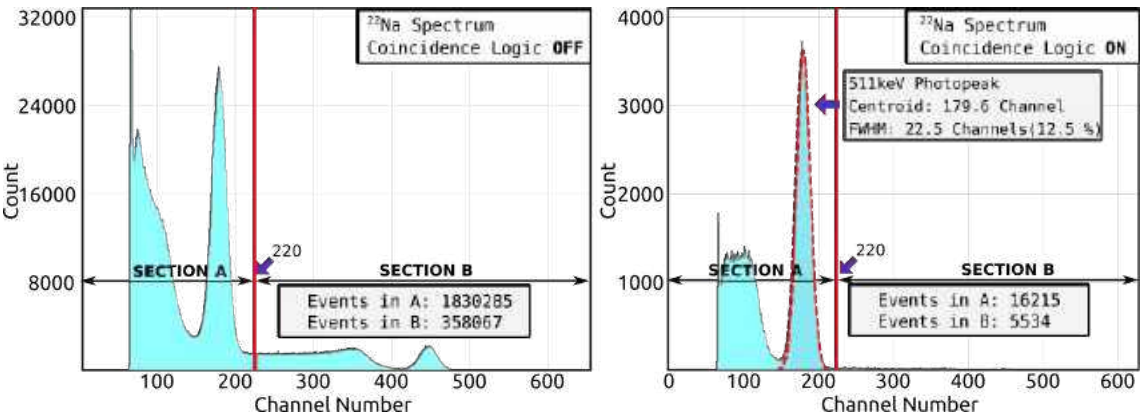

FIGURE 5.7: Effect of the coincidence gate on the high energy peak presence in the data. Right - ^{22}Na spectrum with coincidence gate enabled. The 511 keV photopeak has also been fitted with a Gaussian function. Left - full spectrum without any coincidence gate.

5.5 Angular Correlation measurements

Since the 511keV gamma pair is emitted in diametrically opposite directions, and peak coincidence count rate is observed when detectors are placed facing each other, and the source is placed in their centre. For verification, an experimental setup was prepared as follows.

An optical spectrometer was dismantled in order to use the rotary stage which has graduations for measuring the angle. A gamma spectrometer was attached on each of the telescopic forks, and coincidence counts in 5 minute intervals for different angles subtended with a point source placed at the midpoint were acquired. Results are shown in Figure 5.8, and confirms the initial hypothesis.

A digital goniometer was later procured in order to make the apparatus more self reliant. This instrument consists of two steel scales of 300mm each, with a central pivot that measures the subtended angle with a resolution of 0.05 degrees. In addition, a slider may be machined which will allow easy anchoring of the spectrometers on these scales.

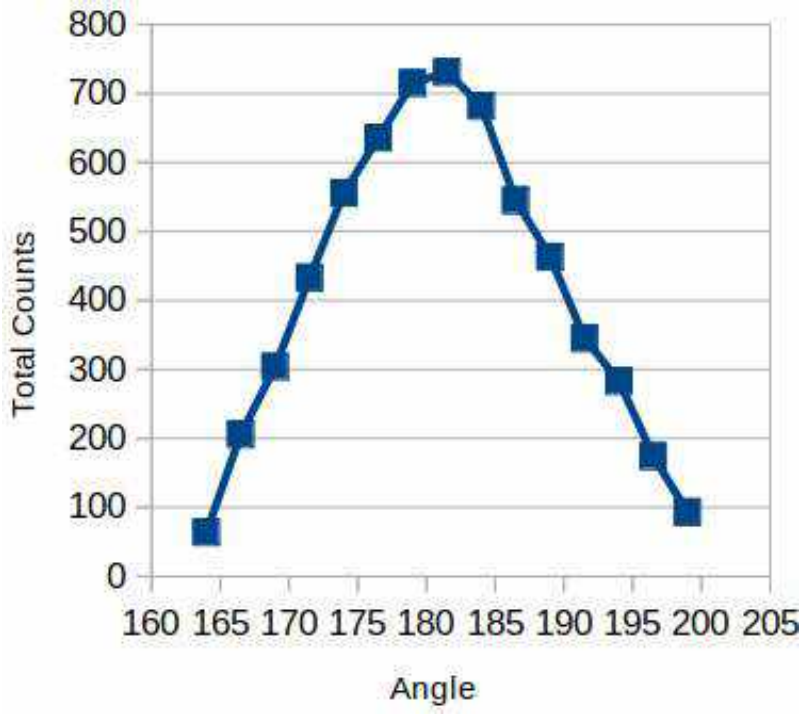

FIGURE 5.8: Results from the angular correlation measurements conducted with a rotational stage. Peak coincidence count rate is recorded when the angle subtended between the spectrometers and the centrally placed source is 180 degree.

CHAPTER 6

Software

CNSpec is a complete Data Acquisition, Visualization and Analysis software we have written to complement the MCA, Alpha and Gamma Spectrometers, and the $\gamma - \gamma$ coincidence system. It uses the Python programming language, and is made available under an open source license. The source code can be downloaded from Github [14].

The firmware of the devices which runs on the microcontrollers was developed using the C language since it provides the most efficient development time without compromising on performance. For the software side, complex visualization and analytical tools are required in addition to a complete user interface. For this purpose, Python was the primary choice since it has a rapid development time as compared to other languages, and comes with a wide set of free and open source modules for analysis such as Numpy

and Scipy. For plotting graphs and surface plots, PyQtGraph is yet another popular module. Python can thus effectively tackle the various mathematical and visualization challenges. In addition to this, it runs on multiple operating systems, which is also known as cross-platform behaviour.

CNSpec has been designed to handle list mode data from the Dual Parameter MCA, and also histogram data from the 1K and 4K MCAs. Parameters such as peak position(centroid channel), area under curves and FWHM can be extracted with its analytical utilities. Other important features incorporated as of now in the software are multi point calibration, Gaussian Fitting including a low-energy tail (Lorentzian part) variant to obtain peak information, and a summation tool to calculate the total number of counts in a given spectral region. Data-loggers to automatically estimate half lives of peaks by periodically recording summation of counts in a region are also available.

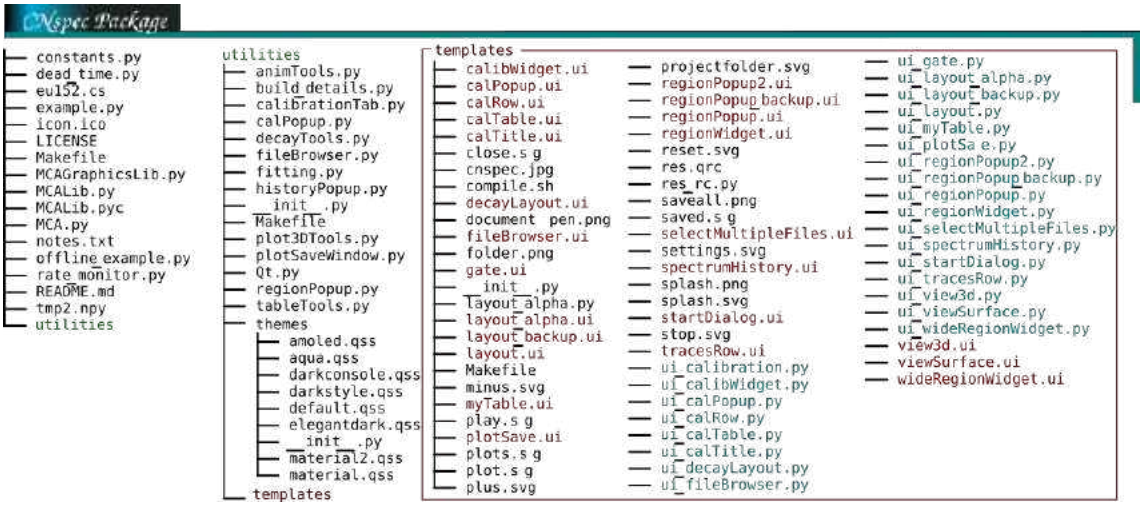

FIGURE 6.1: List of files that make up the CNSpec package

The software features can be summarised as follows:

- Data collection from USB connected instruments described in the previous chapters.
- Automatic detection of the connected instrument (Alpha spectrometer/Gamma Spectrometer/ Multi-Channel Analyzer), followed by appropriate user interface generation.
- Plotting histogram and providing options to select regions for analysis

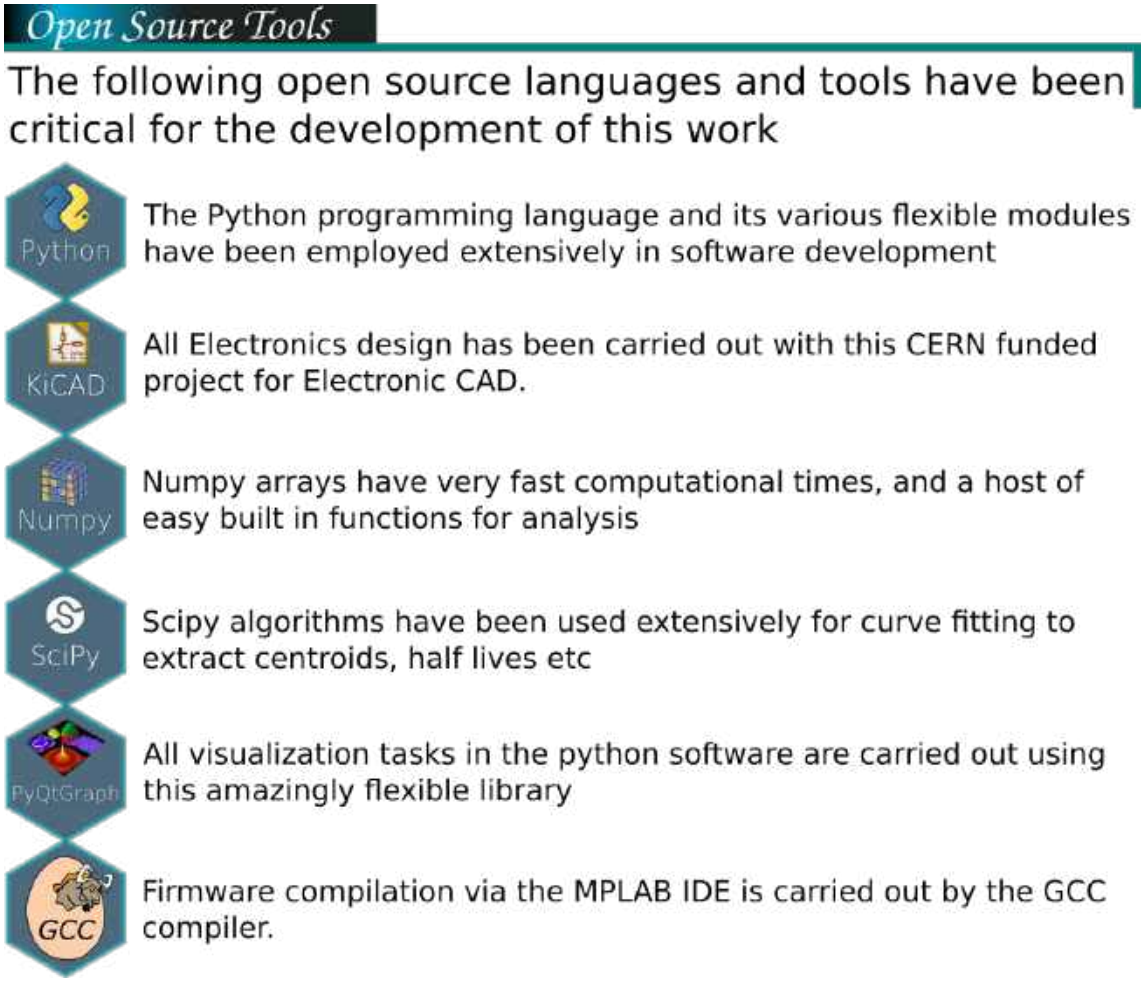

- Centroid estimation using curve fitting with standard Gaussian, or a Gaussian+Lorentzian function for low energy tail estimation. Exponential decay fitting for half life estimation.
- Summation tool for calculating total decay events.
- Multi point calibration utility.
- Decay rate measurement for half life calculation.
- 3D surface plots for gamma-gamma coincidence as well as growth profiles.
- List mode data interpretation and plotting.
- Heat maps and 3D Surface plots, and coincidence analysis via energy gates.
- One-click installation tools for Debian based systems such as Ubuntu as well as Windows.

6.1 The Python Library

A fully functional communications and analysis library for the Python language can be accessed by advanced users. The same library is also used by the graphical interface. It can be used to develop customized graphical interfaces or simply to acquire and analyse data via pre-programmed logic sequences. It also includes function calls for analysis as well, and it can be clubbed with other python modules for visualization, remote publishing etc.

This example is a short sequence to acquire data from a Multi Channel Analyzer

```
import time,sys
from MCALib import connect

device = connect(autoscan = True) # automatically detect the hardware

if not device.connected:
        print("device not found")
        sys.exit(0)

device.startHistogram() #start data acquisition
time.sleep(5) #Wait for data collection
device.sync() # fetch data from the hardware
x = device.getHistogram() #assign data to a variable

#plot this data
from matplotlib import pyplot as plt
plt.plot(x)
plt.show()
```

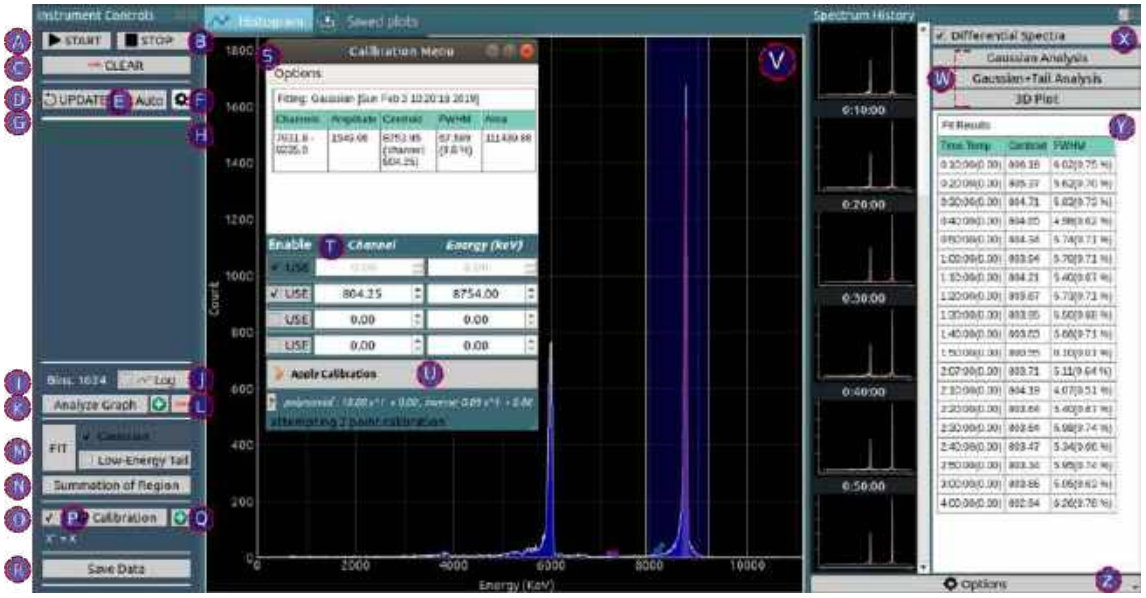

FIGURE 6.2: This annotated screenshot of the CNSpec Software shows data from 212-Bismuth acquired using our Alpha Spectrometer.

6.2 Graphical Interface of CNSPEC

This section contains excerpts from the user manual for the CNSpec software which we have previously authored and uploaded on public platforms in order to facilitate its usage by the community.

Figure 6.2 of the cnspec software displays an alpha particle spectrum, and a description of each of the annotated parts is as follows:

(A) Start Histogram : The hardware is instructed to start data collection which is basically sorting input pulses into bins based on their height.

(B) Stop Histogram : The hardware stops data collection and ignores subsequent events

(C) Clear Histogram: The spectrum stored in the MCA is in the form of an array or a circular buffer, and this command clears it. The plot in the software is also cleared.

(D) Update : Histogram data is fetched from the connected hardware and plotted. In case of list mode data the collection part is redundant because the software is continuously fetching latest data to prevent buffer overflows.

(E) Auto-Update : Invoke the update function in fixed intervals. This is particularly useful for logging data for half-life extraction purposes if a region is already inserted in the spectrum during the collection process.

(F) Collection interval (seconds) for the auto-update function.

(G) Progress bar which indicates the time remaining for the next spectrum refresh (update).

(H) Pulse Counter : total input pulses which are automatically refreshed in real time. Clicking on the counter resets it. For the dual MCA mode, this shows 3 values - coincidence counts [counts from channel A, counts from channel B]

(I) The total number of bins in the connected hardware, or offline data being shown.

(J) Change the Y axis counts to a log scale.

Utilities for data analysis

(K) Open the utilities dock for inserting and viewing graph region selectors.

(L) Region Selection : Insert graph region selectors for defining regions for analysis.

(M) Gaussian Fit : First, insert a region, and center it around the peak to be analyzed. A standard gaussian function is then fitted to the selected data with a least square minimization algorithm to extract important parameters - The centroid which identifies the peak position, FWHM which is a measure of the peak quality. If the energy value of the peak is already known, the centroid can be used as a reference point to calculate the calibration polynomial.
The Gaussian function can also be augmented with a low energy tail(Lorentzian) component to consider attenuation by scattering agents, or degradation of the detectors over time.

(N) Calculate the sum total of the events in bins inside a selected region.

(O) Enable Calibration: Up to 3 point calibration can be applied, and reference points can be added manually or automatically through curve fitting of peaks.

(P) Display the calibration window.

(Q) Manually add a reference point for calibration (channel and corresponding energy in keV must be provided).

(R) This opens a spreadsheet with numerical values for the histogram - channel vs counts. The spreadsheet can be saved in a csv file, or as a png image of the spectrum.

(S) **Calibration menu:**

(T) Channel vs energy table. If only a single channel - energy pair is supplied, the origin coordinate(0,0) is used as a reference to calculate the slope for the calibration polynomial. No offset correction is possible with just one point.

(U) Apply the calculated calibration polynomial . This changes the X axis of the spectrum from channel units to keV.

(V) The spectrum - channels/energies on the X axis, and events recorded in each bin on the Y Axis.

(W) **Spectrum History :**Each call to the update routine saves the latest copy of the spectrum into a new memory location. With the differential spectrum mode enabled, one can analyse various parameters such as centroid shifts, and change in the activity of the source as a function of time.

(X) Plot a 3D growth profile.

(Y) Results of the analysis are shown in tabular form, and may be saved into a collection of files in a directory.

The tab next to the 'SPECTRUM' tab is called SAVED plots, and can be used to load saved data. Once a directory is selected, it displays thumbnails of saved data or quick identification. All saved data can be analysed in an 'offline' mode. This is particularly useful when dealing with large list mode files. For publication quality plots, the 'light theme' may be enabled from the main menu.

6.2.1 Advanced features

1. **Data Logger :** Each region inserted into the spectrum is continuously monitored. Total events are stored for each spectrum update, and this enables plotting the graph

of activity as a function of time. The acquisition interval can be set using the input field next to the AUTO-UPDATE checkbox, and decay constants and half-lives are auto calculated by this tool. In case the interval is short, and too few counts are registered in each interval due to weak activity of the source, the half life fitting algorithm may fail - if that happens the user can also club counts in n adjacent intervals to obtain wider time intervals with cumulative counts in each, thereby improving the data available for fitting.

2. **Threshold setting :** Low energy channels which contain information due to electrical noise, and not actual input radiation events, can be filtered out by setting a threshold value. A built-in 12 bit DAC connected to the threshold comparator in the hardware does this job, and its value should be set a little above the noise threshold.

6.2.2 Gaussian Fitting for Extraction of Peak Centroid

The least square minimization routine from the Scipy library is used to determine the parameters of a standard gaussian function that will best fit a defined region in the spectrum.

This process involves defining an error function $gauss_erf$, and some approximate guess values. Once the values have been determined, a smooth overlapping Gaussian curve is also generated as shown in Figure 6.4. A trapezoid function is used to calculate the area under the curve which can be a useful parameter in some cases.

For asymmetric peaks caused by detector degradation, or imperfect vacuum, a Lorentzian function is added to this. A similar least square minimization approach is also followed for calculating the decay constant from activity recorded as a function of time.

The following code segment deals with Gaussian fitting. The numpy library has been imported and renamed as np. The leastsq function from scipy.optimize does all the major work.

```
1 def gauss_erf(p,x,y):#p = [height, mean, sigma]
2         return y - p[0] * np.exp(-(x-p[1])**2 /(2.0 * p[2]**2))
3
```

```
def gauss_eval(x,p):
        return p[0] * np.exp(-(x-p[1])**2 /(2.0 * p[2]**2))

def gaussianFit(X,Y,region,name=False,**kwargs):
        FIT = {}
        start,end= region
        start = (np.abs(X-start)).argmin() #Find closest index
        end = (np.abs(X-end)).argmin()
        X = np.array(X[start:end])
        Y = np.array(Y[start:end])
        size = len(X)
        maxy = max(Y)
        halfmaxy = maxy / 2.0
        mean = sum(X*Y)/sum(Y)

        halfmaxima = X[int(len(X)/2)]
        for k in range(size):
                if abs(Y[k] - halfmaxy) < halfmaxy/10:
                        halfmaxima = X[k]
                        break
        sigma = mean - halfmaxima
        par = [maxy, mean, sigma] # Amplitude, mean, sigma
        try:
                plsq = leastsq(self.gauss_erf, par,args=(X,Y))
        except:
                return None
        if plsq[1] > 4:
                print('fit failed')
                return None

        par = plsq[0]
        Xmore = np.linspace(X[0],X[-1],1000)
        par[1] += (X[1]-X[0])/2.0 #Move centroid to the center of the bins.
        Y = self.gauss_eval(Xmore, par)
```

```
38
39          FIT['area'] = np.trapz(Y,dx = (Xmore[1]-Xmore[0]) )
40          FIT['amplitude'] = par[0]; FIT['centroid'] = par[1];
41          FIT['fwhm'] = abs(par[2]*2.355) #FWHM = sigma*2.355
42          FIT['type'] = 'gaussian'
43          FIT['X'] = Xmore
44          FIT['Y'] = Y
45          return FIT
```

6.2.3 Calibration using ^{137}Cs

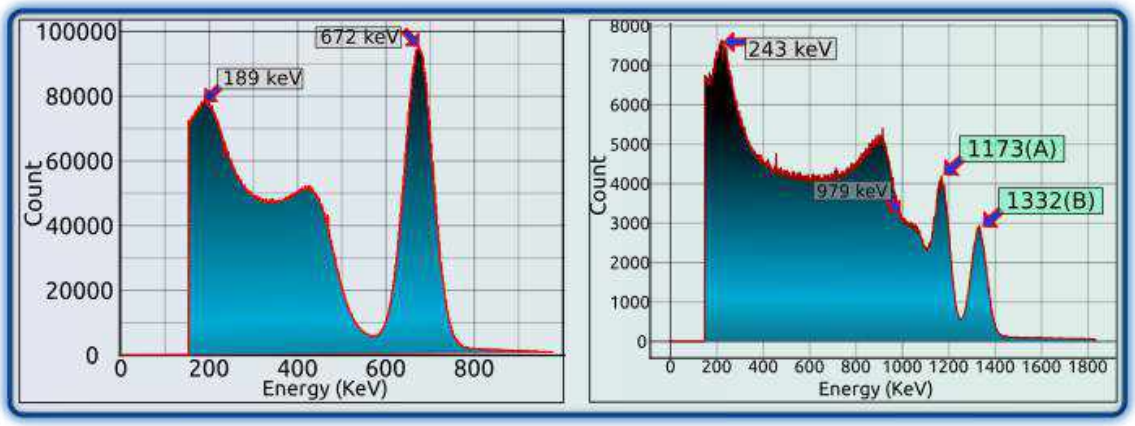

FIGURE 6.3: Single point calibration using ^{137}Cs, and linearity check with ^{60}Co

^{137}Cs source has a single photopeak energy, and is therefore a common choice for single point calibration of gamma spectrometer.

However, since single point calibrations are not equipped to correct offset errors, it is advisable to use a source with at least two gamma emissions at known energies, such as ^{60}Co.

This is a multi-peak source which has two photopeak energies and can be used for applying a slope as well as offset correction.

Instructions for calibration

- Locate a source in front of the detector window, and click on the 'START' button to accumulate data. Wait for a sufficient amount of events to be recorded such that the photopeak has a smooth appearance. Periodically refresh the data using the update button and observe that the plot smoothens as the spectrum builds up.
- Select the photopeak using a region tool
- Use the FIT button(Keyboard shortcut 'f').
- The software will display the extracted parameters such as centroid and FWHM in a dialog box.
- In this dialog box, enter the known energy of the peak against the centroid(channel number). For Cs-137, the photopeak position energy is 662 keV.
- Click on 'Apply calibration polynomial' and observe that the X-axis now displays energy units rather than channels.
- Finally, clear the spectrum, and record data from an unknown source.
- locate the photopeaks of the unknown source with the calibrated instrument.

6.3 Gamma Gamma Coincidence

Coincidence measurements using multiple spectrometers allows for better identification of events with simultaneous multiple gamma emissions. This requires precise digitization of signals from multiple detectors, as well as timestamped data.

6.3.1 Calibration using ^{22}Na

^{22}Na source has a photopeak at 511 keV from positron annihilation, and a high energy peak at 1275 keV. The 511 keV peak is used for calibrating the dual MCA. Offset correction can also be included by using the high energy peak for the calibration as well.

Steps to calibrate the instrument

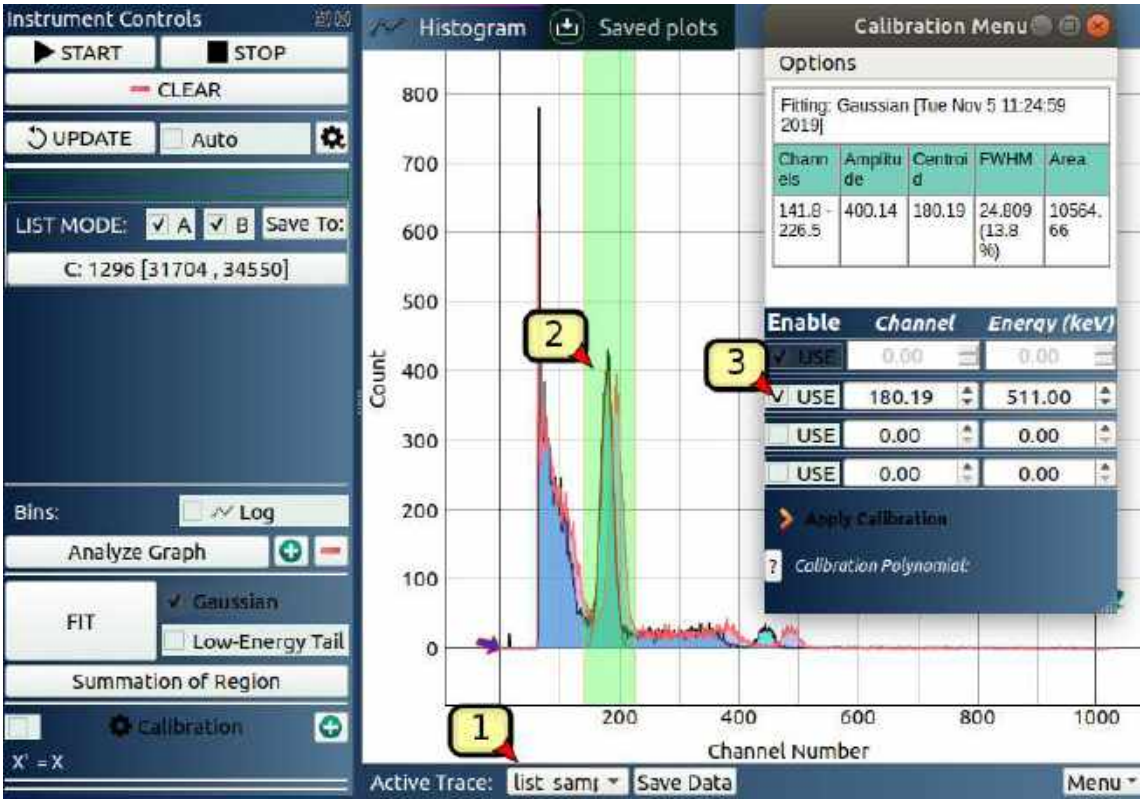

FIGURE 6.4: Single point calibration using 511 keV peak from ^{22}Na

- place the source in front of the window, and acquire the corresponding spectrum by clicking 'start', and waiting for a sufficient spectrum to build up.
- Click on update to fetch the latest spectrum from the hardware, or select the 'auto-update' button.
- select the first input trace (Labelled **1**), which has a black outline.
- Insert a selection region around the 511keV photopeak(labelled **2**), and ensure that it covers this peak
- Click on the fit button, or press 'f'.
- After a succesful fit , the software will show the parameters in a dialog box.
- In the pop-up window that is now displayed, enter the known energy of the peak against the channel number extracted from the peak.
- Click on 'Apply calibration polynomial' to apply this calibration.

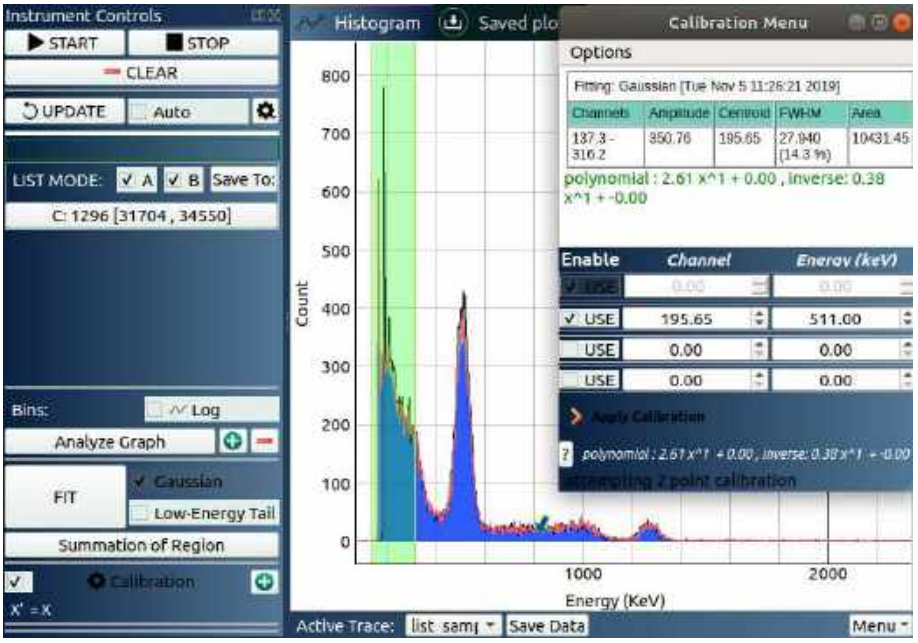

FIGURE 6.5: Spectrum after single point calibration using 511 keV peak from ^{22}Na

- Now select the second trace(from the menu **labelled 1**), and move the region to cover the 511keV peak from trace 2 (red colour)
- repeat the calibration process, and click on apply calibration.

6.3.2 3D data and heat maps

The coincidence data is also represented in the form of a surface plot and a heat map as shown in figure 6.6 . in order to calculate total coincident counts in a region, click on the ROI(Region of Interest) button, and drag the rectangular box to cover it. The total counts are shown in the bottom of the window, and the 3D surface plot automatically updates and rescales to show the selected area.

6.3.3 Applying energy gates

The ideal way for enhanced analysis currently is to use the saved csv file with a tool such as CERN-Root. However, some energy gating features have been implemented.

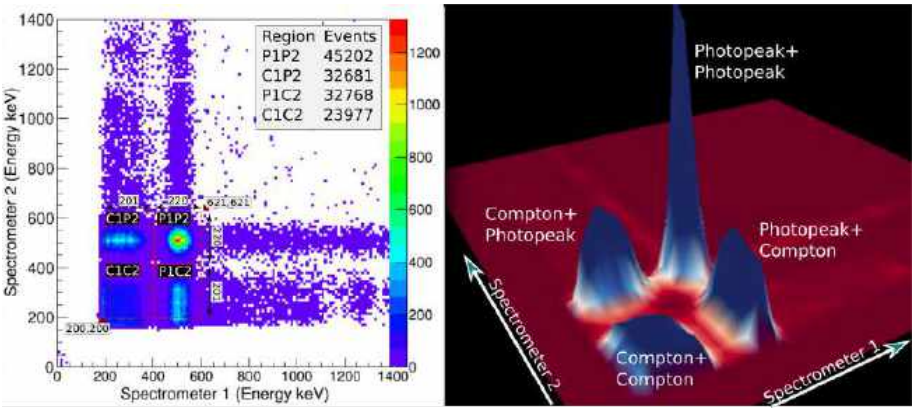

FIGURE 6.6: Coincidence spectrum from ^{22}Na shown as a heat map and a surface plot

In this, one can isolate the counts obtained through input 1 where the corresponding Input 2 signal is between channels A and B. In order to configure a gate on B, first insert a region, and center it around the events to be used as the source for the gate. Now press the c key on the keyboard, which will bring up a popup window where you must select which trace is the source(S), and which trace is to be updated(U). Once this is selected you will observe that U is automatically updated to represent the events that were in coincidence with the events in S which are within the specified region.

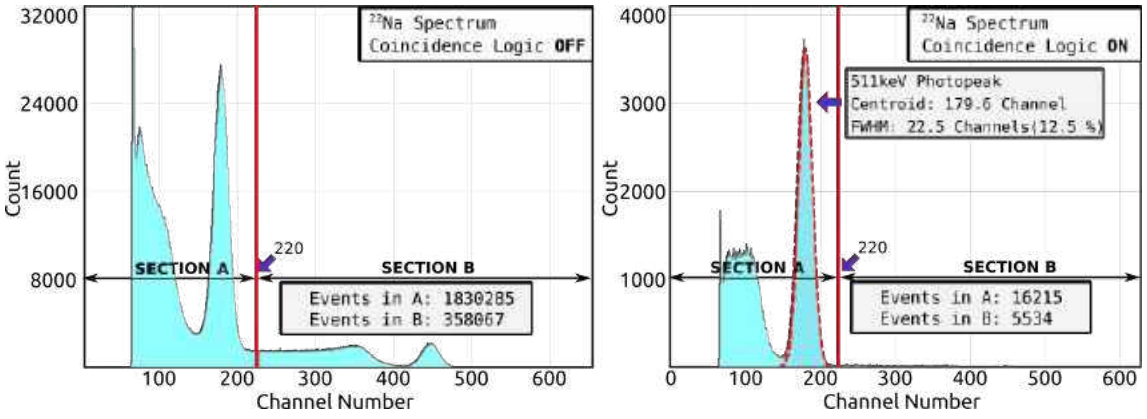

FIGURE 6.7: Coincidence gate applied for 511keV events from B shows the high energy 1275 keV events getting rejected

6.4 Offline Analysis of Data

Several high level functions included in the Python library enable rapid analysis of data saved in the comma separated values(CSV) format. An example is shown below.

```
import time,sys
import numpy as np
from MCALib import connect

dev = connect()

fname = 'mydata.csv'
dev.loadFile(fname)

# Get the data. Supply an optional name argument in case of multiple
# files/connected hardware.
x = dev.getHistogram() #name = fname / name='/dev/ttyUSB0'

# print the whole array. No decimal Points.
# Suppress scientific notation
np.set_printoptions(threshold = np.inf,precision = 0,suppress=True) #
print (x)

#plot the loaded spectrum
import matplotlib.pyplot as plt
plt.plot(x) #Plot RAW data

FIT = dev.gaussianTailFit([750,850]) #Apply a gaussian+Lorentzian
# FIT between 700 and 900 channel, and overlay it.

if FIT: # If fit was successful.
        plt.plot(FIT['X'],FIT['Y']) #Plot fitted data
        print('Gaussian+low energy tail Fit : ',FIT['centroid'],FIT['fwhm'])
```

```
29
30 FIT = dev.gaussianFit([500,600]) #Apply a gaussian FIT between
31 # 500 and 600 channel.
32 if FIT:
33         plt.plot(FIT['X'],FIT['Y']) #Plot fitted data
34         print('Gaussian Fit : ',FIT['centroid'],FIT['fwhm'])
35
36 plt.show()
```

The code above can be executed with Python3 by running the command below:

```
python3 example.py
```

The results are below. With Python, it is very simple for beginners to achieve results with minimal struggles related to programming syntax.

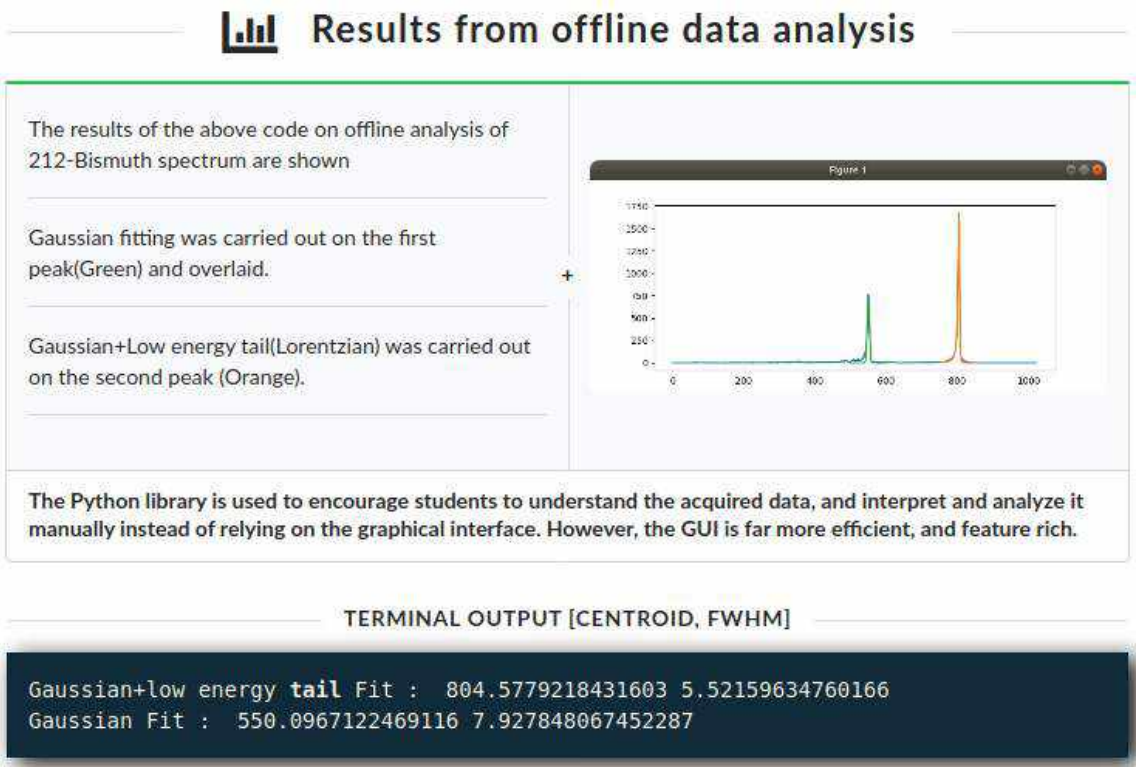

6.5 Installation

Since this software targets end-users who may not be well versed in programming tools, it is essential to generate one-click installers for different operating systems. We have built executable installers for the Windows platform, and deb installers for Debian based systems such as Ubuntu. For others, a Python-pip based installer has also been made available.

Installation on Windows

The setup file can be downloaded from https://csparkresearch.in/gammaspec. The windows installer was prepared using PyInstaller to create a distributable bundle from which a setup file was made using InnoSetup.

Installation on Ubuntu

The deb file can be obtained from https://csparkresearch.in, and installed using a package installer such as Gdebi. Deb file preparation was done with dpkg. Once the software reaches a stable form, it will be added to the standard Debian repository.

Installation from source

The source code for the software can be downloaded from github[14].

Some Python modules must first be installed in order to execute the software. Mainly - pyqt5 ,pyqt5.qtsvg, pyserial ,pyqtgraph , scipy , numpy

Exceute using the command - python3 MCA.py

CHAPTER 7

Workshops and other programs

I have participated in several training programs and workshops as a resource person and given some invited talks, aimed at propagating the use of new and innovative technology in classrooms and labs.

Two Day workshop on Nuclear Physics at Calicut University

I have been involved as a resource person in the "Two Day workshop on Nuclear Physics" at Calicut University conducted during 3-4 Jan 2020. I conducted a session on measurement of half life of the ^{212}Bi isotope extracted from Thorium Nitrate salt.

Training workshop at Amity university

Conducted a workshop for MSc students at Amity University, on using the gamma-gamma coincidence unit, Gamma and Alpha spectrometers, and Multi-channel analyzers.

Three Day workshop on Computer Interfaced Science Experiments

I Participated as a resource person in the "Three Day workshop on Computer Interfaced Science Experiments" conducted at Calicut University during 27-29 Dec 2019. Teachers

were trained on a host of Physics and Electronics experiments developed using computer interfaced data acquisition system ExpEYES. I conducted sessions on using digital sensors for pressure, acceleration, humidity, angular velocity, and a LIDAR for physics experiments. These sessions were streamed online, and can be found at . KuttyPy, an electronics development board whose design I have been involved in, was also introduced

SciPy.in-2019 International Conference

SciPy.in is an international conference organised at IIT Bombay on Python for Scientific computing. I organised a two hour workshop as an invited speaker, and also gave a lightning talk on using Python for computer interfaced data acquisition tools.I was an invited speaker, and conducted a workshop on learning microcontrollers using Python and KuttyPy, a device that I have developed.

Educode-2018 Conference

I conducted a workshop on "Physics experiments using ExpEYES" at Educode-2018, conducted at Brussels, Belgium, during 27-29 Aug 2018.

Invited talk at IISER Mohali

Gave a talk to the students of the outgoing batch of 2018 at IISER Mohali on the subject of Entrepreneurship as a career. It was organized by the Technology Business Incubator, IISER Mohali.

Workshop at MA College, Kerala

participated as a resource person in a Three day workshop on Computer Interfaced Science experiments using ExpEYES at Mar Athanasius College, Kerala.

India Science Fest, IISER Pune

Hosted a stall of science demos in this 2 day fest organised by Aspiring Minds at the IISER Pune campus. Over 10,000 people from in and around Pune are estimated to have attended.India Science Fest 2020 took take place on January 11-12, 2020, in Pune at the campus of IISER (Indian Institute of Science and Education). With major themes such as Artificial Intelligence and Neuroscience , the festival which included autonomous vehicles, AI generated art, and a host of science related panel discussions, lectures, and workshops was open to the public. Along with a passionate physics lecturer Praveen Patil from Makerspace Belgaum , I put up a booth where audiences were introduced to a host of computer interfaced experiments designed as part of my research.

One Day workshop at P T Sarvajanik College, Surat

Conducted a One Day workshop on Computer Interfaced Science Experiments at P T Sarvajanik College, Surat. Two sessions spanning the entire day were conducted by me on electronics and physics experiments at the P T Sarvajanik College for Science, Surat for an audience consisting of science teachers from in and around the district. It was met with a very positive response, and a proposal was mooted to expand the format to include teachers from the entire state over a longer duration.

Science Hack Day 2019, Belgaum

Science Hack Day is a 3-day event which is a progressive space where developers, designers, hackers, programmers, professionals, as well as schoolkids come together to learn and build. People from any background are welcome to attend – "no experience in science or hacking is necessary, just an insatiable curiosity". I have been a consistent part of this annual event and have hosted workshops for over a 100 kids where they have learnt to build solar lanterns, basic electronic circuits, and attain soldering skills.

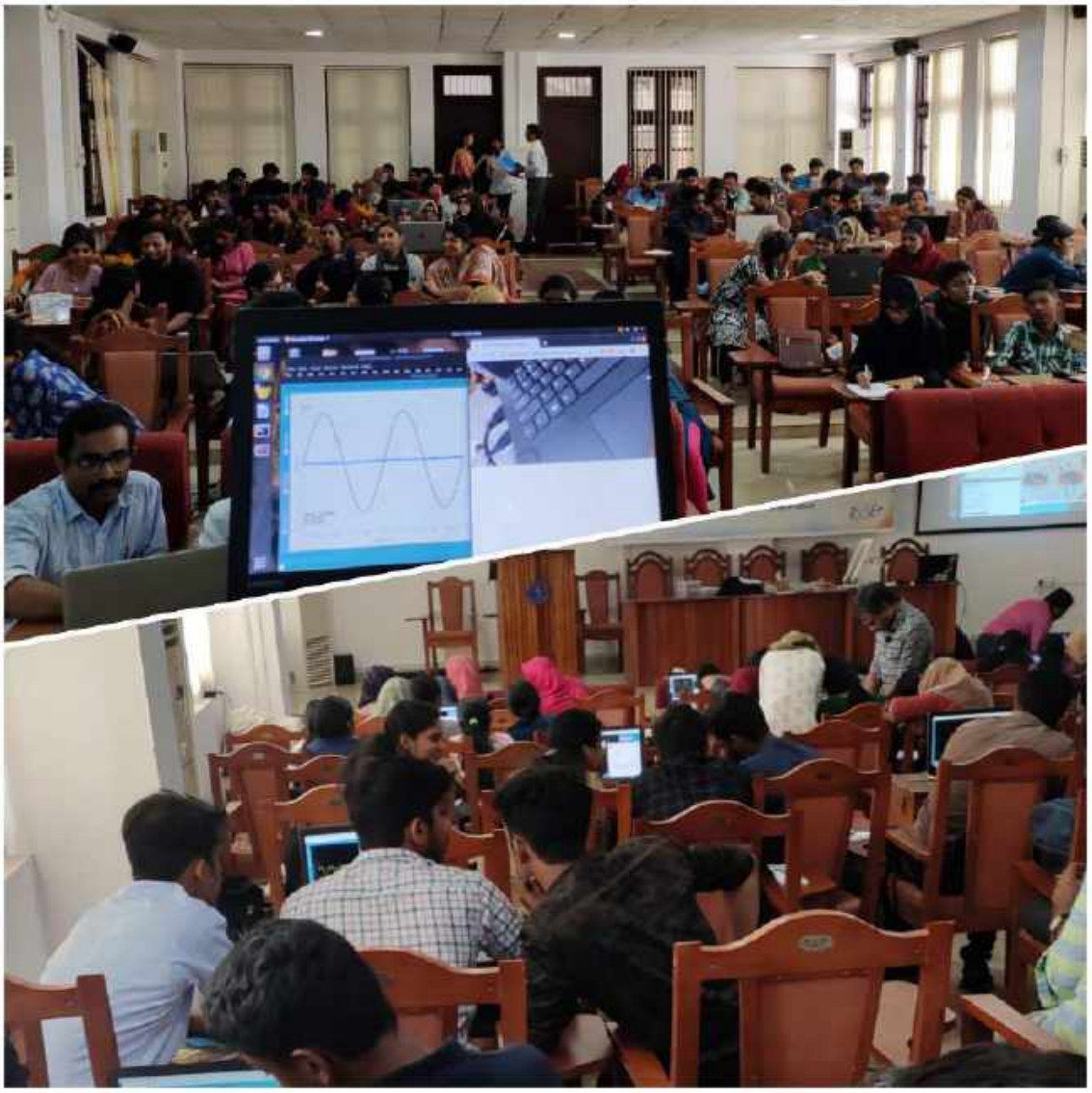

FIGURE 7.1: 3 Day workshop on Computer Interfaced Science Experiments at Calicut University

FIGURE 7.2: India Science Fest organised at IISER Pune

FIGURE 7.3: Scipy.in-2019 International Conference, IIT Bombay

FIGURE 7.4: Workshop at P T Sarvajanik College of Science and Education, Surat

FIGURE 7.5: Science Hack Day 2019, Belgaum

FIGURE 7.6: Conference Educode-2018, an open source centered conference held at Brussels

Conclusions

Through completion of the research goals described in this thesis, I hope to have made a significant contribution to the development of better pedagogical utilities and equipment. Identification of natural sources, development of indigenous detectors and associated instrumentation, and the development of strong theoretical models to back the spectral results have defined my research.

The Alpha Spectrometer design in its present form is well adapted to the needs of an undergraduate lab, but can also be adapted to study more interesting phenomena such as Rutherford scattering. This will require minor modifications to the detector position, and the introduction of a motorized stage for moving the gold film and the source around it.

The dual parameter MCA can also be used with signals from the Alpha Spectrometer, and efforts may be made to develop an Alpha-Gamma coincidence measurement setup. It will be necessary to machine the parts essential to combine the gamma spectrometer with the Alpha detector inside vacuum, and this may be a challenge.

The establishment of a commercial entity to further propagate our designs has ensured that the research can reach a wide audience. This also necessitated polishing of hardware designs as well as software to make it commercially viable, rather than remain a prototype or a proof of concept. This entity also enabled us to follow a design process that relied on continuous feedback received from end users instead of developers and technically savvy individuals, thereby keeping the focus on the intended audience. We have therefore followed design principles tried and tested by product design divisions of industries, and have reached fruitful conclusions.

We hope that the research foundation built during the course of this thesis will be expanded to serve a wide audience from the academic and research community.

Bibliography

[1] Jithin B.P. and O.S.K.S. Sastri, "Novel coincidence setup using indigenously developed portable USB gamma spectrometer and associated analysis software," *Nuclear Instruments and Methods in Physics Research, Section A: Accelerators, Spectrometers, Detectors and Associated Equipment*, vol. 964, p. 163 793, 2020, ISSN: 01689002. DOI: 10.1016/j.nima.2020.163793.

[2] Jithin B.P., V. V. V. Satyanarayana, S. Gora, O. S. K. S. Sastri, and B. P. Ajith, "Measurement Model of an Alpha Spectrometer for Advanced Undergraduate Laboratories," *Physics Education*, vol. 35, no. Jan-March 2019, 2019. [Online]. Available: http://www.physedu.in/pub/2019/PE18-08-518.

[3] Jithin B.P., S. Gora, V. Satyanarayana, O. Sastri, and B. Ajith, "Gamma Spectra of Non-Enriched Thorium Sources using PIN Photodiode and PMT based Detectors," *Physics Education*, no. Apr jun 2020, 2020. [Online]. Available: http://www.physedu.in/pub/2020/PE19-12-600.

[4] S. Gora, Jithin B.P., V. V. V. Satyanarayana, O. S. K. S. Sastri, and B. P. Ajith, "Alpha Spectrum of 212 Bi Source Prepared using Electrolysis of Non-Enriched ThNO 3 Salt," *Physics Education -IAPT*, vol. 35, no. Jan-Mar 2019, 2019. [Online]. Available: http://www.physedu.in/pub/2019/PE18-07-511.

[5] Jithin B.P., "SEELablet : A Technological Platform for Development of Innovative Experiments for Undergraduate Education," *APT Tunes*, vol. May 2018, 2018. [Online]. Available: https://aptkerala.org/images/stories/apttunes/APT_TUNES2018.pdf.

[6] O. S. K. S. Sastri, S. Aditi, J. Bhardwaj, S. Gora, V. Sharda, and B. P. Jithin, "Numerical Solution of Square Well Potential With Matrix Method Using Worksheets," *IAPT*, no. Jan - Mar 2020, 2019. [Online]. Available: http://www.physedu.in/pub/2020/PE19-11-590.

[7] A. Sharma, S. Gora, J. Bhagavathi, and O. S. K. S. Sastri, "Simulation study of nuclear shell model using sine basis," *American Journal of Physics*, vol. 576, 2020. DOI: 10.1119/10.0001041.

[8] Jithin B.P. and O.S.K.S Sastri, "Indigenously developed gamma spectrometer," in *Proceedings of the DAE Symp. on Nucl. Phys. 63 (2018) 1072*, 2018, pp. 1072–1073. [Online]. Available: http://sympnp.org/proceedings/63/G19.pdf.

[9] Jithin B.P. and O.S.K.S. Sastri, "Gated MCA technique for demonstration of coincidence phenomena with a set of indigenously developed gamma spectrometers," in *Recent Issues in Nuclear and Particle Physics, Viswa Bharati*, 2019.

[10] ——, "Compact dual-parameter MCA for γ-γ Coincidence Measurements," in *Proceedings of the DAE Symp. on Nucl. Phys. 64 (2019) 920*, 2019. [Online]. Available: http://sympnp.org/proceedings/64/G37.pdf.

[11] ——, "Background Gamma Radiation Surveying in the IndianPeninsula with a Portable USB Spectrometer," in *Proceedings of the DAE Symp. on Nucl. Phys. 64 (2019)*, 2019. [Online]. Available: http://sympnp.org/proceedings/64/G28.pdf.

[12] Jithin B.P., "Learning Microcontrollers with Python," in *Scipy India*, 2019.

[13] ——, "Simulation of N-Well Kronig- Penney Potential using Matrix Approach.," in *NACISP-2018*, IAPT, 2018.

[14] Jithin B P, *CN Spec Source Code*. [Online]. Available: https://github.com/csparkresearch/cnspec.

[15] Jithin B.P., *KuttyPy Source Code*, 2019. [Online]. Available: github.com/csparkresearch/kuttypy-gui.

[16] R. Grover and S. Chandra, "Scenario for growth of electricity in India," *Energy Policy*, vol. 34, no. 17, pp. 2834–2847, 2006, ISSN: 03014215. DOI: 10.1016/j.enpol.2005.04.021. [Online]. Available: http://linkinghub.elsevier.com/retrieve/pii/S030142150500131X.

[17] B Lalremruata, S. Kailas, B. Atomic, and V. Bhoraskar, "Existing and upcoming particle accelerators in India," no. November, 2017. DOI: 10.13140/RG.2.2.24839.50087.

[18] D. Press Information Bureau, Govt of India, *Use of nuclear energy - PIB report*, 2018. [Online]. Available: http://pib.nic.in/newsite/PrintRelease.aspx?relid=178349 (visited on 01/19/2019).

[19] PTI, *nuclear energy: India to add 7,000 MW nuclear power capacity: Power Minister Piyush Goyal - The Economic Times*. [Online]. Available: https://economictimes.indiatimes.com/industry/energy/power/india-to-add-7000-mw-nuclear-power-capacity-power-minister-piyush-goyal/articleshow/60034058.cms (visited on 08/10/2018).

[20] GOVERNMENT OF INDIA DEPARTMENT OF ATOMIC ENERGY, "LOK SABHA UNSTARRED QUESTION NO. 6071," Tech. Rep. [Online]. Available: http://dae.nic.in/writereaddata/parl/budget2018/lsus6071.pdf.

[21] World Nuclear Association, *Nuclear Power in India | Indian Nuclear Energy - World Nuclear Association*. [Online]. Available: http://www.world-nuclear.org/information-library/country-profiles/countries-g-n/india.aspx (visited on 01/19/2019).

[22] E. Gent, *Why India Wants to turn its beaches into nuclear fuel*. [Online]. Available: http://www.bbc.com/future/story/20181016-why-india-wants-to-turn-its-beaches-into-nuclear-fuel.

[23] R. B. Grover and R. R. Puri, "Development of human resources for Indian nuclear power programme," Tech. Rep., 2013, pp. 1051–1064. [Online]. Available: https://www.ias.ac.in/article/fulltext/sadh/038/05/1051-1064.

[24] Punjab Technical University, "Scheme and Syllabus of M.Sc. Physics M.Sc. Applied Physics," Tech. Rep., 2012. [Online]. Available: https://www.ptu.ac.in/userfiles/file/syllabus/others/M_Sc_Physics_PTU-GZS_Campus_Bathinda---22-07-2014.pdf.

[25] CLEAPPS, "L93 Managing Ionising Radiations and Radioactive Substances in Schools and Colleges," Tech. Rep., 2019. [Online]. Available: http://science.cleapss.org.uk/resource/L093-Managing-Ionising-Radiations-and-Radioactive-Substances-in-Schools-and-Colleges.pdf.

[26] G. F. Knoll, *Radiation detection and measurement*. John Wiley, 2010, p. 830, ISBN: 9780470131480. [Online]. Available: https://www.wiley.com/en-us/Radiation+Detection+and+Measurement%2C+4th+Edition-p-9781118026915.

[27] H. Spieler, *Lecture Notes*. [Online]. Available: https://www-physics.lbl.gov/$\sim$spieler/ (visited on 10/10/2020).

[28] ——, *Introduction to Radiation Detectors and Electronics*. [Online]. Available: https://www-physics.lbl.gov/$\sim$spieler/physics_198_notes/ (visited on 10/07/2020).

[29] C Tuvè, M Angelone, V Bellini, A Balducci, M. G. Donato, G Faggio, M Marinelli, G Messina, E Milani, M. E. Morgada, M Pillon, R Potenza, G Pucella, G Russo, S Santangelo, M Scoccia, C Sutera, A Tucciarone, and G Verona-Rinati, "Single crystal diamond detectors grown by chemical vapor deposition," *Nuclear Instruments and Methods in Physics Research, Section A: Accelerators, Spectrometers, Detectors and Associated Equipment*, vol. 570, no. 2 SPEC. ISS. Pp. 299–302, 2007, ISSN: 01689002. DOI: 10.1016/j.nima.2006.09.043.

[30] H Pernegger, *High mobility diamonds and particle detectors*, 2006. DOI: 10.1002/pssa.200671404.

[31] N. Ade, "An investigation of the role of defect levels on the radiation response of synthetic diamond crystals when used as sensors for the detection of mammography X-rays," *Applied Radiation and Isotopes*, vol. 127, no. June, pp. 237–244, 2017, ISSN: 18729800. DOI: 10.1016/j.apradiso.2017.06.021. [Online]. Available: http://dx.doi.org/10.1016/j.apradiso.2017.06.021.

[32] M. Pomorski, M. Ciobanu, C. Mer, M. Rebisz-Pomorska, D. Tromson, and P. Bergonzo, "Position-sensitive radiation detectors made of single crystal CVD diamond," *Physica Status Solidi (A) Applications and Materials Science*, vol. 206, no. 9, pp. 2109–2114, 2009, ISSN: 18626300. DOI: 10.1002/pssa.200982229.

[33] Microchip Technology, *PIC24EP256GP204 - 16-Bit - Microcontrollers and Digital Signal Controllers*. [Online]. Available: https://www.microchip.com/wwwproducts/en/PIC24EP256GP204 (visited on 11/12/2019).

[34] ORTEC, "Preamplifier and Amplifiers," Tech. Rep., 2015, pp. 2.2–2.4.

[35] A. B.P., *Preamp and Shaping Amplifier reference design*, 2015. [Online]. Available: https://www.iuac.res.in/phoenix/usbPhoenix/experiments/mca.html.

[36] D. NG, "Gamma-Gamma Coincidence Techniques," University of Hong Kong, Tech. Rep., 2015. [Online]. Available: http://www.physics.hku.hk/$\sim$physlab/cyp206/3851-2.pdf.

[37] R. Brun and F. Rademakers, "ROOT - An object oriented data analysis framework," *Nuclear Instruments and Methods in Physics Research, Section A: Accelerators, Spectrometers, Detectors and Associated Equipment*, vol. 389, no. 1-2, pp. 81–86, 1997, ISSN: 01689002. DOI: 10.1016/S0168-9002(97)00048-X.